การจำลองกระบวนการแก๊สซิฟิเคชันชีวมวลแบบออโตเทอร์มัลโดยใช้น้ำที่สภาวะยิ่งยวด

นายณัฐพล บุญพิทักษ์

วิทยานิพนธ์นี้เป็นส่วนหนึ่งของการศึกษาตามหลักสูตรปริญญาวิศวกรรมศาสตรมหาบัณฑิต
สาขาวิชาวิศวกรรมเคมี ภาควิชาวิศวกรรมเคมี
คณะวิศวกรรมศาสตร์ จุฬาลงกรณ์มหาวิทยาลัย
ปีการศึกษา 2555

SIMULATION OF AUTOTHERMAL BIOMASS GASIFICATION USING SUPERCRITICAL WATER

Mr. Nathapol Boonpithak

A Thesis Submitted in Partial Fulfillment of the Requirements
for the Degree of Master of Engineering Program in Chemical Engineering
Department of Chemical Engineering
Faculty of Engineering
Chulalongkorn University
Academic Year 2012

Thesis Title	SIMULATION OF AUTOTHERMAL BIOMASS GASIFICATION USING SUPERCRITICAL WATER
By	Mr. Nathapol Boonpithak
Field of Study	Chemical Engineering
Thesis Advisor	Assistant Professor Amornchai Arpornwichanop, D.Eng.

Accepted by the Faculty of Engineering, Chulalongkorn University in Partial Fulfillment of the Requirements for the Master's Degree

……..Dean of the Faculty of Engineering
(Associate Professor Boonsom Lerdhirunwong, Dr.Ing.)

THESIS COMMITTEE

……..Chairman
(Associate Professor Prasert Pavasant, Ph.D.)

……..Thesis Advisor
(Assistant Professor Amornchai Arpornwichanop, D.Eng.)

……..Examiner
(Assistant Professor Soorathep Kheawhom, Ph.D.)

……..External Examiner
(Assistant Professor Woranee Paengjuntuek, D.Eng.)

ณัฐพล บุญพิทักษ์ : การจำลองกระบวนการแก๊สซิฟิเคชันแบบออโตเทอร์มัลโดยใช้น้ำที่สภาวะยิ่งยวด (SIMULATION OF AUTOTHERMAL BIOMASSS GASIFICATION USING SUPERCRITICAL WATER) อ. ที่ปรึกษาวิทยานิพนธ์หลัก: ผศ. ดร. อมรชัย อาภรณ์วิชานพ, 108 หน้า.

ปัญหาของเชื้อเพลิงฟอสซิลที่ปัจจุบันมีปริมาณลดน้อยลงทุกทีและปัญหาด้านสิ่งแวดล้อมที่เป็นพิษ เป็นเรื่องที่จำเป็นต้องมีการใช้พลังงานทดแทนที่สะอาดเพิ่มมากขึ้น โดยเฉพาะเชื้อเพลิงชีวมวลถือได้ว่าเป็นแหล่งพลังงานทดแทนสะอาดที่มีศักยภาพอย่างมาก และสามารถเปลี่ยนไปเป็นแก๊สเชื้อเพลิงได้อีกด้วย โดยผ่านการเผาไหม้ไม่สมบูรณ์ในกระบวนการแก๊สซิฟิเคชัน แต่อย่างไรก็ตามเทคโนโลยีแก๊สซิฟิเคชันยังพบปัญหาในด้านการฟอร์มตัวของน้ำมันดินและต้องใช้พลังงานสูงเมื่อมีการป้อนชีวมวลที่มีความชื้นสูง แต่ปัญหาทั้งหมดนี้สามารถแก้ไขได้โดยใช้เทคโนโลยีแก๊สซิฟิเคชันโดยใช้น้ำที่สภาวะยิ่งยวดเนื่องจากสมบัติของน้ำที่สภาวะยิ่งยวดจะสามารถละลายได้ดีกับสารประกอบอินทรีย์ต่างๆในชีวมวลได้ ดังนั้นวัตถุประสงค์ของงานวิจัยนี้คือการศึกษาพฤติกรรมของกระบวนการแก๊สซิฟิเคชันโดยใช้น้ำที่สภาวะยิ่งยวดโดยดำเนินการให้มีการใช้พลังงานอย่างพอเพียงเพื่อลดพลังงานที่ให้กับระบบ พร้อมทั้งเปรียบเทียบกับเทคโนโลยีแก๊สซิฟิเคชันแบบทั่วไปในการศึกษาได้ใช้ชีวมวลสองชนิดที่มีความชื้นแตกต่างกันคือผักตบชวากับฟางข้าว อีกทั้งในการจำลองกระบวนการได้ศึกษาพารามิเตอร์หลายตัวเช่น อุณหภูมิของแก๊สซิฟิเคชัน, ความเข้มข้นของชีวมวลและความดันที่มีอิทธิพลต่อองค์ประกอบแก๊สผลิตภัณฑ์และประสิทธิภาพของกระบวน ผลการจำลองกระบวนการพบว่า เทคโนโลยีแก๊สซิฟิเคชันแบบทั่วไปเหมาะสมกับกระบวนการที่ใช้ชีวมวลที่มีความชื้นน้อยเช่นฟางข้าว ขณะที่ชีวมวลที่มีความชื้นมากจะเหมาะสมกับกระบวนการแก๊สซิฟิเคชันที่ใช้น้ำสภาวะยิ่งยวด อีกทั้งงานวิจัยนี้ยังได้ทำการหาสภาวะการดำเนินการที่เหมาะสมที่สุดของกระบวนการแก๊สซิฟิเคชันโดยใช้น้ำที่สภาวะยิ่งยวด โดยระเบียบวิธีพื้นที่ผิวตอบสนอง (Response surface methodology) โดยใช้วิธีการออกแบบเซ็นทรัลคอมคอมโพสิต (Central composite design)

ภาควิชา วิศวกรรมเคมี ลายมือชื่อนิสิต.....

สาขาวิชา วิศวกรรมเคมี ลายมือชื่อ อ.ที่ปรึกษาวิทยานิพนธ์หลัก.....

ปีการศึกษา 2555

5370427521 : MAJOR CHEMICAL ENGINEERING

KEYWORDS : BIOMASS GASIFICATION / SUPERCRITICAL WATER / OPTIMIZATION / ENERGY SELF – SUFFICIENT CONDITION / SIMULATION

NATHAPOL BOONPITHAK : SIMULATION OF AUTOTHERMAL BIOMASS GASIFICATION USING SUPERCRITICAL WATER. ADVISOR : ASST. PROF. AMORNCHAI ARPORNWICHANOP, D. ENG., 108 pp.

Depletion of fossil fuel and environmental concerns stimulate the use of clear and renewable energy. Biomass is regarded as a potential energy source and can be efficiently converted to a useful synthesis gas via incomplete combustion in a gasification process. However, the thermal gasification causes a formation of tar and requires high energy input when wet biomass is used. Supercritical water gasification (SCWG) is a possible way to cope with these difficulties because supercritical water behaves like many organic solvents so that organic compounds have complete miscibility with supercritical water. The objective of this study is to examine the performance of a biomass gasification process in supercritical water condition at energy self–sufficient operation, compared with a conventional gasification process. Modeling of the biomass gasification is performed using a process flowsheet simulator. Two different biomass feedstock: rice straw (low water content feedstock) and hyacinth (high water content feedstock), are considered in this study. Simulations are carried out to study effect of key operational parameters, such as gasification temperature, feedstock concentration and pressure, on the gaseous product composition and the efficiency of the gasification process under a energy self-sufficient operation, where no external heat input is required. The simulation results show that the conventional gasification is suitable process when biomass with low moisture content like rice straw is used as feedstock, whereas for biomass with high moisture content like water hyacinth, the application of the supercritical water gasification process is the appropriate option. To determine an optimal operating condition for the supercritical water gasification process, a response surface methodology (RSM) based on a central composite design (CCD) is used in this study.

Department : Chemical Engineering Student's Signature .....

Field of Study : Chemical Engineering Advisor's Signature .....

Academic Year : 2012

ACKNOWLEDGEMENTS

I wishes to express my sincere gratitude and appreciation to my advisor, Assistant Professor Amornchai Arpornwichanop, for his encouraging guidance throughout this research. I would also be grateful to Associate Professor Prasert Pavasant as the chairman of the thesis committee and Assistant Professor Soorathep Kheawhom and Assistant Professor Woranee Paengjuntuek as the member of the thesis committee.

Support from the Thailand Research Fund, Commission of Higher Education and the Computational Process Engineering research group, the Special Task Force for Activating Research (STAR), Chulalongkorn University Centenary Academic Development Project is also gratefully acknowledged.

I would also like to specially thank Miss Bhawasut Chutichai for her help on this research.

Finally, I would like to express the highest gratitude to my family for their inspiration, encouragement and financial support throughout this study.

CONTENTS

PAGE

ABSTRACT IN THAI iv
ABSTRACT IN ENGLISH v
ACKNOWLEDGEMENTS vi
CONTENTS vii
LIST OF TABLES xii
LIST OF FIGURES xiv
LIST OF ABBREVIATIONS xix

CHAPTER

I INTRODUCTION 1
1.1 Background 1
1.2 Objectives 4
1.3 Scope of research 5
1.4 Expected benefits 5

II LITERATURE REVIEWS 6
2.1 Biomass gasification process for syngas production 6
2.2 Supercritical water biomass gasification process 9
2.3 Application of gasification process 10

III THEORY 12
3.1 Biomass 12
3.1.1 Water hyacinth 13
3.1.2 Rice straw 17
3.2 Biomass gasification process 18
3.2.1 Drying 20

CHAPTER PAGE

3.2.2 Pyrolysis 20
3.2.3 Combustion..... 21
3.2.4 Reduction..... 21
3.3 Biomass gasification technologies..... 21
3.3.1 Fixed-bed/Moving bed gasifiers..... 22
3.3.2 Fluidized-bed gasifier..... 24
3.3.3 Entrained-flow gasifier..... 25
3.4 Gasification simulation models..... 26
3.4.1 Thermodynamic equilibrium models..... 27
3.5 Supercritical water gasification process..... 30
3.5.1 Properties of supercritical water..... 32
3.5.2 Advantage of SCW gasification 34
3.5.3 Scheme of an SCWG plant..... 35
3.6 Response surface methodology (RSM) based on central composite design (CCD)..... 37
3.5.1 Analysis of variance 39

IV CONVENTIONAL GASIFICATION TECHNOLOGY 41
4.1 Introduction..... 41
4.2 Simulation model of water hyacinth and rice straw conventional gasification process..... 42
4.3 Conventional gasification at energy self-sufficient condition 46
4.4 Results and discussion 49
4.4.1 Model validation..... 50
4.4.2 Sensitivity analysis 50
4.4.2.1 Effect of gasifier temperature..... 50
4.4.2.2 Effect of steam..... 51
4.4.3 Efficiency analysis..... 56

CHAPTER PAGE

4.4.3.1 Effect of gasifier temperature..... 56
4.3.1.2 Effect of steam 57

V SUPERCRITICAL WATER GASIFICATION TECHNOLOGY FOR SYNGAS PRODUCTION
5.1 Introduction..... 60
5.2 Simulation model of water hyacinth and rice straw supercritical water gasification process..... 61
5.3 Supercritical water gasification at energy self-sufficient condition..... 63
5.4 Results and discussion 67
5.4.1 Model validation..... 67
5.4.2 Sensitivity analysis 67
5.4.2.1 Effect of gasifier temperature..... 67
5.4.2.2 Effect of feedstock concentration..... 73
5.4.2.3 Effect of pressure 73
5.4.3 Efficiency analysis..... 77
5.5 Comparison of water hyacinth and rice straw gasification technology for syngas production..... 82

VI OPTIMIZATION OF SUPERCRITICAL WATER GASIFICATION PROCESS 83
6.1 Introduction..... 83
6.2 Statistical analysis using design of simulations..... 84
6.3 Development of regression model 85
6.3.1 Mean square of error 86
6.3.2 *F*-value..... 86
6.3.3 *P*-value..... 88
6.3.4 Lack of fit 89

CHAPTER PAGE

6.3.5 Mathematical model 89
6.4 Effect of process parameters 90
6.4.1 Effect of single parameter 90
6.4.1.1 Feedstock concentration 90
6.4.1.2 Gasifier temperature 92
6.4.1.3 Pressure 92
6.4.2 Effect of parameter interaction 93
6.4.2.1 Gasifier temperature and feedstock concentration 93
6.4.2.2 Pressure and feedstock concentration 95
6.4.2.3 Pressure and gasifier temperature 96
6.5 Optimization of the efficiency of a biomass gasification process. 96

VII CONCLUSIONS 98
7.1 Conclusions 98
7.2 Recommendation 100

REFERENCES 101

APPENDICES 106

VITAE 108

LIST OF TABLES

TABLE PAGE

3.1 Proximate and ultimate analysis of water hyacinth 17
3.2 Proximate and ultimate analysis of rice straw 18
3.3 Typical gasification reactions at 25 ^{o}C 20
3.4 Properties of supercritical and subcritical water 31
3.5 Relationship between coded and actual values of a variable 40
4.1 Model inputs used for the simulation. 46
4.2 Experimental results versus model predictions. 50
5.1 Description of unit operation blocks used for simulations of biomass gasification process. 64
5.2 Experimental results versus model predictions. 68
6.1 Process parameters in central composite design: coded and natural values 85
6.2 Full factorial central composite design matrix of three independent variables in coded and the response of the dependent variable efficiency ..87
6.3 Model summary statistics 87
6.4 Analysis of variance (ANOVA) for quadratic polynomial model 88
6.5 Regression analysis of a full second-order polynomial model for optimization of reaction conditions 89
6.6 Optimization criteria for maximum efficiency 97
6.7 Results of model validation at the optimum conditions 97

LIST OF FIGURES

FIGURE PAGE

3.1 Potential paths for gasification. 19
3.2 Stages of gasification in an updraft gasifier. 23
3.3 Schematic of a bubbling fluidized-bed gasifier. 25
3.4 Two main types of entrained–flow gasifiers: (a) side-fed entrained-flow reactor, and (b) top-fed entrained-flow reactor 27
3.5 Phase diagram of water showing the supercritical region 30
3.6 Schematic of a pilot plant for supercritical water gasification of biomass ...37
4.1 Simulation model of gasifier. 44
4.2 Simulation calculation procedure 45
4.3 Shows the system of energy balance in the fluidized bed gasifier 47
4.4 Effect of steam to biomass ratio and equivalence ratio on the net heat energies: (a) for water hyacinth and (b) for rice straw 48
4.5 Equivalence ratio (ER) at different temperatures and at different steam to biomass ratio (SBR): (a) for water hyacinth and (b) for rice straw 49
4.6 Hydrogen yield (kg/kg biomass) at different temperatures and at different steam to biomass ratio (SBR): (a) for water hyacinth and (b) for rice straw 52
4.7 Carbon monoxide yield (kg/kg biomass) at different temperatures and at different steam to biomass ratio (SBR): (a) for water hyacinth and (b) for rice straw 53
4.8 Carbon dioxide yield (kg/kg biomass) at different temperatures and at different steam to biomass ratio (SBR): (a) for water hyacinth and (b) for rice straw 54
4.9 Methane yield (kg/kg biomass) at different temperatures and at different steam to biomass ratio (SBR): (a) for water hyacinth and (b) for rice straw 55

FIGURE PAGE

4.10 Efficiency (%) at different temperatures and at different steam to biomass ratio (SBR): (a) for water hyacinth and (b) for rice straw 58

4.11 Efficiency (%) at different temperatures and at different steam to biomass ratio (SBR): (a) for water hyacinth and (b) for rice straw..... 59

5.1 Schematic diagram of the gasification process considered in this study 63

5.2 Simulation of the biomass gasification in supercritical water 63

5.3 The system of energy balance in the supercritical gasifier. 65

5.4 Equivalence ratio (ER) at different temperatures and at different steam to biomass ratio (SBR): (a) for water hyacinth and (b) for rice straw 66

5.5 Hydrogen yield (kg/kg biomass) at different temperatures and at different feedstock concentration (a) for water hyacinth and (b) for rice straw 69

5.6 Carbon monoxide yield (kg/kg biomass) at different temperatures and at different feedstock concentration (a) for water hyacinth and (b) for rice straw 70

5.7 Carbon dioxide yield (kg/kg biomass) at different temperatures and at different feedstock concentration: (a) for water hyacinth and (b) for rice straw 71

5.8 Methane yield (kg/kg biomass) at different temperatures and at different feedstock concentration: (a) for water hyacinth and (b) for rice straw 72

5.9 Effect of pressure on hydrogen yield (kg/kg biomass) at feedstock concentration 20 wt% and temperatures 800 ^{o}C (a) for water hyacinth and (b) for rice straw 74

5.10 Effect of pressure on carbon monoxide yield (kg/kg biomass) at feedstock concentration 20 wt% and temperatures 800 ^{o}C (a) for water hyacinth and (b) for rice straw 75

FIGURE PAGE

5.11 Effect of pressure on carbon monoxide yield (kg/kg biomass) at feedstock concentration 20 wt% and temperatures 800 ^{o}C (a) for water hyacinth and (b) for rice straw 76
5.12 Effect of pressure on methane yield (kg/kg biomass) feedstock concentration 20 wt% and temperatures 800 ^{o}C (a) for water hyacinth and (b) for rice straw 77
5.13 Efficiency (%) at different temperatures and at different feedstock concentration (a) for water hyacinth and (b) for rice straw 79
5.14 Effect of pressure on efficient (%) feedstock concentration 20 wt% and temperatures 800 ^{o}C (a) for water hyacinth and (b) for rice straw 80
5.15 Efficiency (%) of water hyacinth at different temperatures and at different gasification technology. 82
5.16 Efficiency (%) of rice straw at different temperatures and at different gasification technology. 82
6.1 Optimization of supercritical water gasification process. 85
6.2 A comparative plot between simulation and predicted efficiency. 90
6.3 Effect of feedstock concentration on the efficiency. 91
6.4 Effect of gasifier temperature on the efficiency. 91
6.5 Effect of pressure on the efficiency.....92
6.6 Contour plots of the combined effects gasifier temperature and feedstock concentration on the efficiency. 94
6.7 Contour plots of the combined effects pressure and concentration feedstock on the efficiency 94
6.8 Contour plots of the combined effects pressure and gasifier temperature on the efficiency 95

LIST OF ABBREVIATIONS

SCW	Supercritical water	(-)
SCWG	Supercritical water gasification	(-)
RKS	Redlich Kwong Soave equation	(-)
BM	Boston Mathias Modification	(-)
SCM	Shrinking core model	(-)
GM	Grainy Pellet Model	(-)
PAH	Poly- Aromatic hydrocarbons	(-)
CHP	Combined heat and power	(-)
DDGS	Dried distillers grains with solubles	(-)
GHG	Greenhouse gas	(-)
RDF	Refuse-derived fuel	(-)
H/C	Hydrogen to carbon	(-)
IGCC	Integrated gasification combined cycle	(-)
G_{total}	Gibbs free energy	(-)
$G^0_{f,i}$	Gibbs free energy of formation of species *i* at standard pressure of 1 bar.	(-)
$a_{i,j}$	Number of atoms	(-)
λ	Lagrangian multiplier	(-)
T_{sat}	Saturation temperature	(°C)
P_c	Critical pressure	(MPa)
μ	Viscosity	(kg/m.s)
RSM	Response surface methodology	(-)
CCD	Central Composite Design	(-)
ANOVA	Analysis of variance	(-)
n_e	Total number of experiment trial	(-)
Y_{yield}	Predicted response variable	(-)
$\lambda_0, \lambda_i, \lambda_{ii}, \lambda_{ij}$	Constant regression coefficients	(-)
k	Number of variables	(-)

α	Number of factorial run	(-)
n_c	Number of center points	(-)
ER	Equivalence ratio	(-)
SBR	different steam to biomass ratio	(-)
η	Efficiency	(-)
Q	Heat duties	(-)
RSTOIC	Stoichiometric reactor	(-)
SRKMHV2	Soave Redlich-Kwong property method with modified Huron-Vidal mixing rule	(-)
SEP	Separator	(-)
HP	High-pressure pump	(-)
COMP	Compressor	(-)
HP-SEP	High pressure phase separator	(-)
LP-SEP	Low pressure phase separator	(-)
MIX	Mixer	(-)
LHV_{H_2}	The low heating value of hydrogen	(-)
LHV_{biomass}	Low heating value of biomass	(-)
Q_{gasifier}	Energy of gasifier	(-)
MSE	Mean squared of error	(-)
MS_{SSR}	Mean of square regression	(-)
MS_{SSE}	Mean of square residual	(-)
SSR	Sum of square	(-)
SSE	Sum of residual	(-)
DF	Degree of freedom	(-)
LOF	Lack of fit	(-)

CHAPTER I

INTRODUCTION

1.1 Background

The advancement of renewable energy sources is obtaining elevated importance on account of several factors. First of all, an important deficiency of fossil fuel is estimated for the next few decades due to growing worldwide demand, promoted by developing countries. Secondly, fossil fuels are located to a significant extent in politically and socially unstable countries, which make their exports subject to volatility of prices and supply. Finally, global warming problem, largely involved carbon dioxide releases in the atmosphere due to electric power plants and combustion plants utilizing fossil fuels, have demanded on many national governments to look for alternative and more environmentally friendly ways to produce energy (Castello et al., 2011).

Presently, biomass can be considered an efficient fuel source of renewable energy. Biomass, fuel derived from organic matter on a renewable basis, is among the greatest fuel sources of renewable energy in the world. Biomass adsorbs carbon dioxide from the atmosphere during photosynthesis; carbon dioxide is returned to the environment after combustion. Owing to this cycle, biomass is carbon dioxide neutral, making it a favorable fuel source and a best alternative for replacement of fossil fuels as the issues of global warming increases. Biomass materials realized as sources of energy are agricultural residues, such as straw, bagasse and bark.

Among the several technologies suggested for biomass conversion into energy, the gasification is the excellent hopeful way because it procures a gaseous product which can be directly burnt in engines or turbines to produce electrical power (Castello et al., 2011). Regular gasification process is based on the biomass partial oxidation. Air is a low-priced and widely used gasifying agent; however, it contains a

large amount of nitrogen, which lowers the heating value of the synthesis gas (syngas) product. When pure oxygen is used as the gasifying agent instead, the heating value of syngas will increase but the operating costs will also increase due to the oxygen production costs. The heating value and hydrogen content of the syngas can be increased if steam is used as the gasifying agent. When pure steam is used as the gasifying agent, an indirect or external heat supply for endothermic gasification reactions is required. Alternatively, a mixture of steam or carbon dioxide and air or oxygen can be used as the gasifying agent, and the partial combustion of biomass with air/O_2 provides the heat required for the gasification (Puig-Arnavat et al., 2010).

In general, traditional gasification technologies have encountered a number of major difficulties obstructing their advancement. The first problem in biomass gasification is to deal with the tar formed during the process (Balat, et. al., 2009). Tar derived from biomass gasification will be condensed at temperature lower than its dew point, which then blocks and fouls process equipments like fuel lines, filters, engines and turbines. The quality of the product gas is usually low as it is polluted by impurities like char and tar. As a result, expensive clean gas systems are demanded to complete the required quality standard. Chen et al. (2004) was reported that in case, the producer gas is contaminated by high tar contents and particle which could lead to the corrosion and wear of blades of turbine. Van Paasen et al. (2004) describe that entrained-flow gasifiers are normally operated at high temperature (typically 1300 – 1500 ^{o}C) and do not produce significant amounts of tar. On the other hand, Fixed-bed and fluidized-bed gasifier are normally operated at substantially lower temperature levels and do produce significant amount of tar. Furthermore, traditional gasification technologies require dry biomass to avoid excessive drying costs (Ortiz et al., 2011). Supercritical water gasification (SCWG) is a possible way to solve these problems due to the usual properties of water at supercritical state (i.e. temperature and pressure higher than 375 ^{o}C and 21 bar, respectively) (Castello et al., 2011). The critical point marks an important change in the thermo-physical properties of water. This changes the water from a highly polar solvent at an ambient condition to a nonpolar solvent and makes it the best solvent for non-polar organic compounds. Good miscibility of intermediate solid organic compounds as well as gaseous products in liquid SCW

allows single–phase chemical reactions during gasification, removing the interphase barrier of mass transfer. Supercritical water is characterized by its high ion product, which implies high H^+ or OH^- concentration in supercritical water. This allows SCW to act like an acid or base catalyst in the reactions. In addition, tar production is low because tar precursors, such as phenol molecules, are completely soluble in SCW and so can be efficiently reformed in SCW gasification. SCWG achieves higher thermal efficiency for very wet biomass and char formation is low in SCWG (Basu, 2010).

Although SCWG seems to be an interesting and potential option for biomass gasification, it has not been investigated widely. Most of the studies have focused on experimental activities, mainly analyzing the product gas composition for different feedstock by using small laboratory devices. Model compounds such as cellulose, lignin, glucose and glycerol (Saisu et al., 2003; Hao et al., 2003; Kabyemela et al., 1999) have been extensively tested to get information on the chemistry of biomass gasification in supercritical water. On the other hand, gasification of the real biomass, such as sawdust and different starches (Antal et al., 2000), clover grass and corn silage (D'Jesus et al., 2006), baby food and zoo mass (Kruse, 2005) in supercritical water was also investigated. A lately review on biomass gasification in near- and supercritical water was given by Matsumura et al. (2005).

To date, there are few studies on the prediction of the gasification products and efficiency from a theoretical point of view. The interest of such a work is to predict the thermodynamic limits as a guideline for process design, evaluation and improvement (Yan et al., 2006). Lu et al. (2007) analyzed the thermodynamic equilibrium of a supercritical water gasification using minimization of Gibbs free energy. This approach requires the knowledge of thermodynamical properties, such as the fugacity coefficients, in order to evaluate the activity of each species in the mixture at the operating conditions prevailing within the reactor. This estimation can be performed using Equations of State (EoS). Withag et al. (2012) presented a system model for the gasification process of biomass model compounds in supercritical water. The thermodynamic model in ASPEN was used under the assumption of chemical equilibrium and the model compound was employed to represent the

organics in the wet biomass. The research focuses on predicting the influence of several parameters on the thermal efficiency of the process.

In this study, the performance analysis of a biomass gasification process in supercritical water condition at energy self-sufficient operation is carried out and compared with that of a conventional gasification process. Modeling of the biomass gasification is performed using a process flowsheet simulator. Two different biomass feedstock: rice straw (low water content feedstock) and hyacinth (high water content feedstock), are considered in this study. A systematic thermodynamic analysis of the gasification processes is performed based on the total Gibbs free energy minimization method. Simulations are done to study effect of key operational parameters, such as gasification temperature, concentration feedstock, biomass moisture and pressure, on the gasification process under energy self-sufficient operation, where no external heat input is required. Hydrogen yield in the synthesis gas product and thermal efficiency of the gasification process are considered and suitable operating conditions of the biomass gasification for hydrogen production are identified.

1.2 Objectives

1. To investigate the performance of a supercritical water biomass gasification process in terms of syngas production and process efficiency at energy self-sufficient condition and to compare with a conventional biomass gasification process.
2. To study the effect of key operational parameters, such as gasification temperature, feedstock concentration and pressure on the gasification process under energy self-sufficient condition.
3. To find the optimal operating condition of the supercritical water gasification process for synthesis gas production.

1.3 Scopes of work

1. To simulate supercritical water biomass and conventional gasification processes at energy self–sufficient condition.

2. To analyze effects of operating parameters, such as gasification temperature, feedstock concentration and pressure on the gasification process under a self-sufficient operation.

3. To compare the performance of the supercritical water and conventional biomass gasification using different feedstock, i.e., water hyacinth and rice straw.

3. To determine optimal operating conditions of the supercritical water gasification process with the aim to maximize the process efficiency using a response surface methodology.

1.4 Expected benefits

1. To understand the effect of gasifier temperature, feedstock concentration and pressure on the synthesis gas production of the supercritical water gasification process at energy self-sufficient condition.

2. To know that the supercritical water biomass gasification is suitable for which type of biomass.

3. To obtain the suitable operating conditions of the supercritical water biomass gasification for synthesis gas production.

CHAPTER II

LITERATURE REVIEWS

2.1 Biomass gasification process for syngas production

At present, gasification of biomass is widely accepted as a popular technical to produce fuel gas for the application in boilers, engine, gas turbine or fuel gas. In this section, various aspects of biomass gasification were reviewed. The most widely used configurations of biomass gasifiers and the effect of various operating parameters on the quality of syngas are discussed in detail. Warnecke (2000) has classified the gasifiers in four categories which are based on the fluid and/or solid movement inside the reactor. 1. Quasi non-moving or self-moving feedstock 2. Mechanically-moved feedstock (downdraft gasifier, updraft gasifier, cross-draft gasifier) 3. Fluidically-moved feedstock (bubbling bed (BB) gasifier, circulating fluidized bed (CFB) gasifier, entrained-bed gasifier) 4. Special reactors (spouted bed gasifier, cyclone gasifier) Among those listed above, downdraft, updraft, BB and CFB gasifiers are widely used in the commercial market. Commercially, about 75% of the gasifiers sold are downdraft gasifiers, 20% fluidized bed, 2.5% updraft, and 2.5% of the other types (Knoef , 2000) Syngas composition varies widely and mostly depends upon the gasifier type, feedstock, feedstock pre-treatment, gasifying medium and operating parameters like temperature, pressure, and nature of interaction between reactants in the gasification process. Zainal et al. compared the best optimal value for the downdraft gasifier with respect to equivalence ratio using furniture wood and wood chips as feedstock. The effect of equivalence ratio for each syngas component was analyzed with the conclusion of an optimal equivalence ratio of 0.38 for the gasifier performance for that particular feedstock. Both Skoulou et al. and Sheth et al. report an optimal equivalence ratio of 0.2 for downdraft gasification of olive kernels and olive tree cutting and furniture wood. The optimum equivalence ratio varies for different biomass due to the amount of oxygen elementally present in the biomass as

well as the ash content. Antal et al. (2000) presents biomass feedstocks, including corn- and potato-starch gels, wood sawdust suspended in a cornstarch gel, and potato wastes, were delivered to three different tubular flow reactors by means of a “cement” pump. When rapidly heated to temperatures above 650 °C at pressures above the critical pressure of water (22 MPa), the organic content of these feedstocks vaporized.

Some authors, trying to avoid complex processes and develop the simplest possible model that incorporates the principal gasification reactions and the gross physical characteristics of the reactor, have developed models using the process simulator ASPEN Plus (Puig-Arnavat et al., 2010). Mathieu et al. (2002) analyzed the performance of a fluidized bed gasifier by devising a model which was based on minimization of Gibbs free energy in ASPEN Plus simulator. A sensitivity analysis was also carried out with respect to oxygen factor, air temperature, oxygen content in air, operating pressure and injection of steam. Lv et al. (2003) also studied the effects of steam to biomass ratio, reactor temperature, equivalence ratio and biomass particle size on production of hydrogen rich gas during biomass air-steam gasification. The extra hydrogen content was attributed to water gas reaction and steam reforming reactions. Further steam reforming weakens after 700 ^{o}C when Boudouard reaction and water gas reaction paly dominant role.at higher pressures hydrogen and CO decreases and CO_2 and CH_4 content increases. A model was prepared by Paviet et al. (2009) addressing a thermochemical process occurring a wood biomass downdraft gasifier where they highlighted the effects of char conversion, air fuel ratio on temperature and product gas composition using the Redlich Kwong Soave equation of state with Boston Mathias Modification (RKS-BM). It was selected basing upon its reliable heat duty. Damartzis et al. (2012) performed the assessment of a combined heat and power (CHP) biomass bubbling fluidized bed gasification unit coupled with an internal combustion engine (ICE) by using a comprehensive mathematical model based on the Aspen Plus process simulator. The model is based on a combination of modules that Aspen Plus simulator provides representing the 3 steps of gasification process (drying, pyrolysis, and oxidation), gas cleaning and ICE. The proposed model is capable of dealing with a wide variety of biomasses (olive kernel, corn cob/stalks, rapeseed and sunflower stalks) using air as the fluidization agent and to predict the

system's performance in terms of cold gas and thermal efficiency. Doherty et al. (2009) develops a computer model of a circulating fluidized bed biomass gasifier that can predict gasifier performance under various operating conditions. An original model was developed using ASPEN Plus. The model is based on Gibbs free energy minimisation. The restricted equilibrium method was used to calibrate it against experimental data. This was achieved by specifying the temperature approach for the gasification reactions. The model predicts syn-gas composition, conversion efficiency and heating values in good agreement with experimental data. Operating parameters were varied over a wide range. Parameters such as equivalence ratio (ER), temperature, air preheating, biomass moisture and steam injection were found to influence syn-gas composition, heating value, and conversion efficiency.

Gasification Process has proven to be the most economical and efficient method of converting biomass to useful energy. However, gasification technologies have encountered a number of major difficulties obstructing their advancement. First problem in biomass gasification is to deal with the tar formed during the process (Balat, et. al., 2009). Tar derived from biomass gasification will be condensed as temperature is lower than its dew point, which then block and foul process equipments like fuel lines, filters, engines and turbines. The quality of the product gas is usually low as it is polluted by impurities like char and tar. As a result, expensive clean gas systems are demanded to complete the required quality standard. Chen et al. (2004) was reported that in case, the producer gas is contaminated by high tar contents and particle which could lead to the corrosion and wear of blades of turbine. Van Paasen et al. (2004) describe that entrained-flow gasifiers do not produce significant amounts of tar because of at high temperature (typically 1300 – 1500 ^{o}C). On the other hand, Fixed-bed and fluidized-bed gasifier are normally operated at substantially lower temperature levels and do produce significant amount of tar. Furthermore, traditional gasification technologies require dry biomass to avoid excessive drying costs (Ortiz et al., 2011).

2.2 Supercritical water biomass gasification process for syngas production

Supercritical water gasification (SCWG) is a possible solution to solve these problems. Owing to the unique properties of water at supercritical state (i.e. temperature and pressure higher than 375 ^{o}C and 221 bar, respectively), extremely fast kinetics can be achieved, thus avoiding the formation of tar and char and significantly improving the product gas quality. (Castello et al., 2011). To this regard, Matsumura et al. (2005) reviewed the supercritical water gasification (SCWG) of biomass. There are two approaches to biomass gasification in supercritical water. The first, a low-temperature catalytic gasification, employs reaction temperature ranging from 350 to 600 ^{o}C, and gasifies the feedstock with the aid of metal catalysts. The second, ahigh-temperature supercritical water gasification, employs reaction temperatures ranging from 500 ^{o}C to 750 ^{o}C, without catalyst or with non-metallic catalysts. Reviews are made on the reaction mechanism, catalyst, and experimental results for these two approaches. Engineering technologies for the SCWG gasification and an example of process analysis are also introduced. Ji et al. (2006) performed the simulation study of operating conditions for hydrogen purification and recovery in supercritical water gasification of biomass. The gas product from biomass gasification in supercritical water contains about 55% H_2 and 33% CO_2 in mole fraction. Others like CH_4 and CO exist in the gas product with less amounts. Hydrogen is the targeted product. Its purification is a very important step. Water is generally used as the solvent to purify the hydrogen by separating CO_2 and other gases from the gas product. The hydrogen purification can be carried out through separators, generally a high-pressure separator followed by low-pressure separators. The operating conditions of temperature, pressure, and the amounts of water used have a significant effect on the efficiency of hydrogen purification. Simulation of hydrogen purification at a wide range of operating conditions has been carried out. The appropriate operating conditions have been indicated, at which, to the greatest extent, the hydrogen produced can be purified and recovered. The results of this work will have a significant contribution to the design of a process of supercritical water gasification of biomass. Voll et al. (2009) studied in the present work the Gibbs free energy minimization, using a non-linear programming formulation and an approximation in

the gas fugacities, was used to calculate the equilibrium composition for supercritical water gasification of methanol, ethanol, glycerol, glucose and cellulose. The proposed formulation mathematically ensures finding the global optimal solution with no need of an initial estimate and the numerical results are close to the ones calculated using non-ideal gas formulation. Therefore, the proposed approach is reliable and easy to use, without numerical difficulties, such as an undesirable local minimum. The model predictions show a good agreement with the experimental studies in all cases studied in this work. Withag et al. (2012) presents a system model for the process of gasification of biomass model compounds in supercritical water. Supercritical water gasification of wet biomass (water content of 70 wt% or more) has as the main advantage that conversion may take place without the costly drying step. The thermodynamic model is generated in ASPEN Plus 12.1 under the assumption of chemical equilibrium and using model compounds to represent the organics in the wet biomass. Here a mixture of water and methanol as a biomass model compound is used to mimic wet biomass. It is also possible to use other model compounds like glucose or cellulose. The research focuses on predicting the influence of several parameters on the thermal efficiency of the process. One of the important parameters under investigation is the heat exchanger effectiveness. The possibility of tailoring the product gases and in situ CO_2 capturing using water are also modeled and described.

2.3 Applications of biomass gasification

Pairojpiriyakul et al. (2012) presents thermodynamic analysis of hydrogen production from glycerol at energy self-sufficient conditions. A thermodynamic analysis based on the principle of minimizing the Gibbs free energy is performed for hydrogen production from glycerol. Two levels of energy self-sufficient, (i) within the reformer and (ii) within the overall system, are considered. The obtained results demonstrate that the maximum hydrogen production significantly decreases from 5.65 mol H_2/mol glycerol for the reformer level to 3.31 mol H_2/mol glycerol for the system level, emphasizing the significant demand of energy for feed preheating. Kumar et al. (2010) presents optimization and economic evaluation of industrial gas production and combined heat and power generation from gasification of corn stover

and distillers grains. The objectives of this study were to maximize the net energy efficiency for biomass gasification, and to estimate the cost of producing industrial gas and combined heat and power (CHP) at a feedrate of 2000 kg/h. Aspen Plus-based model for gasification was combined with CHP generation model and optimized using corn stover and dried distillers grains with solubles (DDGS) as the biomass feedstocks. Overall, high net energy efficiencies for gas and CHP production from biomass gasification can be achieved with optimized processing conditions. However, the economical feasibility of these conversion processes will depend on the relative local prices of fossil fuels. Gutiérrez Ortiz et al. (2011) presents thermodynamic analysis of the autothermal reforming of glycerol using supercritical water. Simulations run so as to calculate the O_2 needed to enter the Gibbs reactor (reformer) for achieving the thermoneutral condition (no external heat to sustain the reformer operation is required). Thus, the effect of the main operating parameters (reforming temperature, water to glycerol mole ratio, glycerol purity in the feed of crude glycerol, oxygen to glycerol mole ratio and the inlet feed temperature) aimed to the hydrogen production has been investigated, by obtaining the mole fraction and molar flow-rate of components in syngas, as well as the hydrogen yield. By this way, the most thermodynamic favorable operating conditions at which glycerol may be converted into hydrogen by autothermal reforming using SCW have been identified.

CHAPTER III

THEORY

3.1 Biomass

Biomass is a biorenewable resource derived from organic material of biological origin (Brown, 2003). The cell walls of both woody and herbaceous (non-woody) biomass consist of lignocellulose, or fiber, which is composite structural material formed by plants that consists of variable amounts of cellulose, hemicellulose, and lignin.

The properties of biomass are defined by the material composition and heating value. The proximate analysis reports the moisture content, fixed carbon, volatile matter, and ash on a mass basis and is determined by heating the material under controlled conditions. Volatile matter is the fraction of substance that decomposes and escapes as gases upon heating at moderate (about 400°C) temperatures in a non-oxidizing environment. The remaining fraction is a mixture of fixed carbon and ash; the fixed carbon is determined by oxidation to carbon dioxide so that the non-combustible ash remains. The ultimate analysis reports the weight percent of carbon, hydrogen, nitrogen, oxygen, sulfur, chlorine, moisture, and ash of the substance.

The composition and heating value of biomass are vastly different from those of coal. Biomass contains about 35% less carbon than coal, and as a result, heating values of biomass are 20 – 30% lower than coal. Biomass also contains a larger percentage of oxygen, and in general, chemically bonded oxygen is partly responsible for the lower heating values of biomass (Brown, 2003).

The moisture and ash content of biomass are important factors when evaluating it as a fuel. In a gasification reactor, where drying is the first stage of conversion, biomass with high moisture content consumes otherwise useful heat to

evaporate the liquid water, thereby causing less efficient gasification. Osowski and Osowski (2006) state that feedstocks with up to 50% moisture content can be successfully gasified. However, depending on the plant scale, the use of a dryer may be necessary prior to gasification for feedstocks with higher moisture contents. Because ash is non-combustible material, feedstocks with higher ash contents have lower energy values. In addition, the specific composition of the ash is also important because it can affect the physical properties of the reactor and composition of the producer gas. Elements such as potassium, chlorine, sulfur, and heavy metals can cause high temperature corrosion of reactor components (Liao et al., 2007). In addition, elements such as chlorine and sulfur form acidic gases such as HCl and H_2S which must be cleansed from the product stream.

The heating value is the net energy released upon oxidizing a fuel under isothermal conditions. There are two heating values reported in the literature, the higher heating value (HHV) and lower heating value (LHV). The higher and lower heating values are often termed respectively the gross calorific value and net calorific value. The higher heating value pertains to reaction products containing condensed liquid water, while the lower heating value refers to products containing water vapor. The difference between the higher and lower heating values is the contribution of latent heat of vaporization of water.

3.1.1 Water hyacinth

Water hyacinth is an aquatic plant which can live and reproduce floating freely on the surface of fresh waters or can be anchored in mud. Plant size ranges from a few inches to a meter in height. Its rate of proliferation under certain circumstances is extremely rapid and it can spread to cause infestations over large areas of water causing a variety of problems. It grows in mats up to 2 meters thick which can reduce light and oxygen, change water chemistry, affect flora and fauna and cause significant increase in water loss due to evapotranspiration. It also causes practical problems for marine transportation, fishing and at intakes for hydro power and irrigation schemes. It is now considered a serious threat to biodiversity.

The plant originated in the Amazon Basin and was introduced into many parts of the world as an ornamental garden pond plant due to its beauty. It has proliferated in many areas and can now be found on all continents apart from Europe. It is particularly suited to tropical and sub-tropical climates and has become a problem plant in areas of the southern USA, South America, East, West and Southern Africa, South and South East Asia and Australia. Its spread throughout the world has taken place over the last 100 years or so, although the actual course of its spread is poorly documented. In the last 10 years the rapid spread of the plant in many parts of Africa has led to great concern.

The plant is a perennial aquatic herb (Eichhornia crassipes) which belongs to the family Pontedericeae, closely related to the Liliaceae (lily family). The mature plant consists of long, pendant roots, rhizomes, stolons, leaves, inflorescences and fruit clusters. The plants are up to 1 metre high although 40 cm is the more usual height. The inflorescence bears 6 - 10 lily-like flowers, each 4 - 7cm in diameter. The stems and leaves contain air-filled tissue which give the plant its considerable buoyancy. The vegetation reproduction is asexual and takes place at a rapid rate under preferential conditions. (Herfjord et al., 1994).

The problem

Water hyacinth can cause a variety of problems when its rapid mat-like proliferation covers areas of fresh water. Some of the common problems are listed below:

- Hindrance to water transport. Access to harbours and docking areas can be seriously hindered by mats of water hyacinth. Canals and freshwater rivers can become impassable as they clog up with densely intertwined carpets of the weed. It is also becoming a serious hazard to lake transport on Lake Victoria as large floating islands of water hyacinth form, while many of the inland waterways of south East Asia have been all but abandoned.
- Clogging of intakes of irrigation, hydropower and water supply systems. Many large hydropower schemes are suffering from the effects of water hyacinth.

The Owen Falls hydropower scheme at Jinja on Lake Victoria is a victim of the weeds rapid reproduction rates and an increasing amount of time and money is having to be invested in clearing the weed to prevent it entering the turbine and causing damage and power interruptions. Water hyacinth is now a major problem in some of the world's major dams - the Kariba dam which straddles the Zambia-Zimbabwe border on the Zambezi River and feeds Harare has pronounced infestations of the weed.

- Blockage of canals and rivers causing flooding. Water hyacinth can grow so densely that a human being can walk on it. When it takes hold in rivers and canals it can become so dense that it forms a herbivorous barrage and can cause damaging and dangerous flooding.
- Micro-habitat for a variety of disease vectors. The diseases associated with the presence of aquatic weeds in tropical developing countries are among those that cause the major public health problems: malaria, schistosomiasis and lymphatic filariasis. Some species of mosquito larvae thrive on the environment created by the presence of aquatic weeds, while the link between schistosomiasis (bilharzia) and aquatic weed presence is well known. Although the statistical link is not well defined between the presence of aquatic weeds and malaria and schistosomiasis, it can be shown that the brughian type of filariasis (which is responsible for a minor share of lymphatic filariasis in South Asia) is entirely linked to the presence of aquatic weeds (Bos, 1996).
- Increased evapotranspiration. Various studies have been carried out to ascertain the relationship between aquatic plants and the rate of evapotranspiration compared with evaporation from an open-surfaced water body. Saelthun (1986) suggests that the rate of water loss due to evapotranspiration can be as much as 1.8 times that of evaporation from the same surface but free of plants. This has great implications where water is already scarce. It is estimated that the flow of water in the Nile could be reduced by up to one tenth due to increased losses in Lake Victoria from water hyacinth.

- Problems related to fishing. Water hyacinth can present many problems for the fisherman. Access to sites becomes difficult when weed infestation is present, loss of fishing equipment often results when nets or lines become tangled in the root systems of the weed and the result of these problems is more often than not a reduction in catch and subsequent loss of livelihood. In areas where fishermen eke a meagre living from their trade, this can present serious socio-economic problems. Fishermen on lake Victoria have also noted that, in areas where there is much water hyacinth infestation, the water is ‘still and warm and the fish disappear’. They also complain that crocodiles and snakes have become more prevalent.
- Reduction of biodiversity. Where water hyacinth is prolific, other aquatic plants have difficulty in surviving. This causes an imbalance in the aquatic micro-ecosystem and often means that a range of fauna that relies on a diversity of plant life for its existence, will become extinct. Diversity of fish stocks is often effected with some benefiting and others suffering from the proliferation of water hyacinth. People often complain of localised water quality deterioration. This is of considerable concern where people come to collect water and to wash.

Quantification of the problem is often extremely difficult. The real effect on fish stocks and flora is unknown. It is hard to calculate the effect on fishing communities. Even quantifying the coverage of the weed is difficult on bodies of water which are as large and geographically complex as Lake Victoria. Satellite methods are the only accurate way of determining the spread of the weed. Success is hard to measure when the exact scale of the problem is not clearly defined and is anyway growing rapidly.
Ultimate analysis, moisture contents and energy contents for the water hyacinth is provided in Table 3.1.

Table 3.1 Proximate and ultimate analysis of water hyacinth (Elliott et al., 1988)

Carbon	wt%	43.0
Hydrogen	wt%	5.8
Oxygen	wt%	29.5
Nitrogen	wt%	5.6
Sulphur	wt%	0
Moisture	wt%	94.9
Ash	wt%	15.3

3.1.2 Rice straw

Rice straw is a byproduct or waste from rice production and utilization is promoted for solving pollution problems as the first priority. In most cases of utilization such as fodder and fuel, rice straw is used because of the cheaper price, not because of particularly favorable properties. Unlike commercial goods, the price of rice straw cannot increase too much based on demand; users would shift to alternative materials as was the case for rice husk power production in Thailand where large increase in price resulted is users shifting to wood waste for example. Some form of government intervention may be required to avoid supply shortage. Beside demand and supply mechanism, biomass supply requires transportation which contributes a major part of the biomass cost and a higher calorific value could provide higher heat or power for the same biomass weight, the biomass with higher calorific values tend to be more cost effective in terms of feedstock supply. On the other hand, investors normally expect better advantages from the new recommended biomass, the higher profit (that derive from the higher heating value) and lower operating problems (that derive from biomass properties). Since rice straw does not have very high heating value and particularly better properties as compared to other biomass, it is not expected to provide a higher profit; therefore, the primary goal at the current stage is to determine the possibility and method to use it competitively. The proximate and the ultimate analysis of rice straw were illustrated in Table 3.2.

Table 3.2 Proximate and ultimate analysis of rice straw (Shen et al, 2008)

Carbon	wt%	36.57
Hydrogen	wt%	4.91
Oxygen	wt%	40.70
Nitrogen	wt%	0.57
Sulphur	wt%	0.14
Chlorine	wt%	1.55
Moisture	wt%	8.5
Ash	wt%	8.61

3.2 Biomass gasification process

Gasification is the conversion of solid or liquid feedstock into useful and convenient gaseous fuel or chemical feedstock that can be burned to release energy or used for production of value-added chemicals. Gasification and combustion are two closely related thermo chemical processes, but there is an important difference between them. Gasification packs energy into chemical bonds in the product gas; combustion breaks those bonds to release the energy. The gasification process adds hydrogen to and strips carbon away from the feedstock to produce gases with a higher hydrogento carbon (H/C) ratio, while combustion oxidizes the hydrogen and carbon into water and carbon dioxide, respectively.

A typical biomass gasification process may include the following steps:

- Drying
- Thermal decomposition or pyrolysis
- Partial combustion of some gases, vapors, and char
- Gasification of decomposition products

Pyrolysis is a thermal decomposition process that partially removes carbon from the feed but does not add hydrogen. Gasification, on the other hand, requires a gasifying medium like steam, air, or oxygen to rearrange the molecular structure of the feedstock in order to convert the solid feedstock into gases or liquids; it can also add hydrogen to the product. The use of a medium is essential for the gasification process.

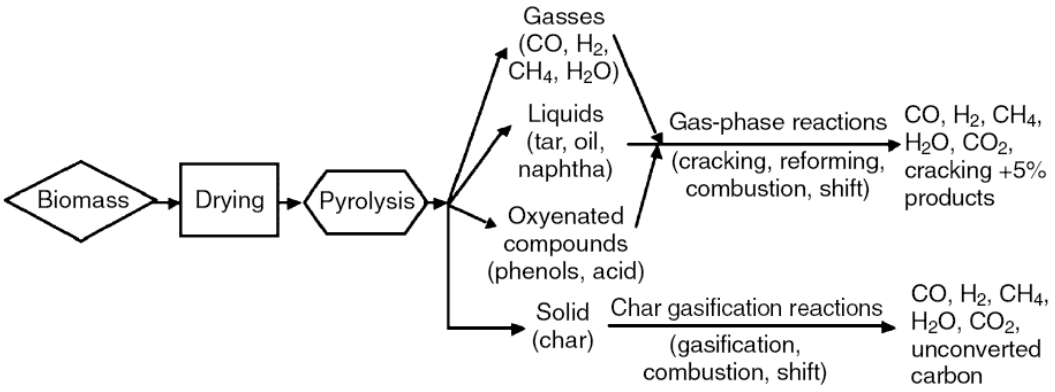

Figure 3.1 Potential paths for gasification

A typical gasification process generally follows the sequence of steps listed on the next page (illustrated schematically in Figure 3.1).

- Preheating and drying
- Pyrolysis
- Char gasification
- Combustion

Though these steps are frequently modeled in series, there is no sharp boundary between them, and they often overlap. The following paragraphs discuss these sequential phases of biomass gasification.

In a typical process, biomass is first heated (dried) and then it undergoes thermal degradation or pyrolysis. The products of pyrolysis (i.e., gas, solid, and liquid) react among themselves as well as with the gasifying medium to form the final gasification product. In most commercial gasifiers, the thermal energy necessary for drying pyrolysis, and endothermic reactions comes from a certain amount of exothermic combustion reactions allowed in the gasifier. Table 3.3 lists some of the important chemical reactions taking place in a gasifier.

Table 3.3 Typical gasification reactions at 25 ^{o}C (Brown, 2003)

Reaction Type	**Reaction**	
Carbon Reactions		
R1 (Boudouard)	$C + CO_2 \leftrightarrow 2CO$	+172
R2 (water-gas or steam)	kJ/mol	
R3 (hydrogasification)	$C + H_2O \leftrightarrow CO + H_2$	+131
R4	kJ/mol	
	$C + 2H_2 \leftrightarrow CH_4$	-74.8
	kJ/mol	
	$C + 0.5\ O_2 \rightarrow CO$	-111 kJ/mol
Oxidation Reactions		
R5	$C + O_2 \rightarrow CO_2$	-394
R6	kJ/mol	
R7	$CO + 0.5O_2 \rightarrow CO_2$	-284
R8	kJ/mol	
	$CH4 + 2O_2 \leftrightarrow CO_2 + 2H_2O$	-803
	kJ/mol	
	$H_2 + 0.5\ O_2 \rightarrow H_2O$	-242
	kJ/mol	
Shift Reaction		
R9	$CO + H_2O \leftrightarrow CO_2 + H_2$	-41.2
	kJ/mol	
Methanation Reactions		
R10	$2CO + 2H_2 \rightarrow CH_4 + CO_2$	-247 kJ/mol
R11	$CO + 3H_2 \leftrightarrow CH_4 + H_2O$	-206 kJ/mol
R14	$CO_2 + 4H_2 \rightarrow CH_4 + 2H_2O$	-165 kJ/mol
Steam-Reforming Reactions		
R12	$CH_4 + H_2O \leftrightarrow CO + 3H_2$	+206 kJ/mol
R13	$CH_4 + 0.5\ O_2 \rightarrow CO + 2H_2$	-36 kJ/mol

3.2.1 Drying

In this stage, the moisture content of the biomass is reduced. Typically, the moisture content of biomass ranges from 5% to 35%. Drying occurs at about 100 - 200 ^{o}C with a reduction in the moisture content of the biomass of <5%.

3.2.2 Pyrolysis (Devolatilisation)

This is essentially the thermal decomposition of the biomass in the absence of oxygen or air. In this process, the volatile matter in the biomass is reduced. This results in the release of hydrocarbon gases from the biomass, due to which the biomass is reduced to solid charcoal. The hydrocarbon gases can condense at a sufficiently low temperature to generate liquid tars.

3.2.3 Oxidation

This is a reaction between solid carbonised biomass and oxygen in the air, resulting in formation of CO_2. Hydrogen present in the biomass is also oxidised to generate water. A large amount of heat is released with the oxidation of carbon ad hydrogen. If oxygen is present in substoichiometric quantities, partial oxidation of carbon may occur, resulting in the generation of carbon monoxide.

3.2.4 Reduction

In the absence (or substoichiometric presence) of oxygen, several reduction reactions occur in the 800–1000 ^{o}C temperature range. These reactions are mostly endothermic. The main reactions in this category are as follows:

Water–gas reaction:

$$\mathrm{C} + H_2\mathrm{O} \rightarrow \mathrm{CO} + H_2 + 131.4\mathrm{kJ/mol} \qquad (3.1)$$

Bounded reaction:

$$\mathrm{C} + CO_2 \leftrightarrow 2\mathrm{CO} \qquad +172\mathrm{kJ/mol} \qquad (3.2)$$

Shift reaction:

$$CO_2 + H_2 \leftrightarrow \mathrm{CO{+}H_2O} \quad -41.2\mathrm{kJ/mol} \qquad (3.3)$$

Methane reaction:

$$\mathrm{C} + 2H_2 \leftrightarrow \mathrm{CH_4} \qquad -74.8\mathrm{kJ/mol} \qquad (3.4)$$

3.3 Biomass gasification technologies

Gasifiers are classified mainly on the basis of their gas - solid contacting mode and gasifying medium. Based on the gas - solid contacting mode, gasifiers are broadly divided into three principal types: (1) fixed or moving bed, (2) fluidized bed, and (3) entrained flow.

3.3.1 Fixed-bed/Moving bed gasifiers

The fixed-bed gasifier has a bed of solid fuel particles through which the gasifying media The fixed-bed gasifier has a bed of solid fuel particles through which the gasifying media gasification occurs. Fixed-bed gasifiers are simple to construct and generally operate with high carbon conversion, long solid residence time, low gas velocity and low ash carry-over.To explain the reaction process in moving-bed gasifiers, and we take the example of a simple updraft gasifier reactor (Figure 3.2).

In a typical updraft gasifier, fuel is fed from the top; the product gas leaves from the top as well. The gasifying agent (air, oxygen, steam, or their mixture), is slightly preheated and enters the gasifier through a grid at the bottom. The gas then rises through a bed of descending fuel or ash in the gasifier chamber.

The air (the gasifying medium), as it enters the bottom of the bed, meet shot ash and unconverted chars descending from the top (Figure 3.5). The temperature in the bottom layer well exceeds the ignition temperature of carbon, so the highly exothermic combustion reaction (Eq. 3.5) takes place in the presence of excess

oxygen. The released heat heats the upward-moving gas as well as the descending solids.

$$C + O_2 \rightarrow CO_2 \qquad \text{-394kJ / mol} \qquad (3.5)$$

The combustion reaction (Eq. 3.6), being very fast, rapidly consumes most of the available oxygen. As the available oxygen is reduced further up, the combustion reaction changes into partial combustion, releasing CO and a moderate amount of heat.

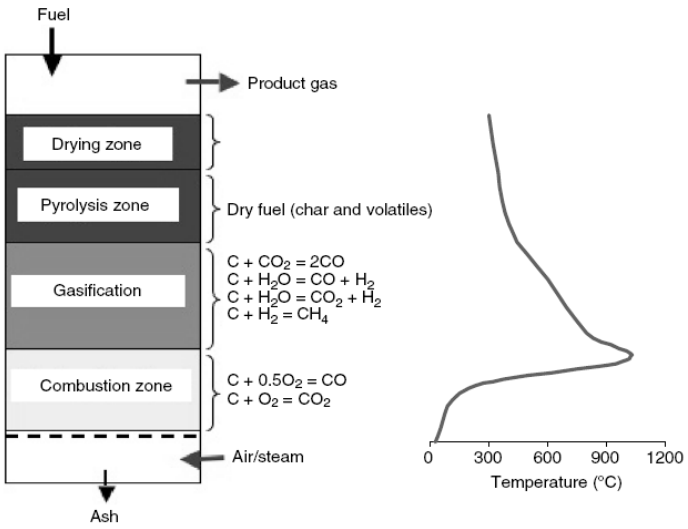

Figure 3.2 Stages of gasification in an updraft gasifier

$$C + 0.5O_2 \rightarrow CO \qquad \text{-111kJ / mol} \qquad (3.6)$$

The hot gas, a mixture of CO, CO_2, and steam (from the feed and the gasifying medium), moves further up into the gasification zone, where char from the upper bed is gasified by Eq. (3.7). The carbon dioxide concentration increases rapidly in the first

combustion zone, but once the oxygen is nearly depleted, the CO_2 enters the gasification reaction (Eq. 3.7) with char, resulting in a decline in CO_2 concentration in the gasification zone.

$$C + CO_2 \leftrightarrow 2CO \qquad \text{-172kJ / mol} \qquad (3.7)$$

$$C + H_2O \leftrightarrow CO + H_2 \quad -131 kJ/mol \qquad (3.8)$$

Sensible heating of the hot gas provides the heat for the two endothermic gasification reactions in Eq. (3.7, 3.8): R1 and R2 (Table 3.3). These are responsible for most of the gasification products like hydrogen and carbon monoxide. Because of their endothermic nature, the temperature of the gas reduces.

The zone above the gasification zone is for the pyrolysis of biomass. The residual heat of the rising hot gas heats up the dry biomass, descending from above. The biomass then decomposes (pyrolyzed) into noncondensable gases, condensable gases, and char. Both gases move up while the solid char descends with other solids.

The topmost zone dries the fresh biomass fed into it using the balance enthalpy of the hot product gas coming from the bottom. This gas is a mixture of gasification and pyrolysis products.

In an updraft gasifier biomass fed from the top descends, while air injected from the side meets with the pyrolysis product, releasing heat (see Chapter 6). Thereafter, both product gas and solids (char and ash) move down in the downdraft gasifier. Here, a part of the pyrolysis gas may burn above the gasification zone. Thus, the thermal energy required for drying, pyrolysis, and gasification is supplied by the combustion of pyrolysis gas. This phenomenon is called flaming pyrolysis.

3.3.2 Fluidized-bed gasifiers

In a bubbling fluidized bed, the fuel fed from either the top or the sides mixes relatively fast over the whole body of the fluid bed (Figure 3.3). The gasifying medium (air, oxygen, steam, or their mixture) also serves as the fluidizing gas and so is sent through the bottom of the reactor.

In a typical fluidized-bed gasifier, fresh solid fuel particles are brought into contact with hot bed solids that quickly heat the particles to the bed temperature and make them undergo rapid drying and pyrolysis, producing char and gases.

Though the bed solids are well mixed, the fluidizing gas remains generally in plug-flow mode, entering from the bottom and leaving from the top. Upon entering the bottom of the bed, the oxygen goes into fast exothermic reactions (R4, R5, and R8 in Table 3.3) with char mixed with bed materials. The bed materials immediately disperse the heat released by these reactions to the entire fluidized bed. The amount of heat released near the bottom grid depends on the oxygen content of the fluidizing gas and the amount of char that comes in contact with it. The local temperature in this region depends on how vigorously the bed solids disperse heat from the combustion zone.

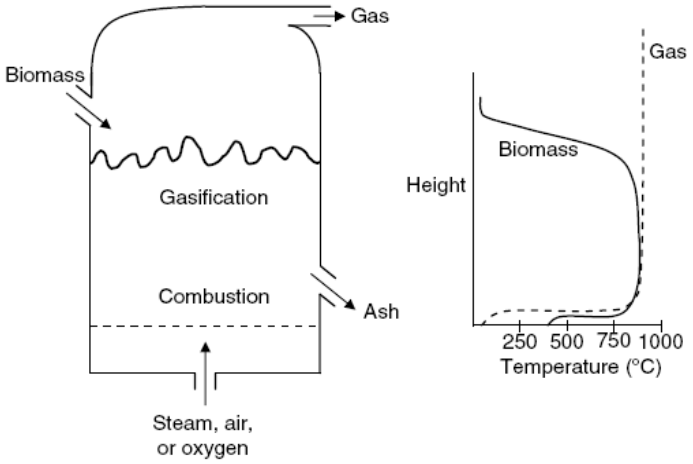

Figure 3.3 Schematic of a bubbling fluidized-bed gasifier

Subsequent gasification reactions take place further up as the gas rises. The bubbles of the fluidized bed can serve as the primary conduit to the top. They are relatively solids-free. While they help in mixing, the bubbles can also allow gas to bypass the solids without participating in the gasification reactions. The pyrolysis products coming in contact with the hot solids break down into noncondensable gases. If they escape the bed and rise into the cooler freeboard, tar and char are formed.

3.3.3 Entrained-flow gasifiers

Entrained-flow gasifiers are preferred for the integrated gasification combined cycle (IGCC) plants. Reactors of this type typically operate at 1400 ^{o}C and 20 to 70

bar pressure, where powdered fuel is entrained in the gasifying medium. Figure 3.4 shows two entrained-flow gasifier types. In the first one, oxygen, the most common gasifying medium, and the powdered fuel enter from the side; in the second one they enter from the top.

In entrained-flow gasifiers, the combustion reaction, R5 (Eq. 3.5), may take place right at the entry point of the oxygen, followed by reaction R4 (Eq. 3.6) further downstream, where the excess oxygen is used up. Powdered fuel (< 75 micron) is injected into the reactor chamber along with oxygen and steam (air is rarely used). To facilitate feeding into the reactor, especially if it is pressurized, the fuel may be mixed with water to make slurry. The gas velocity in the reactor is sufficiently high to fully entrain the fuel particles. Slurry-fed gasifiers need additional reactor volume for evaporation of the large amount of water mixed with the fuel. Furthermore, their oxygen consumption is about 20% greater than that of a dry-feed system owing to higher blast requirements (Higman and van der Burgt, 2008).

3.4 Modelling of gasification process

A mathematical model used to explain a gasifier may be classified into the following groups:

- Thermodynamic equilibrium
- Kinetic
- Computational fluid dynamics (CFD)
- Artificial neural network

Kinetic rate, CFD and artificial neural network models always contain parameters that limit their applicability to different plants. Thus, thermodynamic equilibrium model was selected for the current study. The thermodynamic equilibrium model predicts the maximum achievable yield of a desired product from a reacting system (Li et al., 2001). In other words, if the reactants are left to react for an infinite time, they will reach equilibrium yield. The yield and composition of the product at this condition is given by the equilibrium

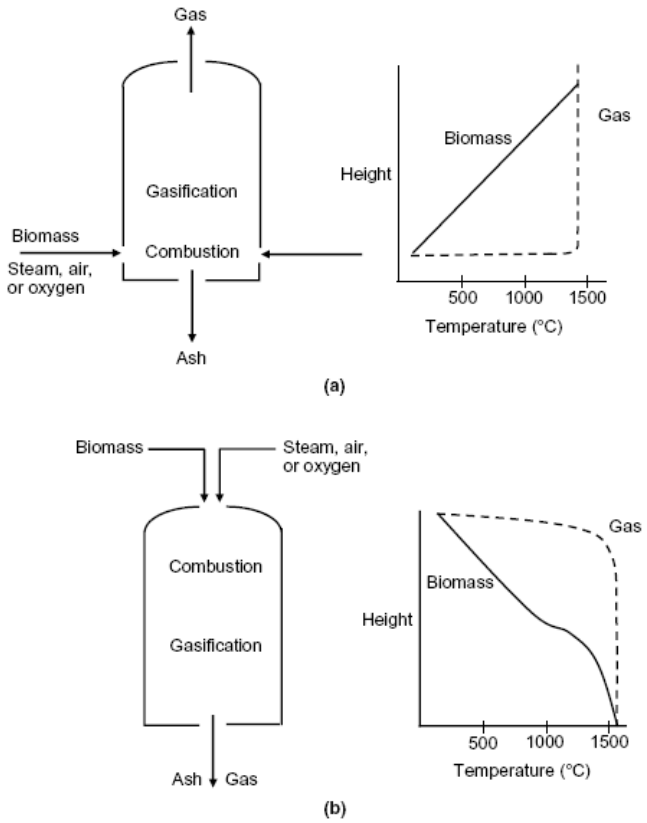

Figure 3.4 Two main types of entrained-flow gasifiers: (a) side-fed entrained-flow reactor, and (b) top-fed entrained-flow reactor

model, which concerns the reaction alone without taking into account the geometry of the gasifier.

Thermodynamic Equilibrium Models

Thermodynamic equilibrium calculation is independent of gasifier design and so is convenient for studying the influence of fuel and process parameters. Though chemical or thermodynamic equilibrium may not be reached within the gasifier, this model provides the designer with a reasonable prediction of the maximum achievable yield of a desired product. However, it cannot predict the influence of hydrodynamic or geometric parameters, like fluidizing velocity, or design variables, like gasifier height. Chemical equilibrium is determined by either of the following:

- The equilibrium constant
- Minimization of the Gibbs free energy

Prior to 1958 all equilibrium computations were carried out using the equilibrium constant formulation of the governing equations. Later, computation of equilibrium compositions by Gibbs free energy minimization became an accepted alternative. This section presents a simplified approach to equilibrium modeling of a gasifier based on the following overall gasification reactions:

$$\mathrm{C} + CO_2 \leftrightarrow 2\mathrm{CO} \qquad (R1)$$

$$\mathrm{C} + H_2O \leftrightarrow H_2 + \mathrm{CO} \qquad (R2)$$

$$\mathrm{C} + H_2 \leftrightarrow CH_4 \qquad (R3)$$

$$\mathrm{CO} + H_2O \leftrightarrow \mathrm{CO}_2 + \mathrm{H}_2 \qquad (R4)$$

From a thermodynamic point of view, the equilibrium state gives the maximum conversion for a given reaction condition. The reaction is considered to be zero dimensional and there are no changes with time (Li et al., 2001). An equilibrium model is effective at higher temperatures (>1500 K), where it can show useful trends in operating parameter variations (Altafini et al., 2003). For equilibrium modeling, one may use stoichiometric or nonstoichiometric methods (Basu, 2006).

Nonstoichiometric Equilibrium Models

In nonstoichiometric modeling, no knowledge of a particular reaction mechanism is required to solve the problem. In a reacting system, a stable equilibrium condition is reached when the Gibbs free energy of the system is at the minimum. So, this method is based on minimizing the total Gibbs free energy. The only input needed is the elemental composition of the feed, which is known from its ultimate analysis. This method is particularly suitable for fuels like biomass, the exact chemical formula of which is not clearly known. The Gibbs free energy, G_{total} for the gasification product comprising N species ($i = 1 \ldots N$) is given by

$$G_{total} = \sum_{i=1}^{N} n_i \Delta G_{f,i}^{0} + \sum_{i=1}^{N} n_i RT \ln\left(\frac{n_i}{\sum n_i}\right) \tag{3.9}$$

where $G_{f,i}^{0}$ is the Gibbs free energy of formation of species *i* at standard pressure of 1 bar. Equation (3.9) is to be solved for unknown values of n_i to minimize G_{total}, bearing in mind that it is subject to the overall mass balance of individual elements. For example, irrespective of the reaction path, type, or chemical formula of the fuel, the amount of carbon determined by ultimate analysis must be equal to the sum total of all carbon in the gas mixture produced. Thus, for each *j*th element we can write

$$\sum_{i=1}^{N} a_{i,j} n_i = A_j \tag{3.10}$$

where $a_{i,j}$ is the number of atoms of the *j*th element in the *i*th species, and A_j is the total number of atoms of element *j* entering the reactor. The value of n_i should be found such that G_{total} will be minimum. We can use the Lagrange multiplier methods to solve these equations. The Lagrange function (L) is defined as

$$L = G_{total} - \sum_{J=1}^{K} \lambda_j \left(\sum_{i=1}^{N} a_{ij} n_i - A_j \right) kJ / mol \tag{3.11}$$

where λ is the Lagrangian multiplier for the *j*th element. To find the extreme point, we divide Eq. (3.11) by *RT* and take the derivative,

$$\left(\frac{\partial L}{\partial n_i}\right) = 0 \tag{3.12}$$

Substituting the value of G_{total} from Eq. (3.11) in Eq. (3.13), and then taking its partial derivative, the final equation is of the form given by

$$\left(\frac{\partial L}{\partial n_i}\right) = 0 \tag{3.13}$$

3.5 Supercritical water gasification process

Water above its critical temperature (374.29 ^{o}C) and pressure (22.089 MPa) is called supercritical (Figure 3.5). Water or steam below this pressure and temperature is called subcritical. The term water in a conventional sense may not be applicable to SCW except for its chemical formula, H_2O, because above the critical temperature SCW is neither water nor steam. It has a water like density but a steam like diffusivity. Table 3.4 compares the properties of subcritical water and steam with those of SCW, indicating that SCW's properties are intermediate between the liquid and gaseous states of water in subcritical pressure; descriptions of each follow the table. Figure 3.5 shows that the higher the temperature, the higher the pressure required for water to be in its liquid phase. Above a critical point the line separating the two phases disappears, suggesting that the division between the liquid and vapor phases disappears. Temperature and pressure at this point are known as critical temperature, and critical pressure, above which water attains supercritical state and hence is called supercritical water (SCW).

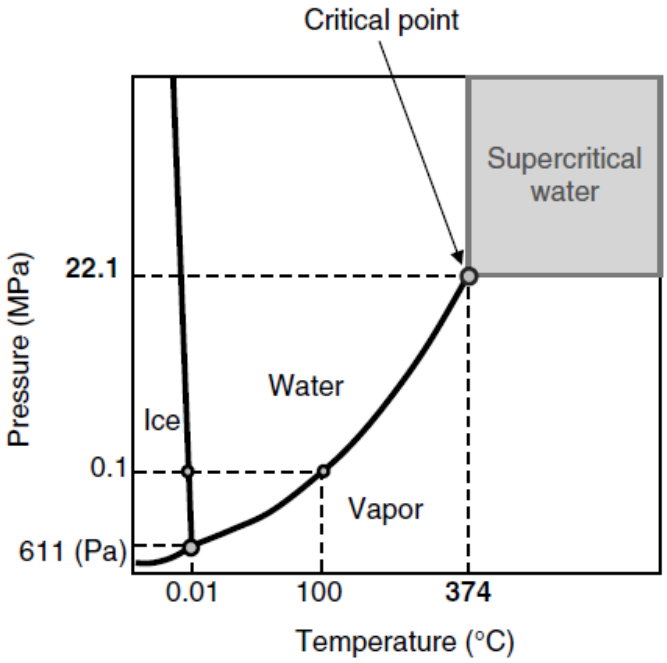

Figure 3.5 Phase diagram of water showing the supercritical region

Subcritical water ($T < T_{sat}$; $P < P_c$) When the pressure is below its critical value, Pc, and the temperature is below its critical value, T_c, the fluid is called subcritical. If the temperature is below its saturation value, the fluid is known as subcritical water, as shown in the lower left block of Figure 3.5.

Subcritical water ($T < T_{sat}$; $P < P_c$) When the pressure is below its critical value, Pc, and the temperature is below its critical value, T_c, the fluid is called subcritical. If the temperature is below its saturation value, the fluid is known as subcritical water, as shown in the lower left block of Figure 3.5.

The critical point marks a significant change in the thermophysical properties of water. There is a sharp rise in the specific heat near the critical temperature

Table 3.4 Properties of supercritical and subcritical water

Property	**Subcritical Water**	**Supercritical Water**	**Supercritical CO_2**	**Subcritical Steam**
Temperture (^oC)	25	400	55	150
Pressure (MPa)	0.1	30	28	0.1
Density, kg/m^3	997	358	835	0.52
Dynamic viscosity,μ (kg/m.s)	890.8×10^{-6}	43.83×10^{-6}	0.702×10^{-6}	14.19×10^{-6}
Diffusivity of small particles (m^2/s)	$\sim 1.0 \times 10^{-9}$	$\sim 1.0 \times 10^{-8}$		$\sim 1.0 \times 10^{-5}$
Dielectric comstant	78.46	5.91		1.0
Thermal conductivity (w/m.k)	607×10^{-3}	330×10^{-3}		28.8×10^{-3}
Prandtl number	6.13	3.33		0.97

followed by a similar drop. The thermal conductivity of water drops from 0.330 W/m.K at 400 ^oC to 0.176 W/m.K at 425 ^oC. The drop in molecular viscosity is also significant, although the viscosity starts rising with temperature above the critical

value. Above this critical point, water experiences a dramatic change in its solvent nature primarily because of its loss of hydrogen bonding. The dielectric constant of the water drops from a value of about 80 in the ambient condition to about 10 at the critical point. This changes the water from a highly polar solvent at an ambient condition to a nonpolar solvent, like benzene, in a supercritical condition.

3.5.1 Properties of supercritical water

The critical point marks a significant change in the thermophysical properties of water. There is a sharp rise in the specific heat near the critical temperature followed by a similar drop. The thermal conductivity of water drops from 0.330 W/m.K at 400 ^{o}C to 0.176 W/m.K at 425 ^{o}C. The drop in molecular viscosity is also significant, although the viscosity starts rising with temperature above the critical value. Above this critical point, water experiences a dramatic change in its solvent nature primarily because of its loss of hydrogen bonding. The dielectric constant of the water drops from a value of about 80 in the ambient condition to about 10 at the critical point. This changes the water from a highly polar solvent at an ambient condition to a nonpolar solvent, like benzene, in a supercritical condition.

The change in density in supercritical water across its pseudo-critical temperature is much more modest, however. For example, at 25 MPa it can drop from about 1000 to 200 kg/m^3 while the water moves from a liquid like to a vapor like state. At subcritical pressure, however, there is an order of magnitude drop in density when the water goes past its saturation temperature. For example, at 0.1 MPa or 1 atm of pressure, the density reduces from 1000 to 0.52 kg/m^3 as the temperature increases from 25 to 150 ^{o}C

The most important feature of supercritical water is that we can “manipulate” and control its properties around its critical point simply by adjusting the temperature and pressure. Supercritical water possesses a number of special properties that distinguish it from ordinary water. Some of those properties relevant to gasification are as follows:

- The solvent property of water can be changed very strongly near or above its critical point as a function of temperature and pressure.
- Subcritical water is polar, but supercritical water is nonpolar because of its low dielectric constant. This makes it a good solvent for nonpolar organic compounds but a poor one for strongly polar inorganic salts. SCW can be a solvent for gases, lignin, and carbohydrates, which show low solubility in ordinary (subcritical) water. Good miscibility of intermediate solid organic compounds as well as gaseous products in liquid SCW allows single-phase chemical reactions during gasification, removing the interphase barrier of mass transfer.
- SCW has a high density compared to subcritical steam at the same temperature. This feature favors the forward reaction between cellulose and water to produce hydrogen.
- Near its critical point, water has higher ion products ([H+][OH−]~10–11 $(mol/l)^2$) than it has in its subcritical state at ambient conditions (~10−14 $(mol/l)^2$).Owing to this high [H+] and [OH–] ion, the water can be an effective medium for acid- or base-catalyzed organic reactions (Serani et al., 2008). Above the critical point, however, the ion product drops rapidly (~10−24 $(mol/l)^2$ at 24 MPa), and the water becomes a poor medium for ionic reactions.
- Most ionic substances, such as inorganic salts, are soluble in subcritical water but nearly insoluble under typical conditions of SCW gasifiers. As the temperature rises past the critical point, the density as well as the ionic product decreases. Thus, highly soluble common salt (NaCl) becomes insoluble at higher temperatures above the critical point. This tunable solubility property of SCW makes it relatively easy to separate the salts as well as the gases from the product mixture in an SCW gasifier.
- Gases, such as oxygen and carbon dioxide, are highly miscible in SCW, allowing homogeneous reactions with organic molecules either for oxidation or for gasification. This feature makes SCW an ideal medium for destruction of hazardous chemical waste through SCWO.
- SCW possesses excellent transport properties. Its density is lower than that of subcritical water but much higher than that of subcritical steam. This, along

with other properties like low viscosity, low surface tension (surface tension of water reduces from 7.2 x 10^{-2} at 25 ^{o}C to 0.07 at 373 ^{o}C), and high diffusivity greatly contribute to the SCW's good transport property, which allows it to easily enter the pores of biomass for effective and fast reactions.

- Reduced hydrogen bonding is another important feature of SCW. The high temperature and pressure break the hydrogen-bonded network of water molecules.

3.5.2 Advantages of SCW gasification

Thermal conversion processes are relatively fast, taking minutes or seconds to complete, while biological processes, which rely on enzymatic reactions, take much longer, on the order of hours or even days. Thus, for commercial use, thermochemical conversion is preferred.

Gasification may be carried out in air, oxygen, subcritical steam, or water near or above its critical point. This chapter concerns hydrothermal gasification of biomass above or very close to the water's critical point to produce energy and/or chemicals.

Conventional thermal gasification faces major problems from the formation of undesired tar and char. The tar can condense on downstream equipment, causing serious operational problems, or it may polymerize to a more complex structure, which is undesirable for hydrogen production. Char residues contribute to energy loss and operational difficulties. Furthermore, very wet biomass can be a major challenge to conventional thermal gasification because it is difficult to economically convert if it contains more than 70% moisture. The energy used in evaporating fuel moisture (2257 kJ/kg), which effectively remains unrecovered, consumes a large part of the energy in the product gas.

Gasification in supercritical water (SCWG) can largely overcome these shortcomings, especially for very wet biomass or organic waste. For example, the efficiency of thermal gasification of a biomass containing 80% water in conventional steam reforming is only 10%, while that of hydrothermal gasification in SCW can be

as high as 70%. Gasification in near or supercritical water therefore offers the following benefits:

- Tar production is low. The tar precursors, such as phenol molecules, are completely soluble in SCW and so can be efficiently reformed in SCW gasification.
- SCWG achieves higher thermal efficiency for very wet biomass.
- SCWG can produce in one step a hydrogen-rich gas with low CO, obviating the need for an additional shift reactor downstream.
- Hydrogen is produced at high pressure, making it ready for downstream commercial use.
- Carbon dioxide can be easily separated because of its much higher solubility in high-pressure water.
- Char formation is low in SCWG.
- Heteroatoms like S, N, and halogens leave the process with aqueous effluent, avoiding expensive gas cleaning. Inorganic impurities, being insoluble in SCW, are also removed easily.
- The product gas of SCWG automatically separates from the liquid containing tarry materials and char if any.

3.5.3 Scheme of an SCWG plant

A typical SCWG plant includes the following key components:

- Feedstock pumping system
- Feed preheater
- Gasifier/reactor
- Heat-recovery (product-cooling) exchanger
- Gas–liquid separator
- Optional product-upgrading equipment

The feed preheating system is very elaborate and accounts for the majority (~60%) of the capital investment in an SCW gasification plant. Figure 3.6 describes the SCWG

process using the example of an SCWG plant for gasifying sewage sludge. Biomass is made into a slurry for feeding. It is then pumped to the required supercritical pressure. Alternatively, water may be pressurized separately and the biomass fed into it. In any case, the feedstock needs to be heated to the designed inlet temperature for the gasifier, which must be above the critical temperature and well above the designed gasification temperature because the enthalpy of the water provides the energy required for the endothermic gasification reactions. This temperature is a critical design parameter.

The sensible heat of the product of gasification may be partially recovered in a waste heat-recovery exchanger and used for partial preheating of the feed (Figure 3.6). For complete preheating, additional heat may be obtained from one of the following:

- Externally fired heater (Figure 3.6)
- Burning of a part of the fuel gas produced to supplement the external fuel
- Controlled burning of unconverted char in the reactor system

After gasification, the product is first cooled in the waste heat-recovery unit. Thereafter, it cools to room temperature in a separate heat exchanger by giving off heat to an external coolant.

The next step involves separation of the reaction products. The solubility of hydrogen and methane in water at low temperature but high pressure is considerably low, so they are separated from the water after cooling while the carbon dioxide, because of its high solubility in water, remains in the liquid phase. For complete separation of CO_2, the gas may be scrubbed with additional water. The gaseous hydrogen is separated from the methane in a pressure swing adsorber. The CO_2-rich liquid is depressurized to the atmospheric pressure, separating the carbon dioxide from the water and unconverted salts.

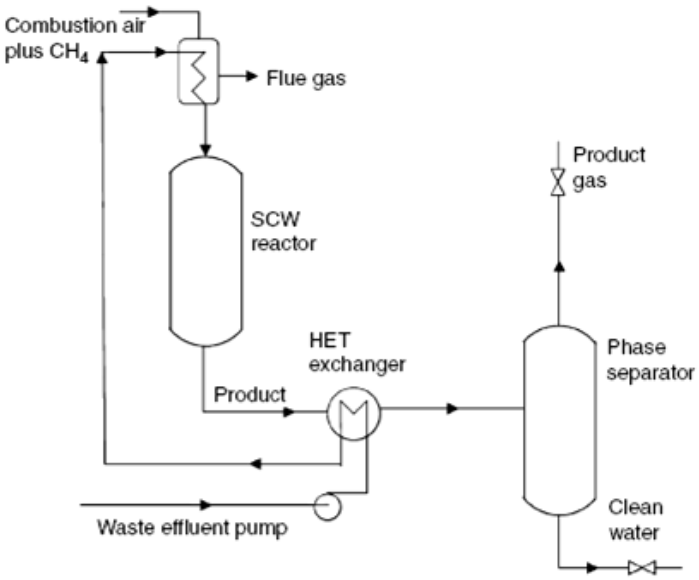

Figure 3.6 Schematic of a pilot plant for supercritical water gasification of biomass

3.6 Response surface methodology (RSM) based on central composite design (CCD)

A response surface methodology (RSM) is a collection of statistical and mathematical methods that are useful for modeling and analyzing engineering problems. In this technique, the main objective is to optimize the response surface that is influenced by various process parameters. RSM also quantifies the relationship between the controllable input parameters and the obtained response surfaces (Kwak, 2005). Box et al., 1951 lay the basic foundations for response surface methodology, which an integration of experimental design, regression, and optimization theory. RSM is widely used to explore and to optimize response surfaces in industrial experiments. For many industrial experiments, the response can be obtained immediately. The result from small exploratory experiments can then be used as a guide to more complicated or large follow-up experiments. In RSM, it is common to begin with a screening experiment to identify important factor or variables. Follow-up experiments seek to improve the performance of the response.

The design procedure for RSM is as follows (Aslan, 2008):

(i) Performing a series of experiments for adequate and reliable measurement of the response of interest.

(ii) Developing a mathematical model of the second-order response surface with the best fit.

(iii) Determining the optimal set of experimental parameters that produce a maximum or minimum value of response.

(iv) Representing the direct and interactive effects of process parameters through two and three-dimensional (3-D) plots.

If all variables are assumed to be measureable, the response surface can be expressed as follows:

$$y = f(x_1, x_2, x_3, \ldots, x_k) \tag{3.14}$$

Where y is the predicted response variable, and x_i the variables of action called factor.

The goal is to optimize the response variable (y). An important assumption is that the independent variables are continuous and controllable by experiments with negligible errors. The task then is to find a suitable approximation for the true functional between independent variables and the response surface. (Aslan, 2008)

The different orders of models lead to different response surface designs with different properties. Among first order designs, full factorial and fractional factorial designs are used extensively in preliminary experiments to identify potentially important factors. Central Composite Design (CCD) is a design commonly used for building a second-order (quadratic) model. CCD contains an imbedded two-level factorial design and axial (or star) points. If there are k factors, the axial number is 2^k. If the distance from the center of the design space to a factorial point is ±1 unit for each factor, the distance from the center of the design space to the axial point is ±α with $\alpha > 1$. The choice of α is crucial to the performance of the design. The value of α depends on the number of experimental run in the factorial portion of the central composite design, which expressed as follows:

$$\alpha = [number\ of\ factorial\ runs]^{1/4} \quad (3.15)$$

If the factorial is a full factor

$$\alpha = (2^k)^{1/4} \quad (3.16)$$

Once the desired ranges of values of the variables are defined, they are coded to lie at ±1 for the factorial points, 0 for the center points and ±α for the axial points. The codes are calculated as functions of the range of interest of each factor as shown in Table 3.5. When the response data are obtained from the test work, a regression analysis is carried out to determine the coefficients of the response model.

The total number of experiment trials (n_e) depends on the number of factors and the number of center points (n_c). The total number of experimental trials is expressed in Eq. (3.17). The reasonable number of the center points is usually three to five.

$$n_e = 2^k + 2k + n_c \quad (3.17)$$

The polynomial model for the yield fatty methyl ester was expressed as follows:

$$Y_{yield} = \lambda_o + \sum \lambda_i X_i + \sum \lambda_i X_{ii}^2 + \sum \lambda_{ij} X_i X_j \quad (3.18)$$

Where Y_{yield} is the predicted response variable, λ_0, λ_i, λ_{ii}, λ_{ij} are constant regression coefficients of the model, and X_i, X_j represent the independent variables (the reaction conditions) in the form of code values. The accuracy and general ability of the above polynomial model could be evaluated by the coefficient of determination R^2.

3.6.1 Analysis of variance

Analysis of variance (ANOVA) is the statistical analysis used to check the significance of the equation with the experimental data. This analysis included the Fisher's *F*-test (overall model significance), its associated probability *p(F)*, correlation coefficient *R*, determination coefficient R^2 which measures the goodness of fit of regression model. It's also includes the Student's *t*-value for the estimated

coefficient and associated probabilities *p(t)*. For each variable, the quadratic models were represented as contour plots (2D). The optimal combination was determined from contour plot. The statistical software was used to generate design, regression analysis, and plot abstention.

Table 3.5 Relationship between coded and actual values of a variable (Box et al., 1951)

Code	Actual value of variable
$-\alpha$	x_{min}
-1	$[x_{max} + x_{min})/2] - [(x_{max} - x_{min})/2\alpha]$
0	$(x_{max} + x_{min})/2$
+1	$[x_{max} + x_{min})/2] + [(x_{max} - x_{min})/2\alpha]$
$+\alpha$	x_{max}

x_{max} and x_{min} = maximum and minimum values of x; k = number of variable

CHAPTER IV

CONVENTIONAL GASIFICATION TECHNOLOGY FOR SYNGAS PRODUCTION

In this chapter, the simulation model of a conventional gasification (fluidized-bed) process is presented. In Section 4.1, a general description of a fluidized-bed process is given. Section 4.2 explains a simulation model of the conventional gasification process using a flowsheet simulator. The operation of the conventional gasification process at energy self–sufficient condition is explained in Section 4.3. Section 4.4 presents the simulation results of the sensitivity analysis for the conventional gasification process at energy self-sufficient condition.

4.1 Introduction

General gasifier configurations are moving/fixed-bed, fluidized-bed, and entrained-flow. In this work, a fluidized-bed gasifier was chosen for conventional gasification process because of its near commercial type. This technology is demonstrated for biomass gasification, has potential for scale-up and high fuel flexibility. In fluidized-bed (bubbling, circulating and twin-bed) gasifier, the gasifying agent is blown through a bed of solid particles at a sufficient velocity to keep the particles in a state of suspension while fuel particles are introduced at the bottom of the reactor, are very quickly mixed with the bed material, and almost instantaneously are heated up to the bed temperature. As a result of this treatment, the fuel is pyrolysed very fast, resulting in a component mix with a relatively large amount of gaseous materials. Further gasification and tar-conversion reactions occur in the gas phase. Twin-bed gasification uses two fluidized-bed reactors. The biomass enters the first reactor, where it is gasified with steam, and the remaining char is transported to the second reactor, where it is burnt with air to produce heat. The heat is transported

to the gasification reactor by the bed material, normally sand. The flue gas and the product gas have two separate exits. This technology is made of coarse solids, called bed materials, which are kept in a semi-suspended condition (fluidized state) by the passage of the gasifying medium through them at the suitable velocities. The brilliant gas-solid mixing and the large thermal inertia of the bed make this type of gasifier relatively insensitive to the fuel's quality (Basu, 2010). Along with this, the temperature regularity significantly reduces the risk of fuel agglomeration. The fluidized-bed design has proved to be especially useful for gasification of biomass. Its tar production lies between that for updraft (~50 g/nm^3) and downdraft gasifiers (~1 g/nm^3), with an average value of around 10 g/nm^3 (Milne et al., 1998).

4.2 Simulation model of water hyacinth and rice straw conventional gasification process

Process modeling is an influential instrument which permits the mathematical demonstration of a process and the complete study of its features and configuration. For the model improvement of the present study, the ASPEN Plus process model simulator was used. Aspen Plus is a powerful and adaptable tool for a wide variety of engineering tasks. It can be used in approximately every feature of process engineering from preliminary design to optimization. A benefit of Aspen Plus is that it allows a user to create a process model starting at any step. The Aspen Plus includes various modules than can be combined to give a full depiction of the fluidized-bed gasifier's behavior. The following assumptions were considered for the simulation of the fluidized bed gasification process:

- The process is at steady state and isothermal conditions.
- Biomass devolatilization takes place immediately and the volatile products consist of H_2, CO, CO_2, CH_4, and H_2O.
- All the gases are uniformly dispersed within the reactor.
- Fluid hydrodynamic within the fluidized-bed reactor has not been taken into consideration.
- Char gasification reactions are assumed to be at chemical equilibrium.

- Char contains only carbon and ash.
- Reactions of sulfur and nitrogen have not been taken into consideration.

Figure 4.1 and 4.2 describes the ASPEN Plus simulation model and its calculation procedure used. Biomass feedstock are water hyacinth and rice straw are specified as a non-conventional. Data used to describe the feedstock, which is based on ultimate and proximate analyses is given in Table 3.1 and 3.2. The fluidized bed gasification process is represented by a series of blocks corresponding to the presence of various sub-processes, namely the feed decomposition, biomass drying, the pyrolysis/devolatilization step and the char gasification.

The biomass drying step concerns the removal of moisture from the sample by vaporization owing to the increased temperature. At about 150 ^{o}C achieving the reduction of moisture to 5 wt% of the original sample. The stoichiometric reactor (RSTOIC) has been used to model the drying of the biomass where as the drying operation is controlled by writing the FORTRAN statement in the calculator block. After being stripped from the moisture, the dry biomass requests to be decomposed to its elemental constituents that is carbon, hydrogen, oxygen, nitrogen, and ash by specifying the yield distribution according to the biomass ultimate analysis. The yield distribution of biomass into its components has been specified by FORTRAN statement in calculator block. CSTR equivalent block was used for the modeling of the formation of volatiles by considering that they follow chemical equilibrium carbon partly constitutes the gas phase, which takes part in devolatilization. It is considered that the assumption for perfect gas mixing which is ensured by the continuous motion of the bed matches the principles of the CSTR reactor. The char gasification is simulated by considering a separate RGIBBS reactor block including the char gasification reactions, while in this way the hydrodynamic parameters are not included into consideration. The restricted equilibrium method was used to calibrate it against experimental data. This was achieved by specifying the temperature approach for the gasification reactions.

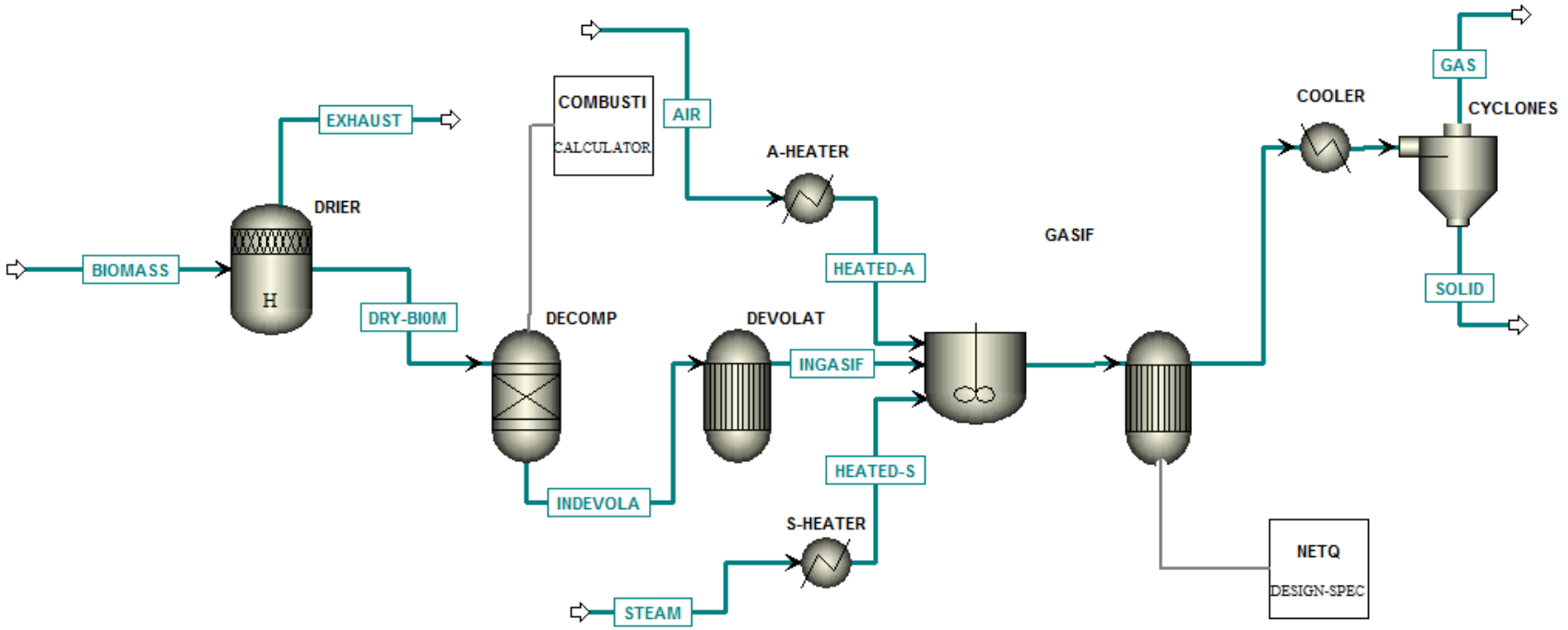

Figure 4.1 Simulation model of gasifier

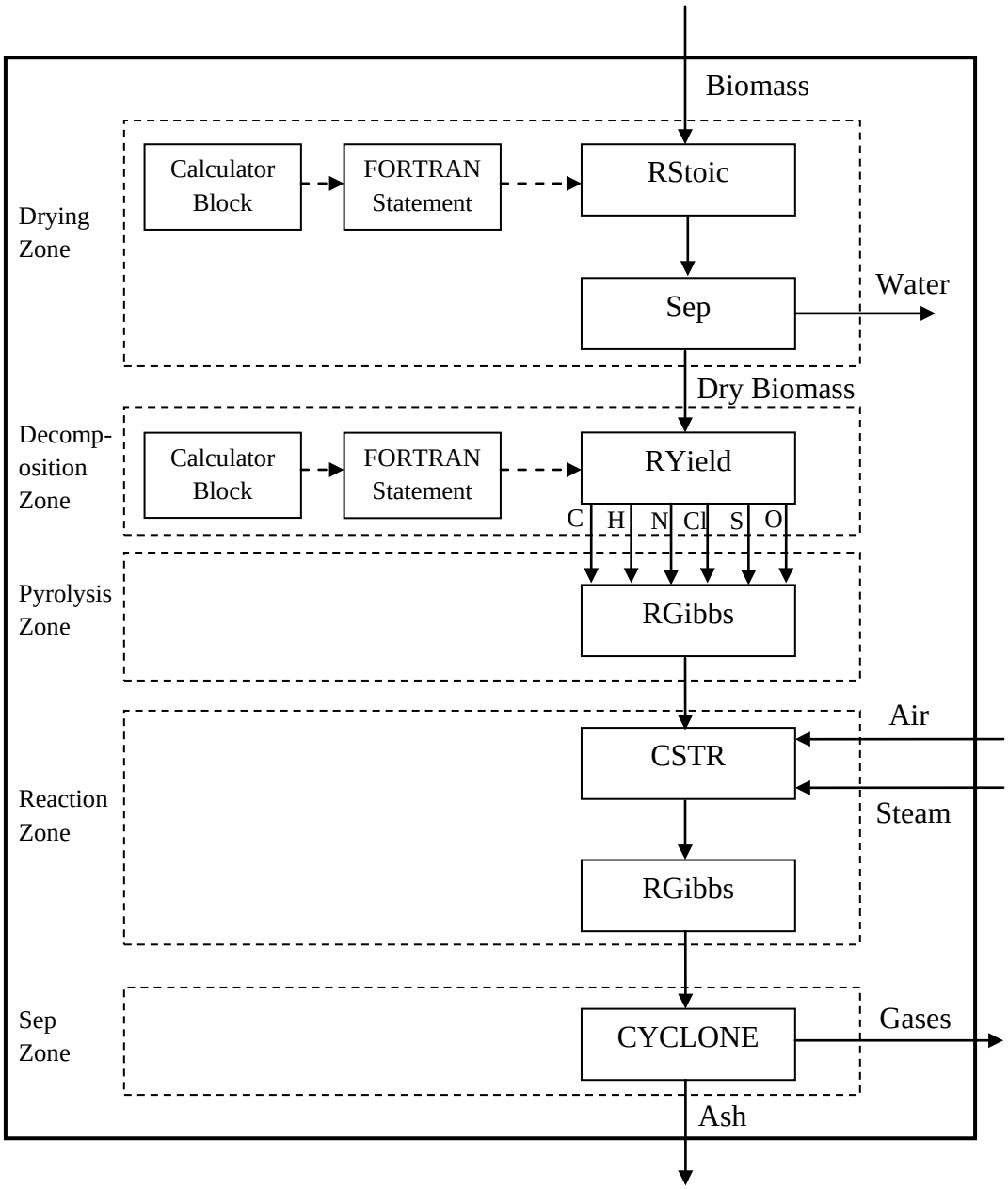

Figure 4.2 Simulation calculation procedure

In separation step, the solid impurities (char or unreacted biomass, ash) are separated with the use of a cyclone separator while the sulfur and nitrogen compounds are simply cast away via a component separator (CYCLONE). The data used for performing the simulations using the process flow sheet are listed in table 4.1

4.3 Conventional gasification at energy self-sufficient condition

This part describes to develop energy efficiency so as to minimize the external heat demand, leading to a energy self-sufficient system. This system is particularly appropriate for efficiency of the process. Figure 4.2 demonstrates the system of energy balance in the fluidized bed gasifier for syngas production.

$$Q_{gasifier(net)} = Q_{Decomposition\,zone} + Q_{Pyrolysis\,zone} + Q_{Reaction\,zone} \quad (4.1)$$

Equation 4.1 shows the energy balance equation for fluidized bed gasifier. Energy self-sufficient condition can be achieved by appropriate adjustment of operating parameters including steam to biomass ratio, equivalence ratio and the gasifier temperature. The energy self- sufficient condition can be found by setting $Q_{gasifier(net)}$ equal to zero.

Table 4.1 Model inputs used for the simulation

Gasifier feed capacity (kg/hr)	10
Steam to biomass ratio (water hyacinth)	0.1 - 0.5
Steam to biomass ratio (rice straw)	1 - 3
Drying temperature (^oC)	150
Pyrolysis temperature (^oC)	150 - 700
Gasification temperature (^oC)	400 - 1000
Gas cooling temperature (^oC)	25
Steam temperature (^oC)	200
Air temperature (^oC)	350
Pressure (bar)	1

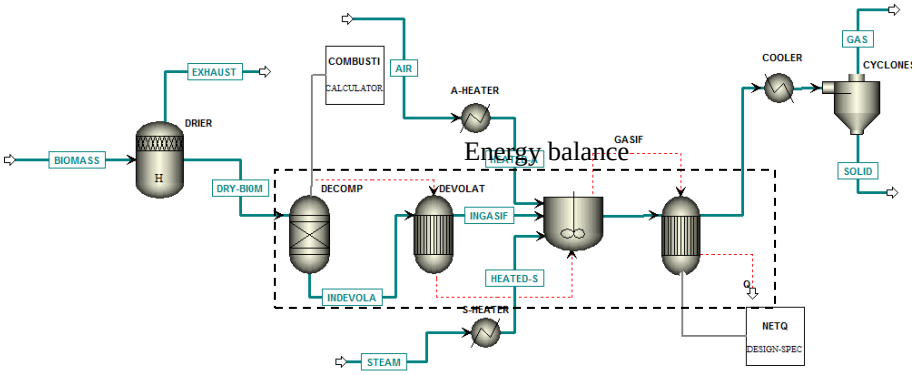

Figure 4.3 The system of energy balance in the fluidized bed gasifier

The results obtained from the calculations in this work represent the maximum achievable hydrogen production based on the energy self-sufficient condition. In a real system, the values will be lower due to deviation from the thermodynamic equilibrium reaction and the presence of heat loss.

Figure 4.4 shows the effect of equivalence ratio (ER) on the net heat energies of water hyacinth and rice straw gasifiers at steam to biomass ratio (0.1, 1) and gasifier temperature 700 ^{o}C. When increasing ER from 0 to 0.1 (water hyacinth) and 0 to 1 (rice straw), the net heat energy gradually decreases. The decrease of the net heat energy is mainly controlled by the strong oxidation reaction particularly at high amount of oxygen. At ER = 0.04 (water hyacinth) and ER = 0.39 (rice straw), it is the minimum heat energy requirement to offer energy self-sufficient condition at gasifier temperature 700 ^{o}C and steam to biomass ratio (0.1, 1).

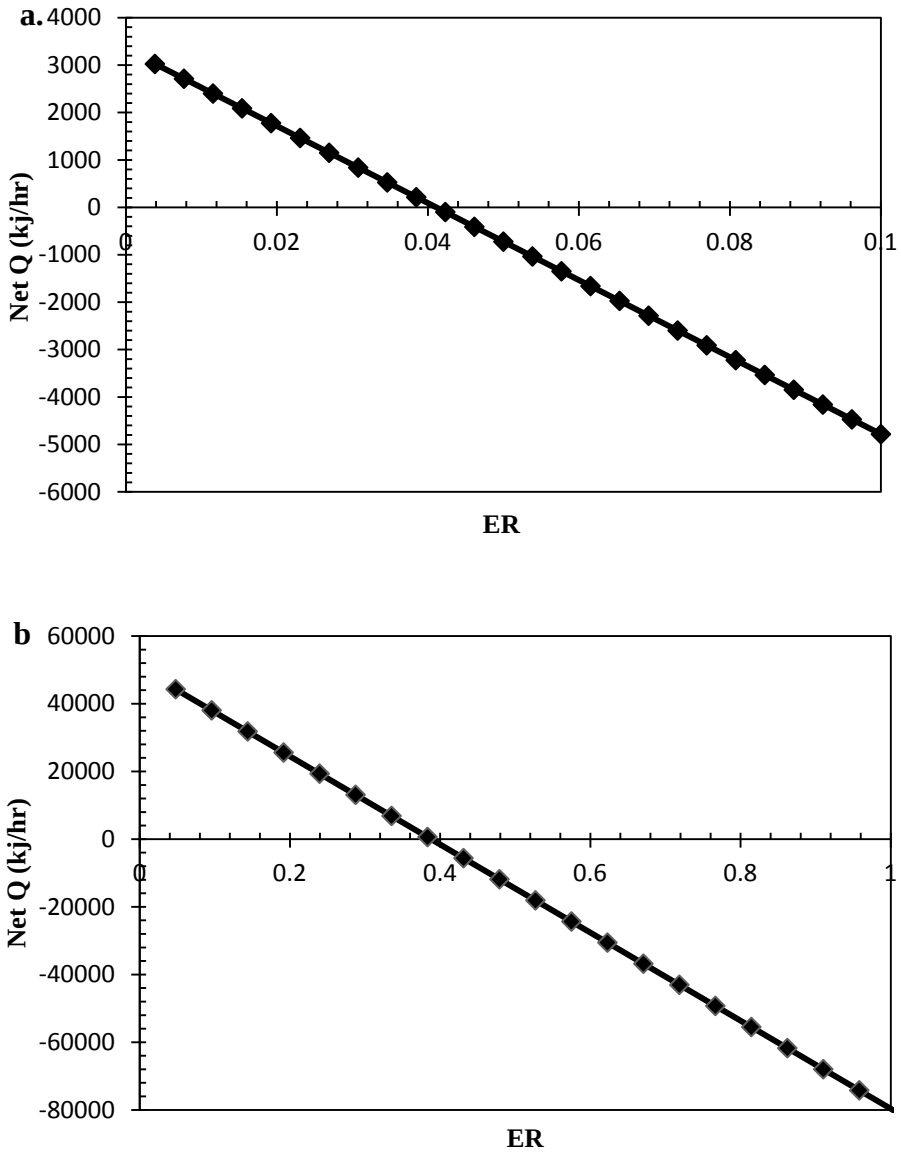

Figure 4.4 Effect of steam to biomass ratio and equivalence ratio on the net heat energies: (a) for water hyacinth and (b) for rice straw

Figure 4.5 shows the equivalence ratio (ER) for (a) water hyacinth and (b) rice straw, which is required for achieving the energy self-sufficient condition, at different gasifier temperature and at different steam to biomass ratio (SBR). Oxygen used is calculated to always achieve setting $Q_{gasifier(net)}$ at zero. From the simulation results, there is no oxygen at the gasifier outlet for all simulations indicating that all oxygen reacts with biomass through oxidation.

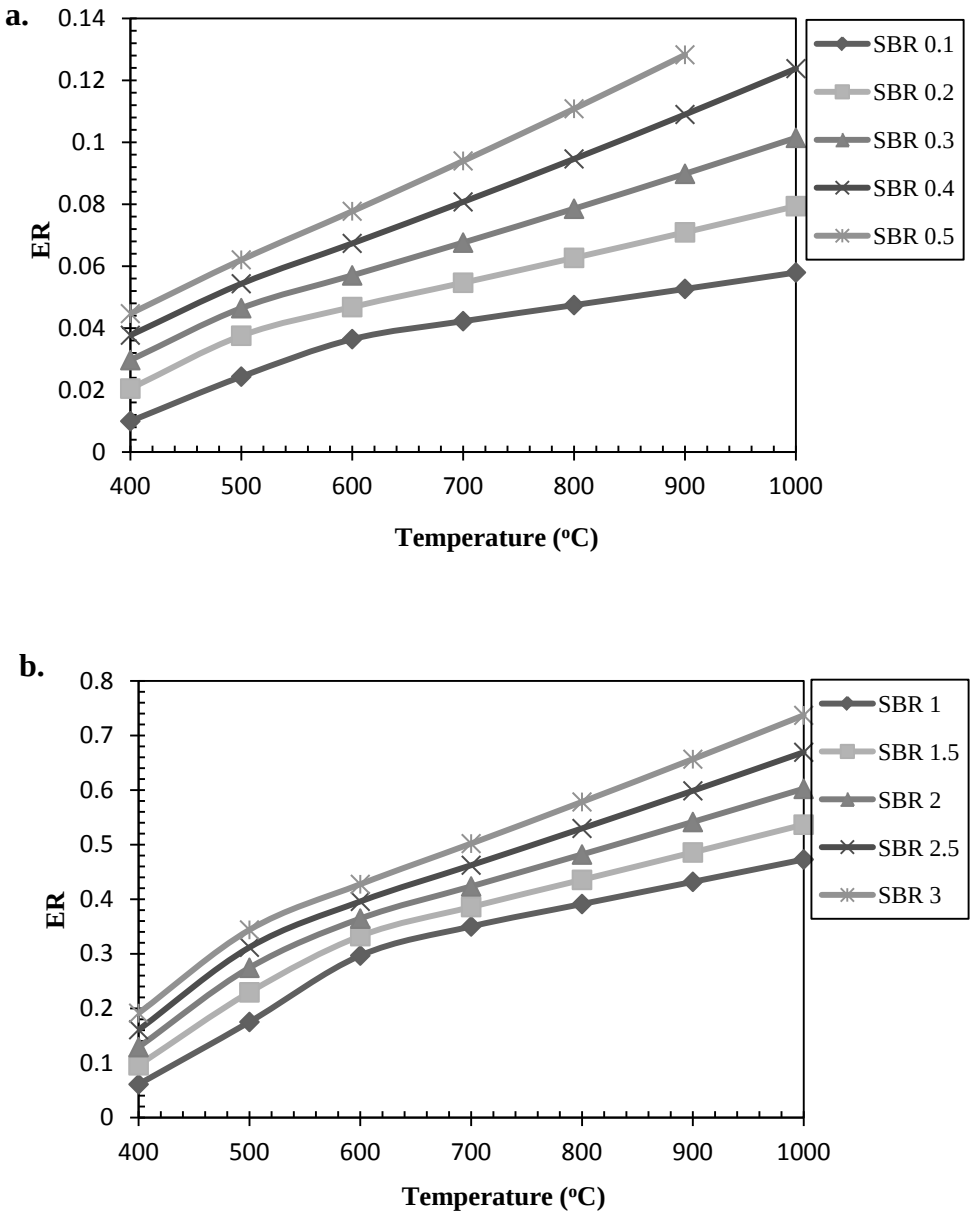

Figure 4.5 Equivalence ratio (ER) at different temperatures and at different steam to biomass ratio (SBR): (a) for water hyacinth and (b) for rice straw

4.4 Results and discussion

In this section, the effect of key process parameters (i.e., temperature and steam to biomass ratio) on the composition of the product gas is analyzed. The product gas composition is required for the calculation of the efficiency of the process that will be discussed in Section 4.3.3

4.4.1 Model validation

The simulation model has been validated using experimental data from fluidized bed gasification of olive kernel gasification the Aristotle University pilot reactor published by Damartzis. Table relates the experimental results to the model predictions using the input data presented at gasification temperature 705 ^{o}C and equivalent ratio 0.2. The model predictions are in good agreement with the experimental data.

Table 4.2 Experimental results versus model predictions

Gas composition (%v/v)	Experimental	Model
H_2	26	32
CO	15	16
CO_2	20	16
CH_4	4	6

4.4.2 Sensitivity analysis

4.4.2.1 Effect of gasifier temperature

The gasifier temperature is a significant parameter that influences the syngas yield of conventional gasification process. The gasifier temperature study was varied from 400 ^{o}C to 1000 ^{o}C. Owing to the self-sufficient condition specified for all simulations, gasifier temperatures considered are also adiabatic gasifier, at which the external heat flow equals to zero, related a definite oxygen input. The effect of gasifier temperature on the composition of the product gas for two biomass is shown in Figure 4.5 - 4.8 (a,b). The gas composition of biomass gasification in the gasifier is result of the combination of a series of complex and competing reaction, as given in Table 3.5. The major water gas reaction, boudouard reaction and steam reforming of biomass gasification in the gasifier were an intensive endothermic process, while the CO shift reaction is an exothermic reaction. Higher temperatures support the reactants in exothermic reaction and support the products in endothermic reaction.

Consequently, endothermic reactions were strengthened with an increase in the gasifier temperature. Figure 4.6 shows that at very low temperature (400^{o}C) the carbon present in the biomass is not utilized completely but as the temperature increase from 400 to 600 ^{o}C carbon is converted into hydrogen and carbon monoxide in conformance with water-gas reaction. At about 600 ^{o}C , the hydrogen yield reaches a maximum value of about 0.005 (kg/kg biomass) for water hyacinth and 0.068 (kg/kg biomass) for rice straw. At still 600 – 1000 ^{o}C, the hydrogen yield starts reducing, since more energy is needed and so more oxygen to oxidixe fuel. Figure 4.7 proposes that high temperature increases the production of carbon monoxide in conformance with boudouard reaction. Figure 4.8 shows that high temperature increases the production of carbon dioxide because at higher temperature more energy is needed and so more oxygen to oxidixe more fuel. According to methanation reaction the methane yield in syngas decreases and that of hydrogen increases with the increases in temperature. Rice straw has higher all composition yields than water hyacinth but general behavior is same. At about range 500 - 600 ^{o}C, the hydrogen yield has a maximum value of about 0.068 (kg/kg biomass) for rice straw and 0.005 (kg/kg biomass) for water hyacinth.

4.4.2.2 Effect of steam

Steam to biomass ratio (denoted by SBR) in the feed of 0.1, 0.2, 0.3, 0.4, 0.5 for water hyacinth and 1, 2, 3, 4, 5 for rice straw were simulated at temperatures of 400 - 1000 ^{o}C, at energy self-sufficient condition. Results are also represented in Figure 4.6 - 4.9 (a,b) for water hyacinth and rice straw respectively. Steam to biomass ratio, like gasifier temperature has a strong influence on both product gas composition and energy input. According to water gas reaction steam increase the mole fraction of hydrogen and carbon monoxide in the syngas. According to carbon monoxide shift reaction the amount hydrogen increases by steam injection and that of carbon monoxide decreases. The same result is predicted by model. As rice straw has higher production of combustible gases thus it may be concluded that steam injection has a more pronounced effect on it. The overall behavior is same for all the two biomass

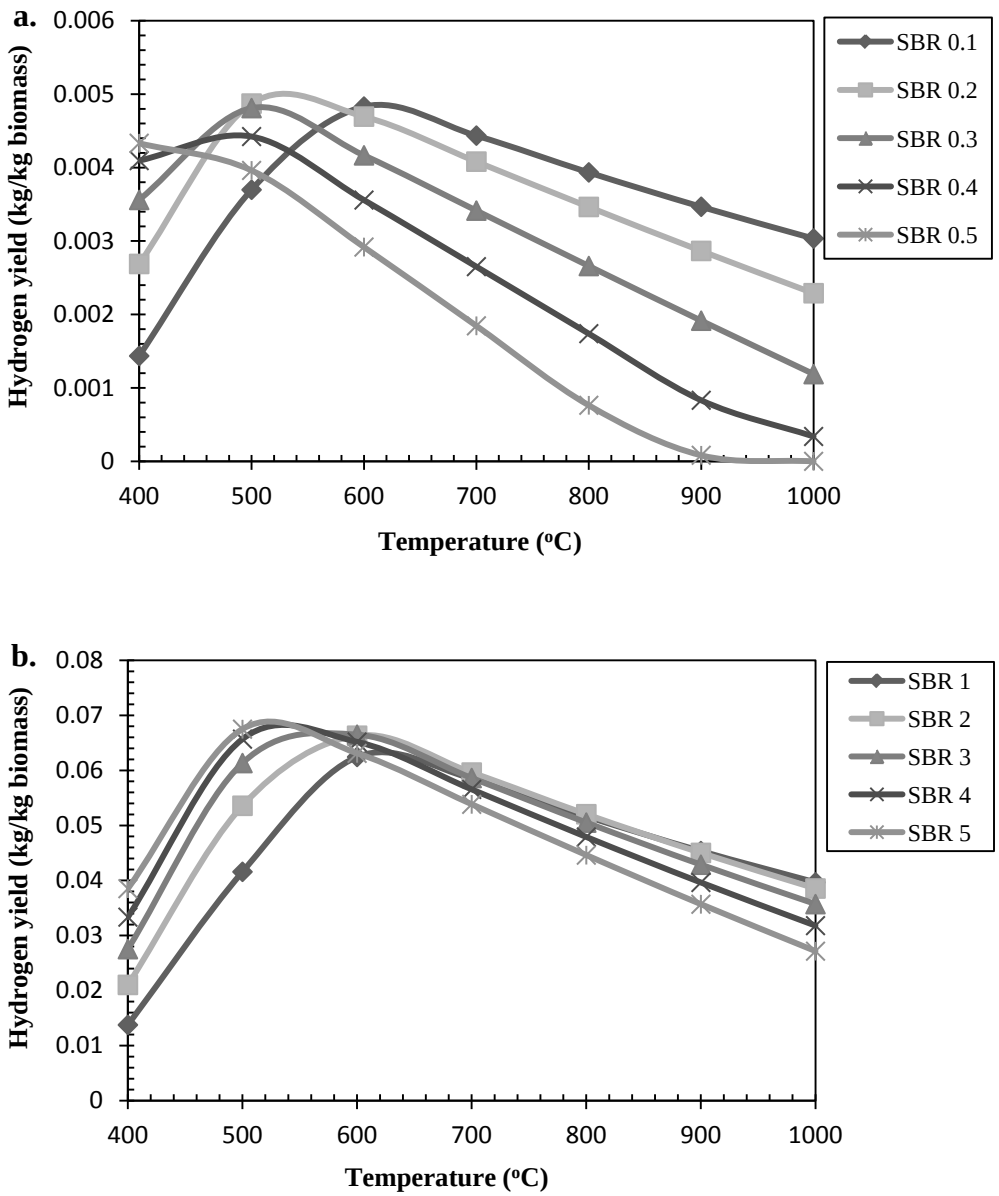

Figure 4.6 Hydrogen yield (kg/kg biomass) at different temperatures and at different steam to biomass ratio (SBR): (a) for water hyacinth and (b) for rice straw

i.e., hydrogen yield and carbon dioxide yield increases with steam injection and that of carbon monoxide decreases.

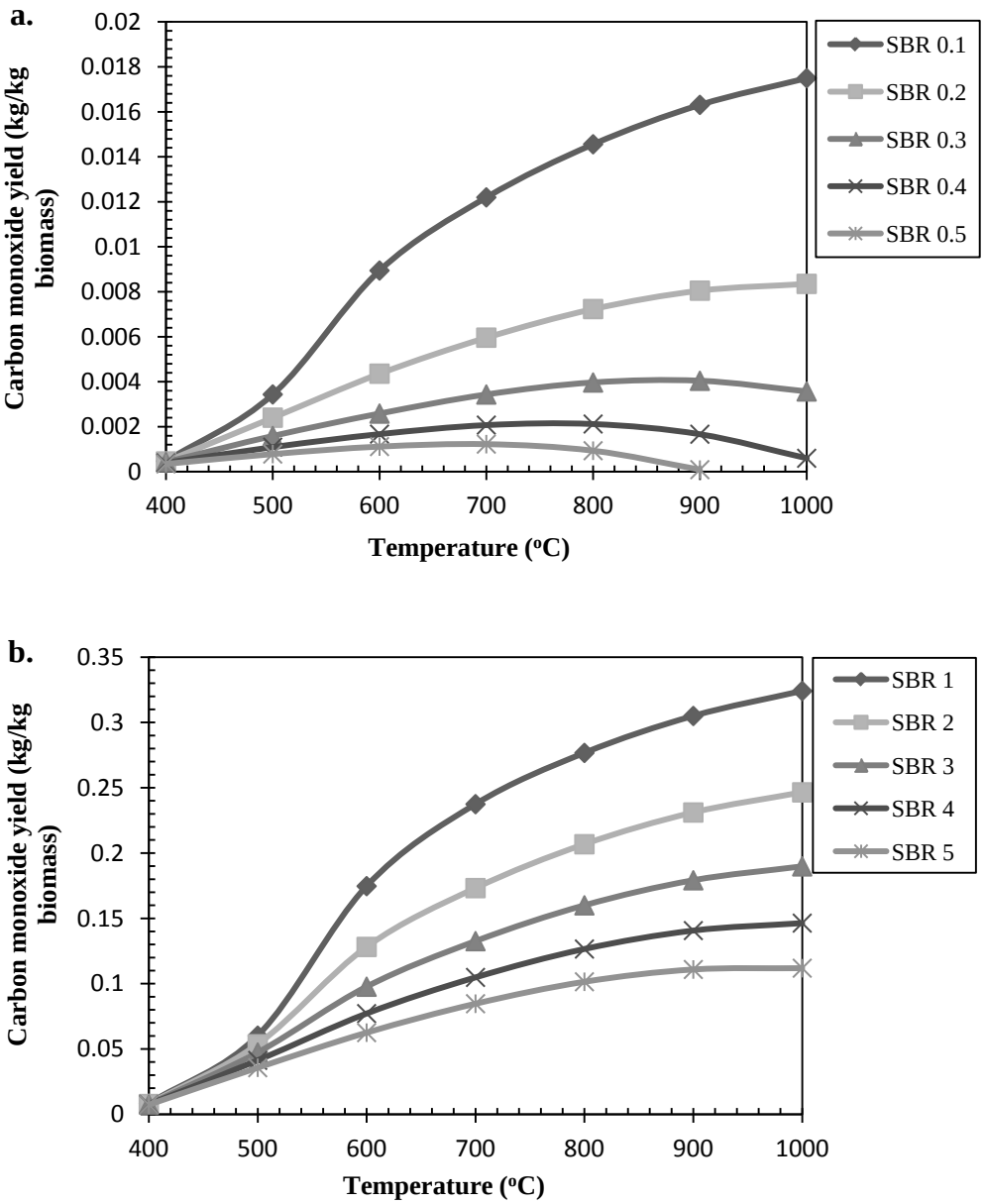

Figure 4.7 Carbon monoxide yield (kg/kg biomass) at different temperatures and at different steam to biomass ratio (SBR): (a) for water hyacinth and (b) for rice straw

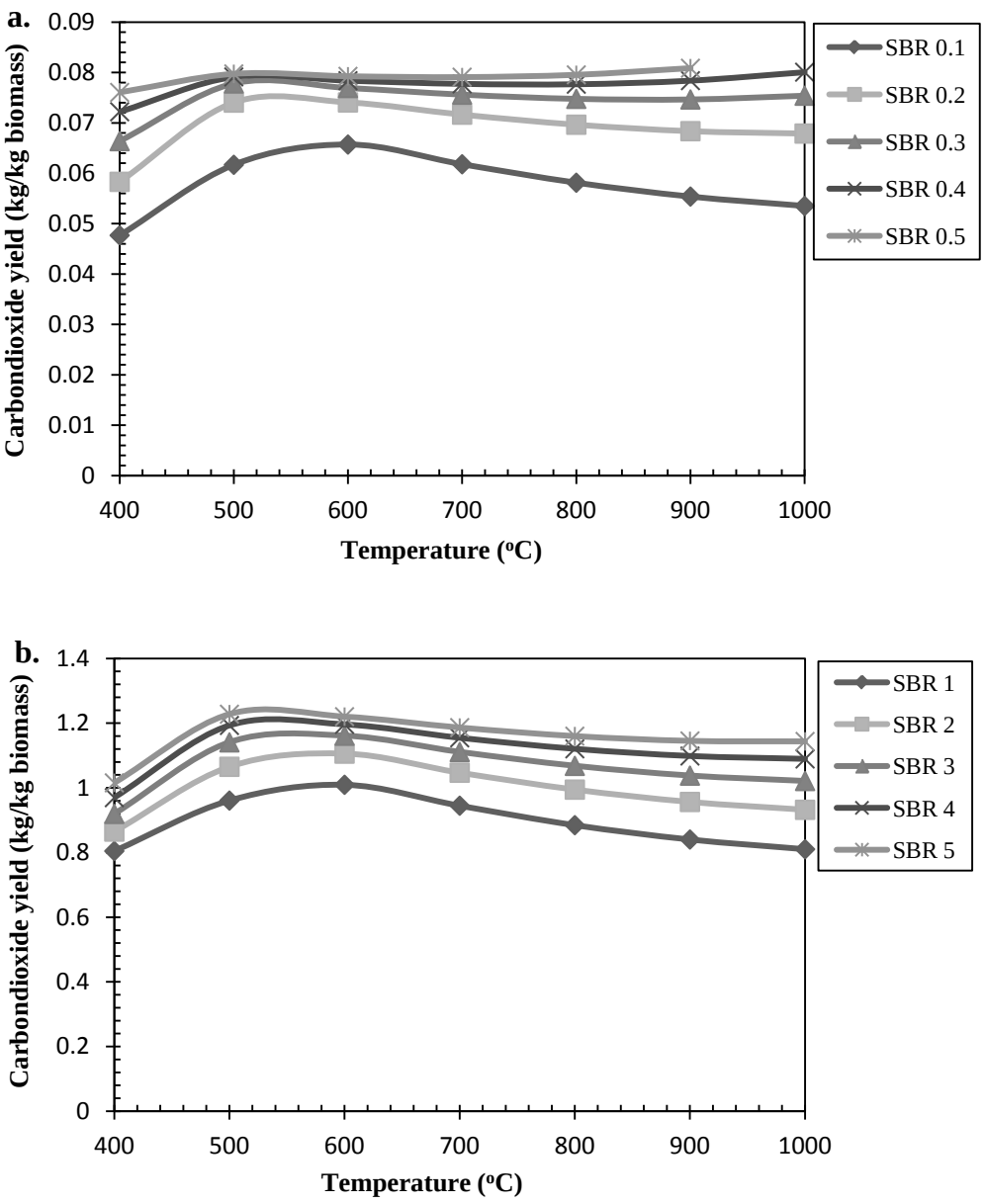

Figure 4.8 Carbon dioxide yield (kg/kg biomass) at different temperatures and at different steam to biomass ratio (SBR): (a) for water hyacinth and (b) for rice straw

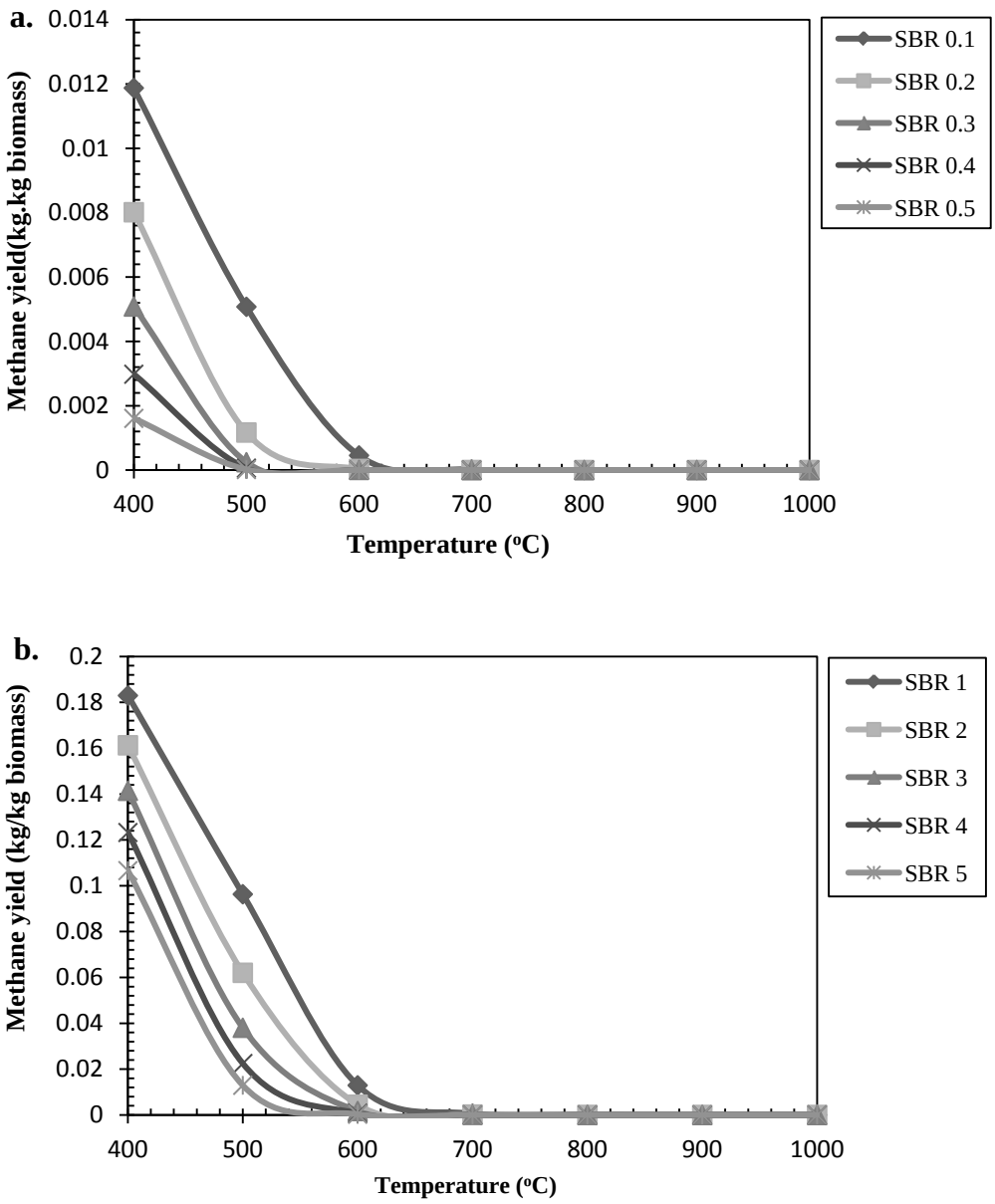

Figure 4.9 Methane yield (kg/kg biomass) at different temperatures and at different steam to biomass ratio (SBR): (a) for water hyacinth and (b) for rice straw

4.4.3 Efficiency analysis

The efficiency is a key factor that defines the economic potentiality of conventional gasification technology. In this part the efficiency of the process is studied while several operating parameters of the process are varied. The efficiency of the process was calculated as per the following definition:

$$\eta = \frac{\text{LHV of hydrogen in product gas}}{\text{LHV of biomass + all other energies}} \qquad (4.2)$$

$$\eta = \frac{n_{H_2} \times LHV_{H_2}}{n_{\text{biomass}} \times LHV_{\text{biomass}} + (Q_{\text{Dryer}} + Q_{A-\text{Heater}} + Q_{S-\text{Heater}})} \qquad (4.3)$$

The moles of each species at chemical equilibrium were calculated using Aspen Plus. The enthalpy of formation and enthalpy change for each species are taken from standard thermodynamic tables (Barin, 1995). The values for all the heat duties (Q) were determined. The efficiency was then determined using the above equation for a range of temperature and steam to biomass ratio at energy self-sufficient conditions. Figure 4.10 show the efficiencies for conventional gasification at general conditions. Figure 4.11, respectively, show the efficiencies for conventional gasification at energy self-sufficient conditions

4.4.3.1 Effect of gasifier temperature.

Figure 4.11 shows the combined effects of gasifier temperature and steam to biomass ratio at energy self-sufficient condition. As gasifier temperature increase, biomass thermally dissolves to produce more gases and volatiles. As temperature increases, the hydrocarbon in presence of steam /air gets reformed to produce hydrogen and carbon monoxide. As the hydrogen yield increases, the efficiency also increases (refer Eq. 4.3) and Figure 4.5 As gasifier temperature more increases, more heat needs and so more oxygen to oxidize with fuel to maintain the gasifier at that temperature. Also at higher temperatures (>700 ^{o}C) the hydrogen yield drops (Figure

4.11). Hence the efficiency first increases, reaches a maximum at around 500 - 600 ^{o}C and then starts reducing for temperatures >700 ^{o}C for two biomass. Figure 4.10 and Figure 4.11 were observed that conventional gasification at self-sufficient conditions gave much higher hydrogen yield than gasification at general conditions. Using energy self-sufficient condition helps to improve the convention gasification technology.

4.4.3.2 Effect of steam.

As we had seen in Figure 4.10, adding steam increases the hydrogen yield. However additional steam also demands additional energy. Therefore, there should be an optimum steam to biomass ratio which will justify the cost of supplying steam. In this analysis, the steam to biomass ratio was varied from 0.1 to 0.5 for water hyacinth and from 1 to 5 for rice straw. At low steam to biomass ratio values the total of hydrogen produced is quite little. As steam to biomass ratio increases, the efficiency increases and this is due to higher hydrogen yields. However at very high steam to biomass ratio values the efficiency drops due to more of energy needed to produce the steam and more oxygen to oxidize with fuel to protract the energy self-sufficient operation.

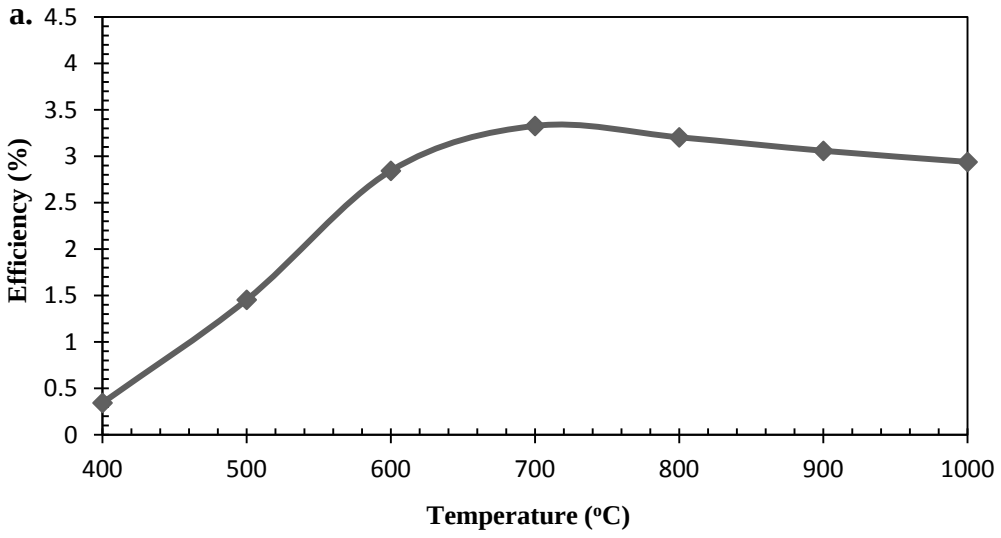

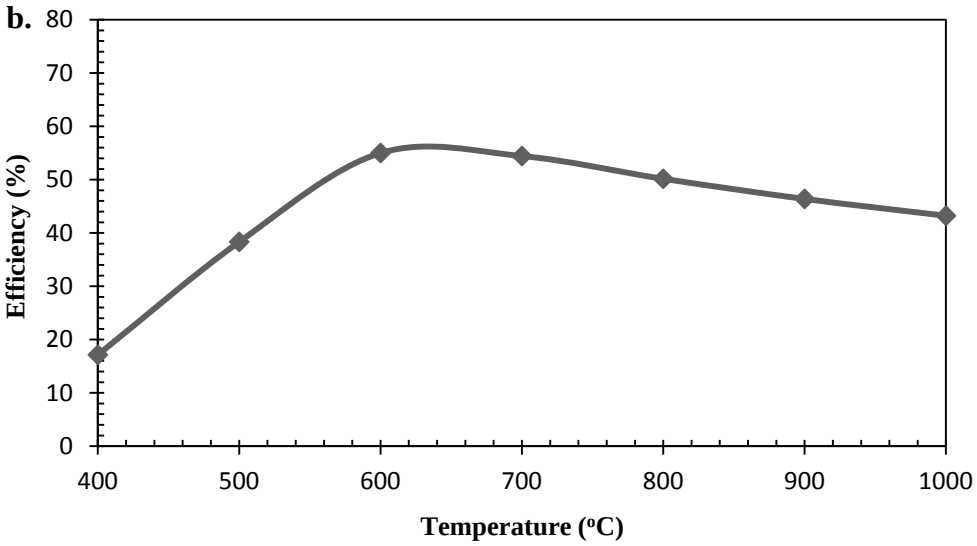

Figure 4.10 Efficiency (%) at different temperatures and at different steam to biomass ratio (SBR): (a) for water hyacinth and (b) for rice straw

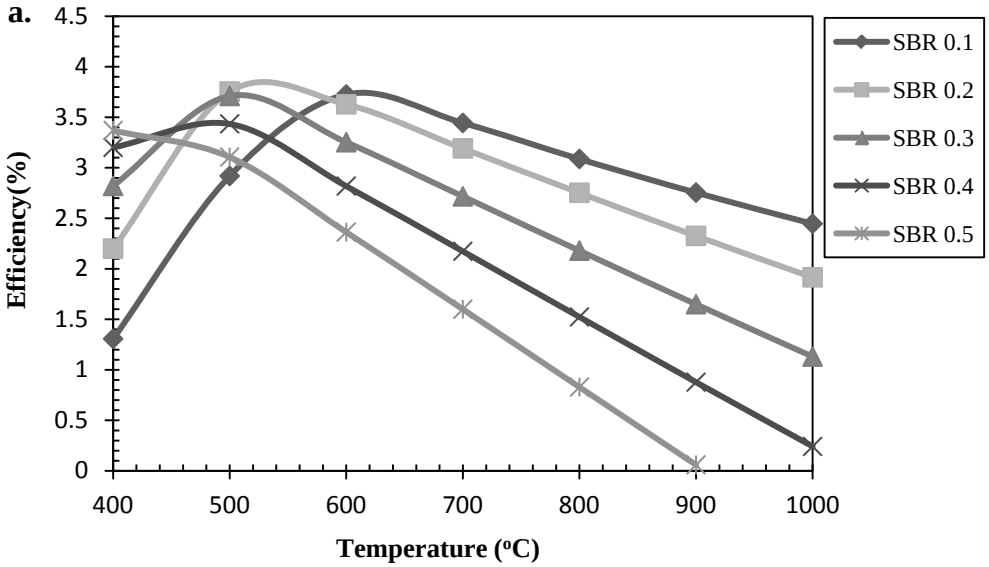

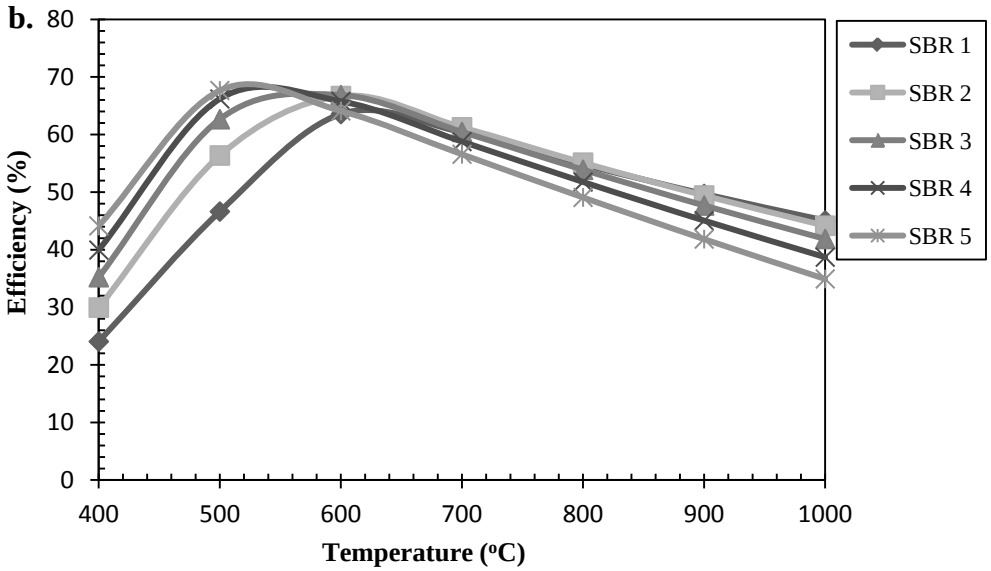

Figure 4.11 Efficiency (%) at different temperatures and at different steam to biomass ratio (SBR): (a) for water hyacinth and (b) for rice straw

CHAPTER V

SUPERCRITICAL WATER GASIFICATION TECHNOLOGY FOR SYNGAS PRODUCTION

In this chapter, the simulation model of a supercritical water gasification process is presented. In section 5.1, a description of the supercritical water gasification technology is given. Section 5.2 explains the simulation of the water hyacinth and rice straw supercritical water gasification process. In Section 5.3, the supercritical water gasification process run at a energy self-sufficient condition is studied. Finally, the simulation results of the sensitivity analysis of the supercritical water gasification process is given in Section 5.4.

5.1 Introduction

Biomass in general includes substantially more moisture than do fossil fuels such as coal. Some watery species, such as water hyacinth, or waste products, such as raw sewage, can have water contents exceeding 90%. Thermal gasification, where air, oxygen, or subcritical steam is the gasification medium, is very effective for dry biomass, but it becomes very useless for a high moisture biomass because the moisture must be substantially driven away before thermal gasification can begin; in addition, a large amount of the extra energy (~2260 kJ/kg moisture) is consumed in its evaporation. For example, Yoshida et al. (2003) saw the efficiency of their thermal gasification system reduce from 61 to 27% while the water content of the feed increased from 5 to 75%. So, for gasification of very wet biomass, hydrothermal gasification in high pressure hot water are superior because the water in these processes is not a liability as it is in thermal gasification. Instead it serves as a reaction medium and a reactant.

The efficiencies of these processes do not decrease with moisture content. For supercritical gasification, Yoshida et al. (2003) found the gasification efficiency to remain nearly unchanged, at 31% and 51%, respectively, even when the moisture in the biomass increased from 5 to 75%.

Supercritical water gasification involves gasification in a watery medium at very a high temperature and pressure exceeding or close to its critical value. While subcritical water has been used effectively for hydrothermal reaction, supercritical water has attracted more attention owing to its unique features. Supercritical water offers rapid hydrolysis of biomass, high solubility of intermediate reaction products, including gases, and a high ion product near (but below) the critical point that helps ionic reaction. These features make supercritical water an excellent reaction medium for gasification, oxidation, and synthesis.

5.2 Simulation model of water hyacinth and rice straw supercritical water gasification process

In order to present a principal system analysis, the process of supercritical water gasification for syngas production has been modeled with the Aspen Plus simulation. This model utilizes equilibrium calculations, which are based on Gibbs free energy minimization. This means that the model can more or less predict catalytic experiments of supercritical water gasification, absolutely rely on the capability of catalyst to have the reaction get to the chemical equilibrium. The Aspen Plus model cannot predict non-catalytic experiments, but this is not essential, due to non-catalytic supercritical water gasification certainly does not complete high carbon conversions and for this reason, not pleasing from a commercial point of view.

The system under study of VERENA pilot plant is shown in Figure 5.1. It is composed of a feed storage for wet biomass, a high pressure pump for pumping the slurry at a supercritical pressure, a heat exchanger to heat the reactants and cool the hot product gases, a supercritical water gasification reactor, a cooler, a valve used to reduce the pressure to atmospheric pressure, high and low pressure separators.

For the given operating conditions, the equilibrium compositions of the product gas obtained from the supercritical water gasification reactor are defined by solving a minimization problem of the total Gibb-free energy of the system. This method is known as a non stoichiometric approach, which a selection of the possible set of reactions is not essential. Here, an R-Gibbs reactor module in Aspen Plus is used to calculate the gas product compositions and heat of overall reaction in the process. The R-Gibbs reactor does not take reaction kinetics into calculation and allows individual reactions to be at a restricted equilibrium (Doherty et al., 2009)

A property method is utilized to determine the thermodynamic and transport properties of a chemical process. The pressures of different components in a process are influenced by the property method used in the calculation; thus, the choice of a property method is of importance. In this study, the Soave Redlich-Kwong property method with modified Huron-Vidal mixing rule (SRKMHV2) is chosen for the simulation of the gasification process for the reason that it can be used to predict the thermodynamic properties at supercritical water conditions (Withag et al., 2012). More detailed information about the property methods can be found in Valderrama (2003).

Modeling of biomass gasification in supercritical water is divided into five sections, as shown in Figure 5.2:

(1) Fuel feed preparation
(2) Air supply
(3) Biomass decomposition
(4) Gasification
(5) Product gas separation

and performed by using a process simulator Aspen Plus. Table 5.1 shows a description of each unit operation block shown in Figure 5.2. In this study, the RYIELD module is used to change the non-conventional stream “BIOMASS” into conventional components based on biomass composition. The RGIBBS module is operated to simulate partial oxidation, gasification steps; the composition of the

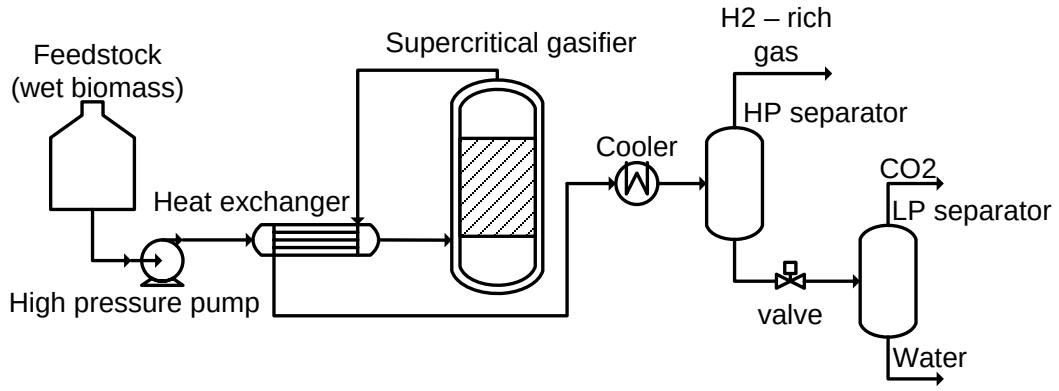

Figure 5.1 Schematic diagram of the gasification process considered in this study

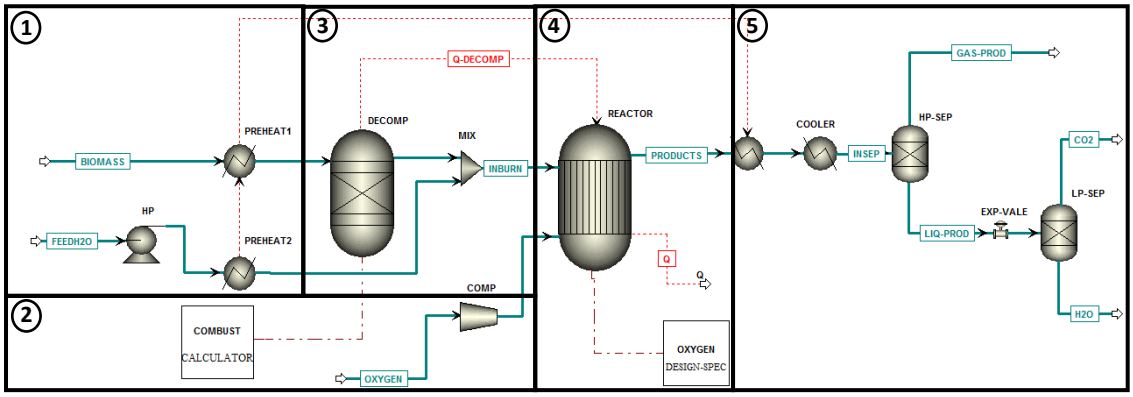

Figure 5.2 Simulation of the biomass gasification in supercritical water

product gas is determined by the minimization of the Gibbs free energy. A high and low pressure phase separator (SEP module) is used to separate the product gas.

5.3 Supercritical water gasification at energy self – sufficient condition

This part describes to develop energy efficiency so as to minimize the external heat demand, leading to a energy self-sufficient system. This system is particularly appropriate for efficiency of the process. Figure 5.3 demonstrates the system of energy balance in the supercritical water gasification process for syngas production.

$$Q_{\text{gasifier(net)}} = Q_{\text{Decomposition zone}} + Q_{\text{sup}ercritical\ \text{gasifier}} \qquad (5.1)$$

Equation 5.1 shows the energy balance equation supercritical gasifier. Nevertheless, depending on the amount of air supplied, energy self-sufficient condition can be achieved by appropriate adjustment of operating parameters

Table 5.1 Description of unit operation blocks used for simulations of biomass gasification process

Block	Unit Module	Description
HP	PUMP	High-pressure pump (pressure = 28 MPa)
PREHEAT1	HEATER	Heat exchanger: preheat biomass slurry (pressure drop = 0.02 MPa),
PREHEAT2		temperature = 75% of gasifier temperature (efficiency = 75%)
COMP	COMPR	Compressor (pressure = 28 MPa)
DECOMP	RYIELD	Yield reactor: decompose biomass into its constituent elements (pressure = 28 MPa, temperature = variable)
REACTOR	RGIBBS	Gibbs reactor: perform partial oxidation and supercritical water gasification (pressure = 28 MPa, temperature = variable)
HP-SEP	FLASH	High pressure phase separator: separate lighter components from the liquid phased (water and dissolved CO_2)
LP-SEP		Low pressure phase separator: separate CO_2 from liquid water (atmospheric pressure)
EXP-VALE	VALVE	Valve: reduce stream pressure (atmospheric pressure)
MIX	MIXER	Mixer: mix biomass with a certain amount of water before it is fed into a supercritical water gasification reactor

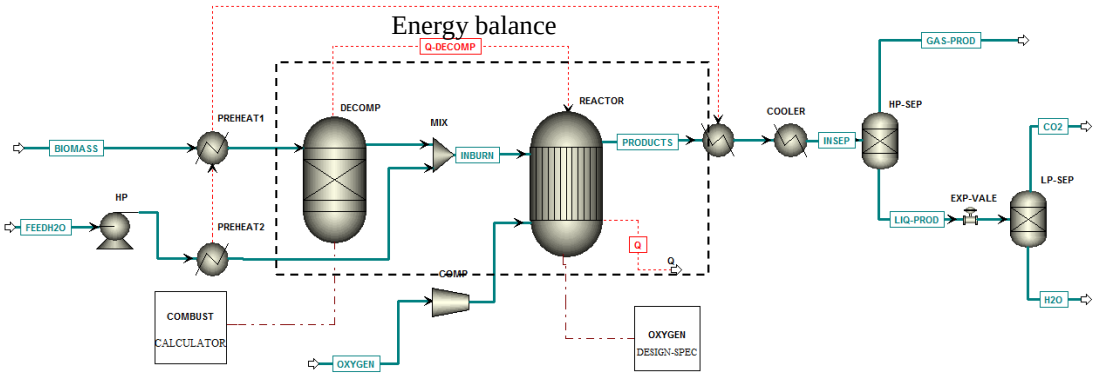

Figure 5.3 The system of energy balance in the supercritical gasifier

including biomass feedstock concentration, equivalence ratio (ER) and the gasifier temperature. The energy self-sufficient condition can be found by setting $Q_{gasifier(net)}$ equal to zero. The results obtained from the calculations in this work represent the maximum achievable hydrogen production based on the energy self-sufficient condition. In a real system, the values will be lower due to deviation from the thermodynamic equilibrium reaction and the presence of heat loss.

Figure 5.4 shows the equivalence ratio (ER) for (a) water hyacinth and (b) rice straw, which is required for achieving the energy self-sufficient condition, at different supercritical gasifier temperature and at different biomass feedstock concentration. Oxygen used is calculated to always achieve the energy self-sufficient condition. From the simulation results, there is no oxygen at the gasifier out for all simulations. Thus, oxygen reacts with biomass via reaction R5

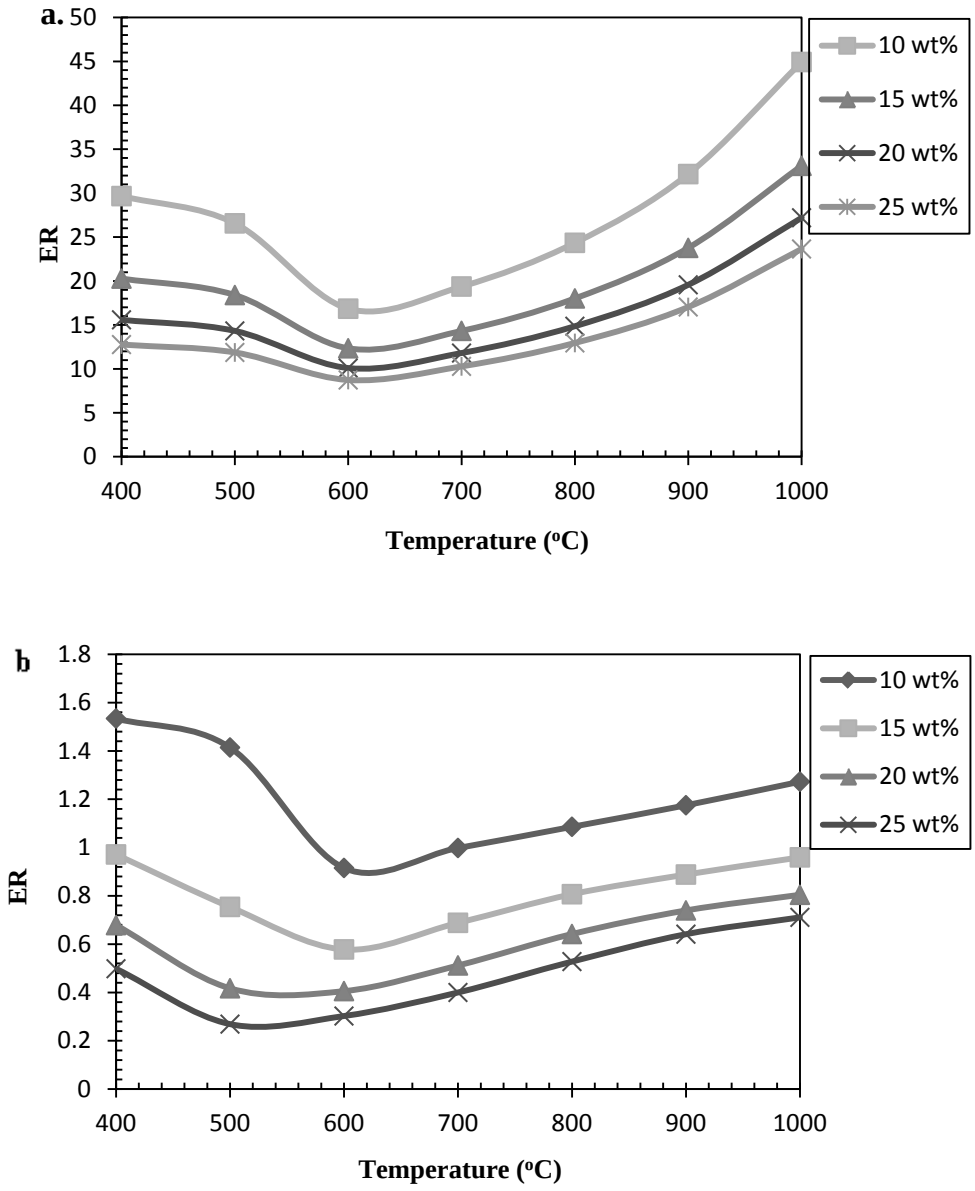

Figure 5.4 Equivalence ratio (ER) at different temperatures and at different steam to biomass ratio (SBR): (a) for water hyacinth and (b) for rice straw

5.4 Result and discussion

A thermodynamic analysis based on Gibbs free energy minimization using the Soave Redlich-Kwong property method with modified Huron-Vidal mixing rule (SRKMHV2) was carried out for the supercritical water gasification of hyacinth and rice straw. In this paragraph the effect of the key process parameters (i.e. supercritical gasifier temperature, different biomass feedstock concentration and pressure) on the composition of the product gas is analyzed. The product gas composition is required for the calculation of the efficiency of the process that will be discussed in Section 5.3.3

5.4.1 Model validation

Initially, The supercritical water gasification model in the exhibit work was validated with the previous biomass gasification in supercritical water reported by Antal et.al., (2000). The fuel for model validation is cornstarch. Experimental date 4/5/99, was selected for a particular comparison and analysis. The input data for experiment date 4/5/99 are as follows: input feedstock concentration 10.4 wt%, gasifier temperature 715 ^{o}C, pressure 28 MPa.

Table 5.2 compares the experimental results as reported by Antal et.al. to the model predictions using the input data presented above. The model predictions are in good agreement with the experimental data. For example hydrogen, carbon monoxide and carbon dioxide are predicted. However the methane is over – predicted which causes an error in the calculation of the gas heating value and ultimate.

5.4.2 Sensitivity analysis

5.4.2.1 Effect of gasifier temperature

The gasifier temperature is a significant effect on supercritical water gasification process. Figure 5.5 - 5.8 shows the predictions of the variation of the dry

Table 5.2 Experimental results versus model predictions.

Gas composition	Experimental	Model
H_2	0.55	0.55205229
CO	0.03	0.02675059
CO_2	0.35	0.34525642
CH_4	0.06	0.07594069

product gases yields of the major species with temperature ranging from 400 - 1000 ^oC at feedstock concentration 10, 15, 20, 25 wt%.. Owing to the energy self-sufficient condition specified for all simulations, gasifier temperatures considered are also adiabatic gasifier, at which the external heat flow equals to zero, related a definite oxygen input. For water hyacinth, the amount of oxygen input is excess compared to biomass supply which makes complete combustion happen. This restrains process of gasification. For rice straw, amount of oxygen supply is not sufficient (less than combustion stoichiometric demands) then gasification occurs. Figure 5.5 - 5.8 (a) show the sensitivity analysis results of supercritical water gasification with water hyacinth. It can be observed from Figure 5.5 (a) that an increase in temperature causes an increase hydrogen yield in conformance with water - gas reaction and become almost constant since about 600 ^oC. Therefore, higher temperature favors hydrogen production. The maximal hydrogen yield of 0.0084 kg/kg biomass is obtained. Accordingly, from the viewpoint of thermodynamics, further increase of temperature is unnecessary for hydrogen production. Figure 5.6 (a) proposes that high temperature gradually increase the production of carbon monoxide, for high feedstock concentration it continuously increases beyond 1000 ^oC. It is also clear that a change in temperature does not affect significantly the yield of carbon monoxide. For Figure 5.7 (a), yield of carbon dioxide increases slowly at low temperature and become nearly unchanged since about 600 ^oC, for all feedstock concentration. In Figure 5.8 (a), it can be observed that an increase in temperature causes a decrease in the yield of methane. This result indicates that the methanation rection R12 in disfavored with the increase in temperature. For rice straw, Figure 5.6 (b) shows that as temperature increases from 400 to 1000 ^oC, the hydrogen yield increases first and then decreases, for all feedstock concentration. This graph shows that at low temperature, hydrogen

production is formed from water-gas reaction and at high temperature more energy and oxygen are needed in order to oxidixe more fuel which reduces amount of hydrogen. From Figure 5.7, 5.9 (b), the carbon monoxide and methane yield of rice straw was observed same behavior with the hyacinth biomass. The carbon dioxide yield is stable throughout the temperature range.

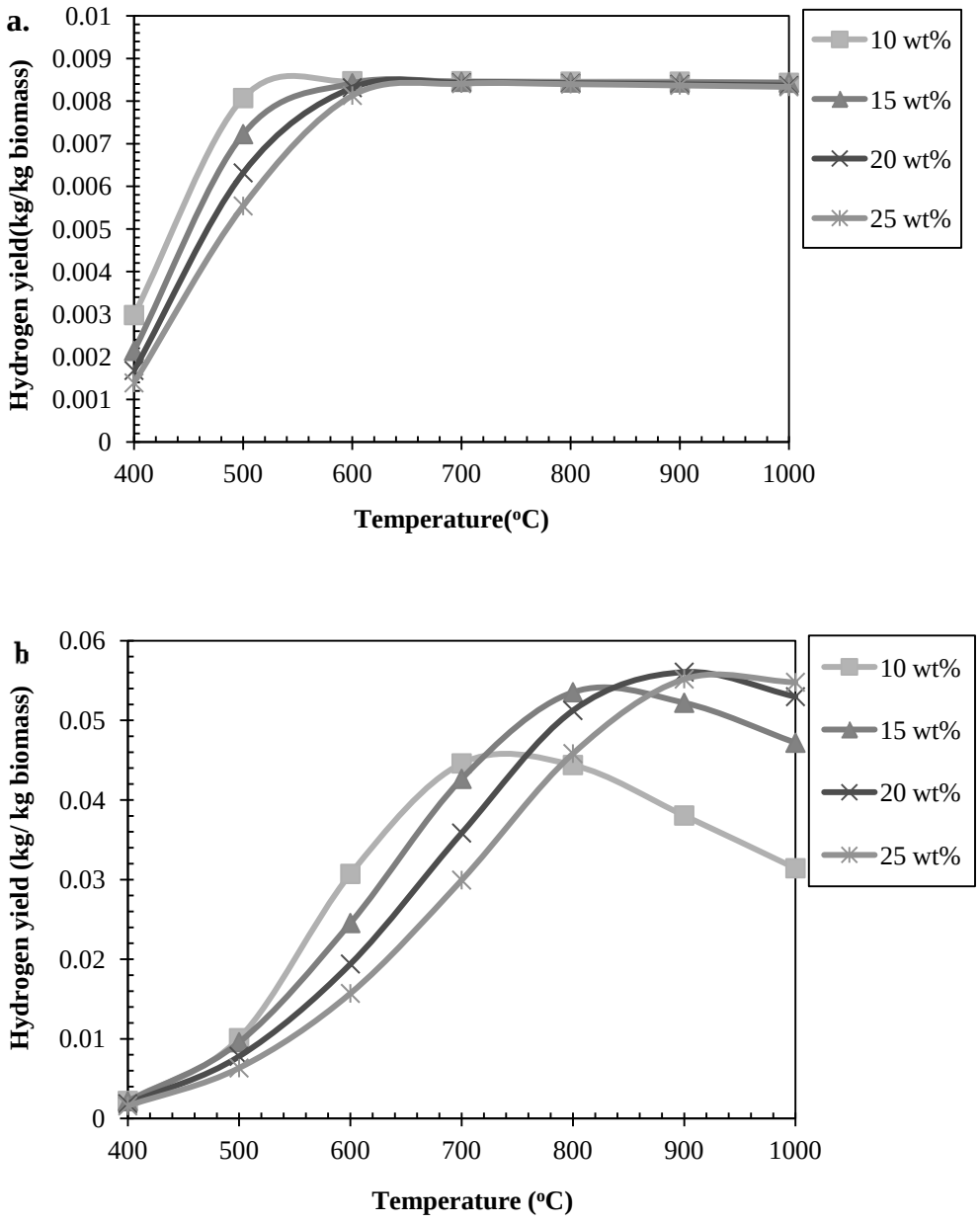

Figure 5.5 Hydrogen yield (kg/kg biomass) at different temperatures and at different feedstock concentration (a) for water hyacinth and (b) for rice straw

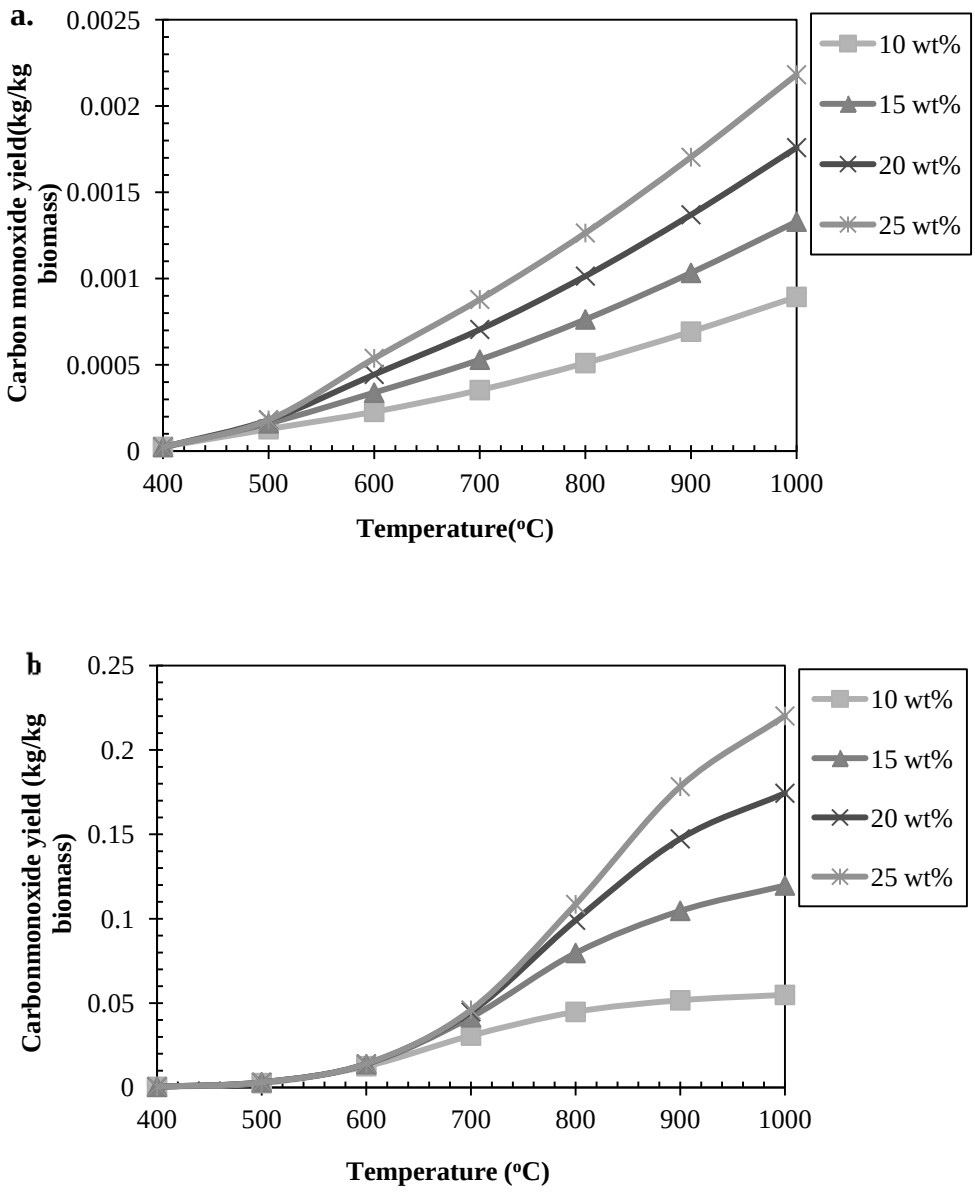

Figure 5.6 Carbon monoxide yield (kg/kg biomass) at different temperatures and at different feedstock concentration (a) for water hyacinth and (b) for rice straw

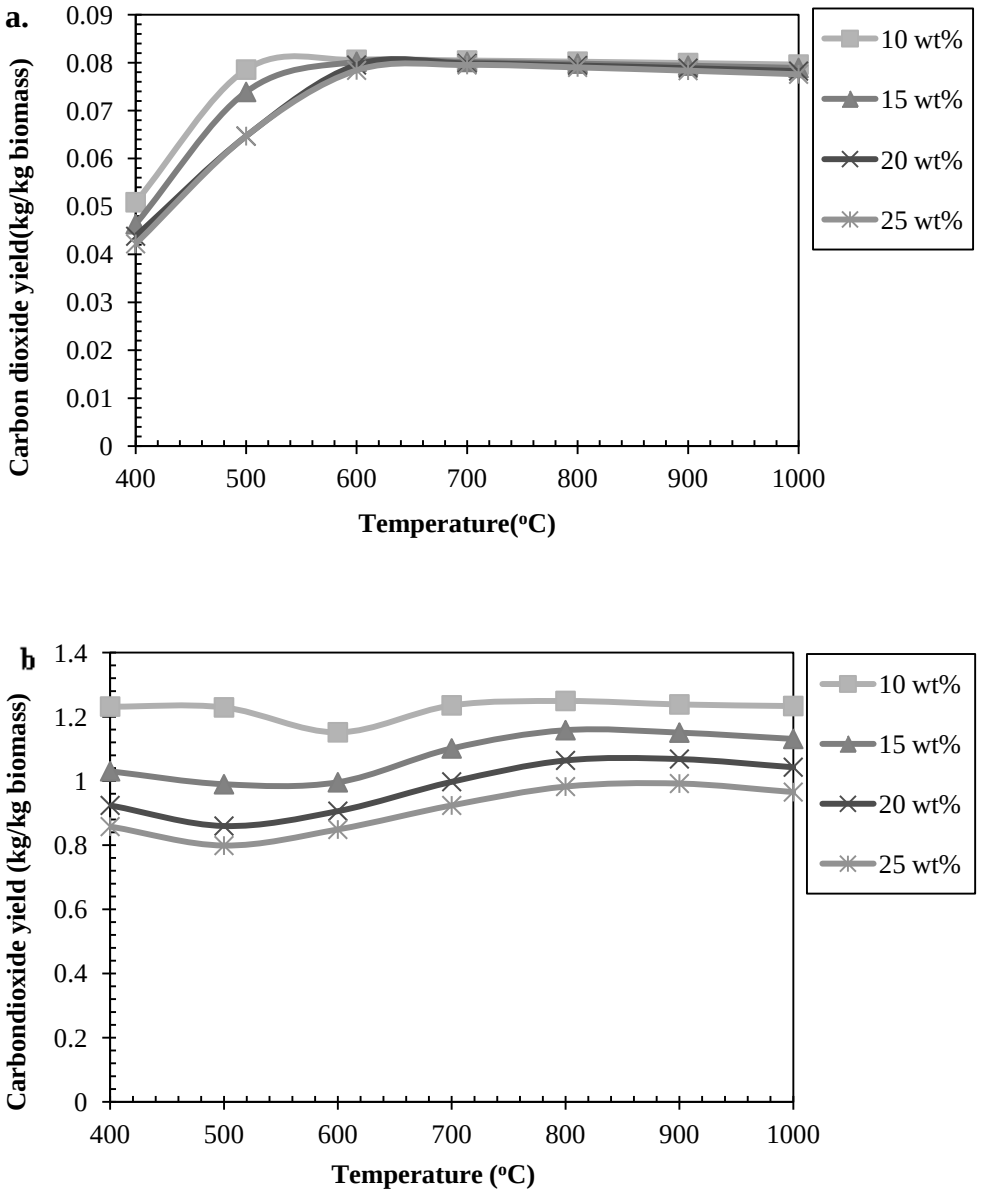

Figure 5.7 Carbon dioxide yield (kg/kg biomass) at different temperatures and at different feedstock concentration: (a) for water hyacinth and (b) for rice straw

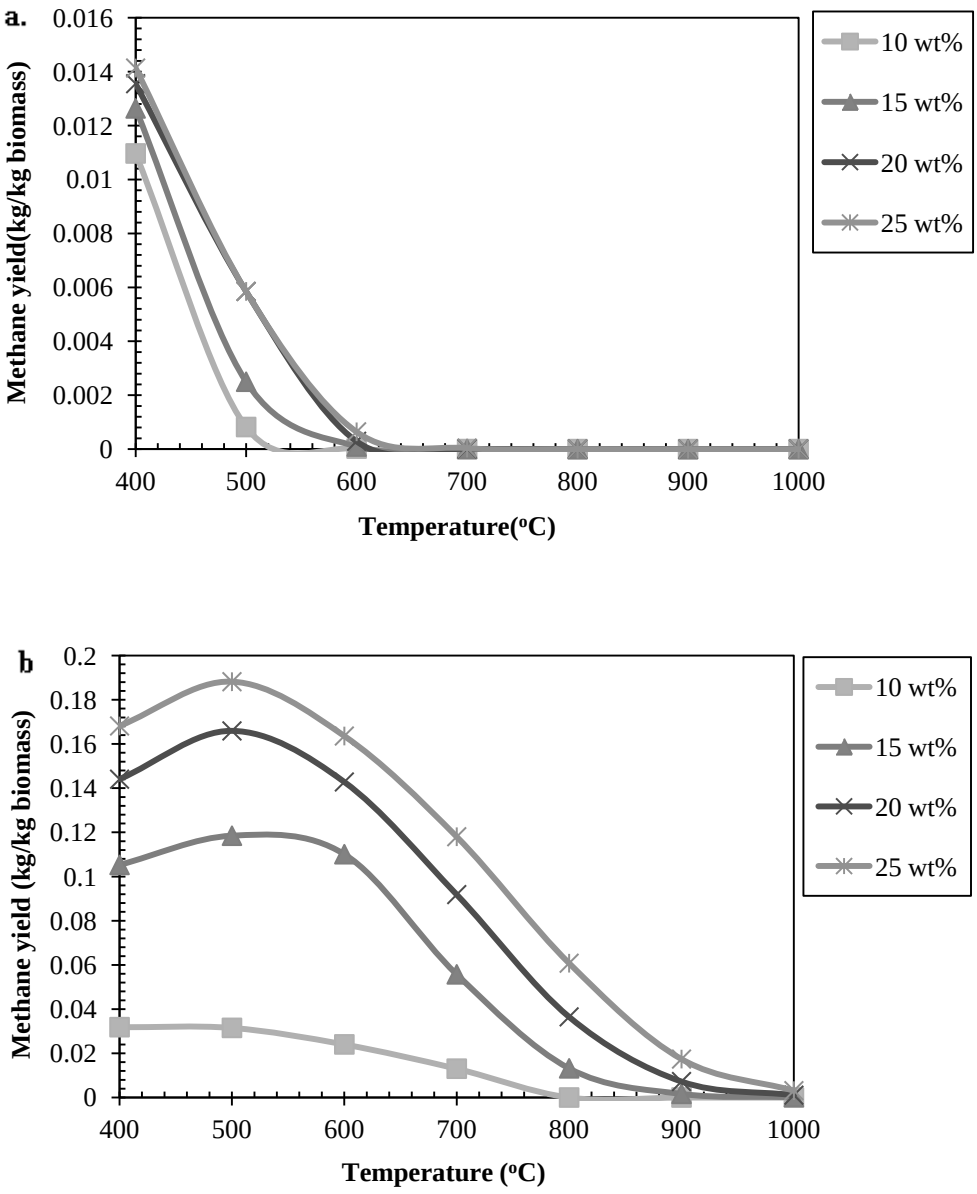

Figure 5.8 Methane yield (kg/kg biomass) at different temperatures and at different feedstock concentration: (a) for water hyacinth and (b) for rice straw

5.4.2.2 Effect of feedstock concentration

Feedstock concentration in the feed of 10, 15, 20 and 25 wt% were simulated at gasifier temperature of 400 - 1000 ^{o}C, at 28 MPa. Results are represented in Figure 5.5 - 5.8 (a) for hyacinth and Figure 5.5 - 5.8 (b) for rice straw. In Figure 5.5 (a), it can be observed that an increase in the feedstock concentration of water hyacinth causes an increase in the water hyacinth composition and a decrease in the composition of hydrogen at temperature range 400 - 600 ^{o}C. This behavior can be explained by considering that less water is present at the higher water hyacinth feed concentrations. The higher water hyacinth feedstock concentration lessens the shift toward the right side of water-gas reaction due to the lower water surplus. At temperature 600 - 1000 ^{o}C, it is clear that a change in this temperature rage does not influence essentially the hydrogen production. In Figure 5.6, 5.8 (a), It can be observed that an increase in the feedstock concentration (water decreases) increases the yield of carbon monoxide and methane. This behavior can be explained by reaction R9 and reaction R12

5.4.2.3 Effect of pressure

Pressure exhibits a complicated effect on biomass gasification in supercritical water. The properties of water, such as density, static dielectric constant and ion product, increase with pressure. As a result, the ion reaction rate increases and free-radical reaction is restrained with an increase of pressure. Hydrolysis reaction presents a significant role in biomass gasification in supercritical water gasification, but it requires the presence of H+ or OH-. With increasing pressure, the ion product increases, and hence the hydrolysis rate also increase. Also, a high pressure is in favor of water-gas shift reaction, but reduce decomposition reaction rate. Figure 5.9 - 5.12 shows the predictions of the variation of the gas yields of the four major species with variant pressures when the biomass feedstock concentration is gasified in supercritical water. The order of gas yields is $CO_2 > H_2 > CO > CH_4$ in the pressure range 23 MPa to 35 MPa. The hydrogen and carbon dioxide yields decrease and the methane yield increases as the pressure increases. In each case, the methane is in contention with

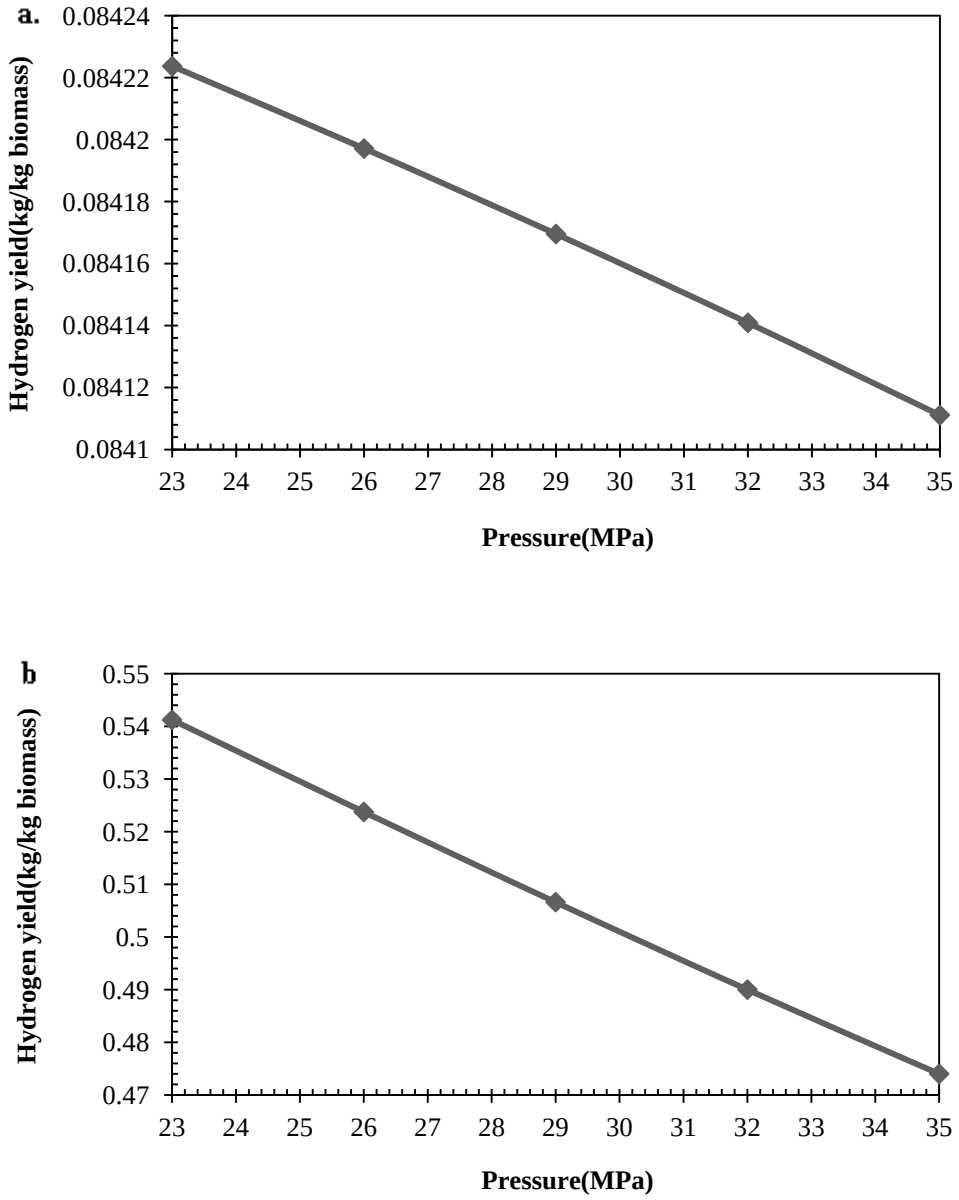

Figure 5.9 Effect of pressure on hydrogen yield (kg/kg biomass) at feedstock concentration 20 wt% and temperatures 800 ^{o}C (a) for water hyacinth and (b) for rice straw

hydrogen formation. The pressure, from 23 MPa to 35 MPa, has no significant effect on the biomass gasification in supercritical water. High pressure appears to favor the methane production in the range of 23 MPa to 35 MPa.

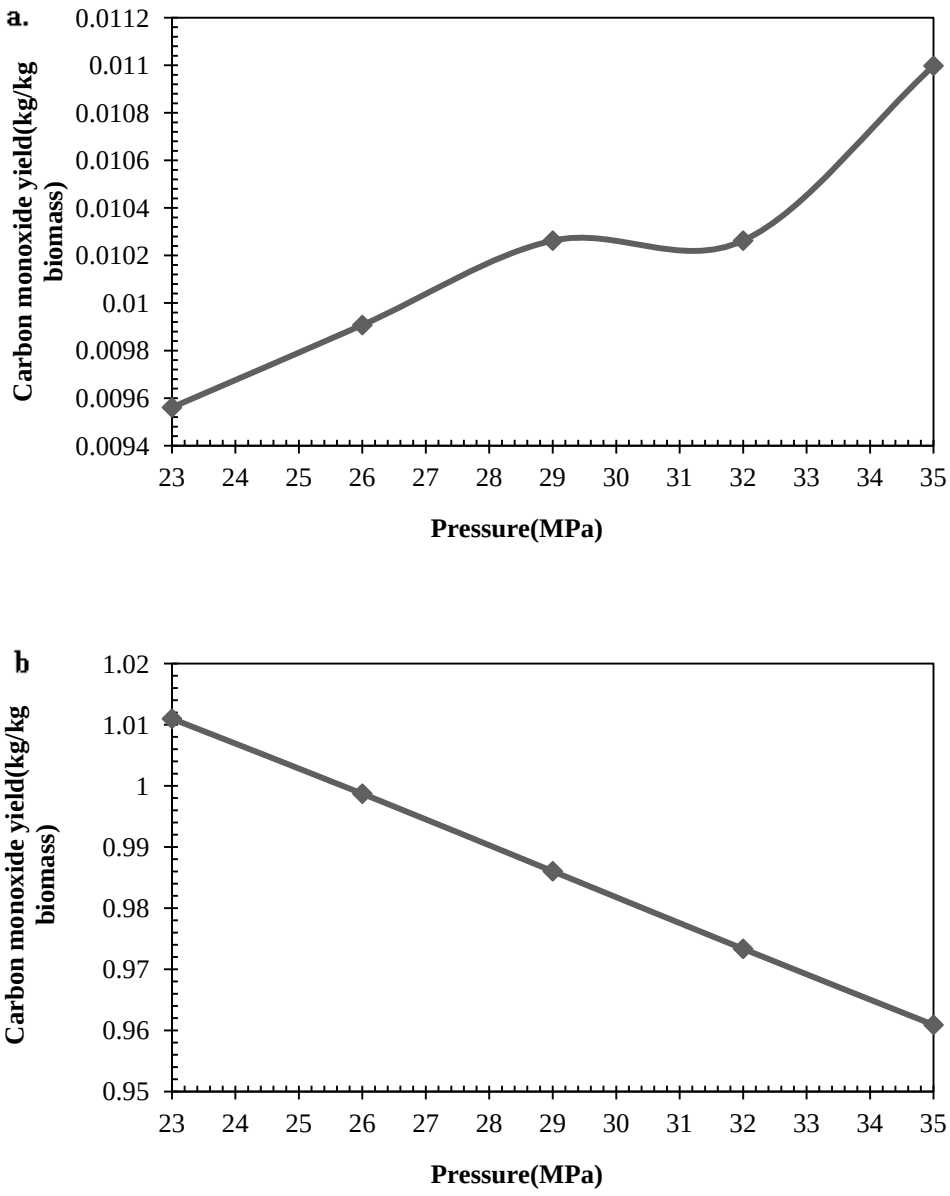

Figure 5.10 Effect of pressure on carbon monoxide yield (kg/kg biomass) at feedstock concentration 20 wt% and temperatures 800 ^{o}C (a) for water hyacinth and (b) for rice straw

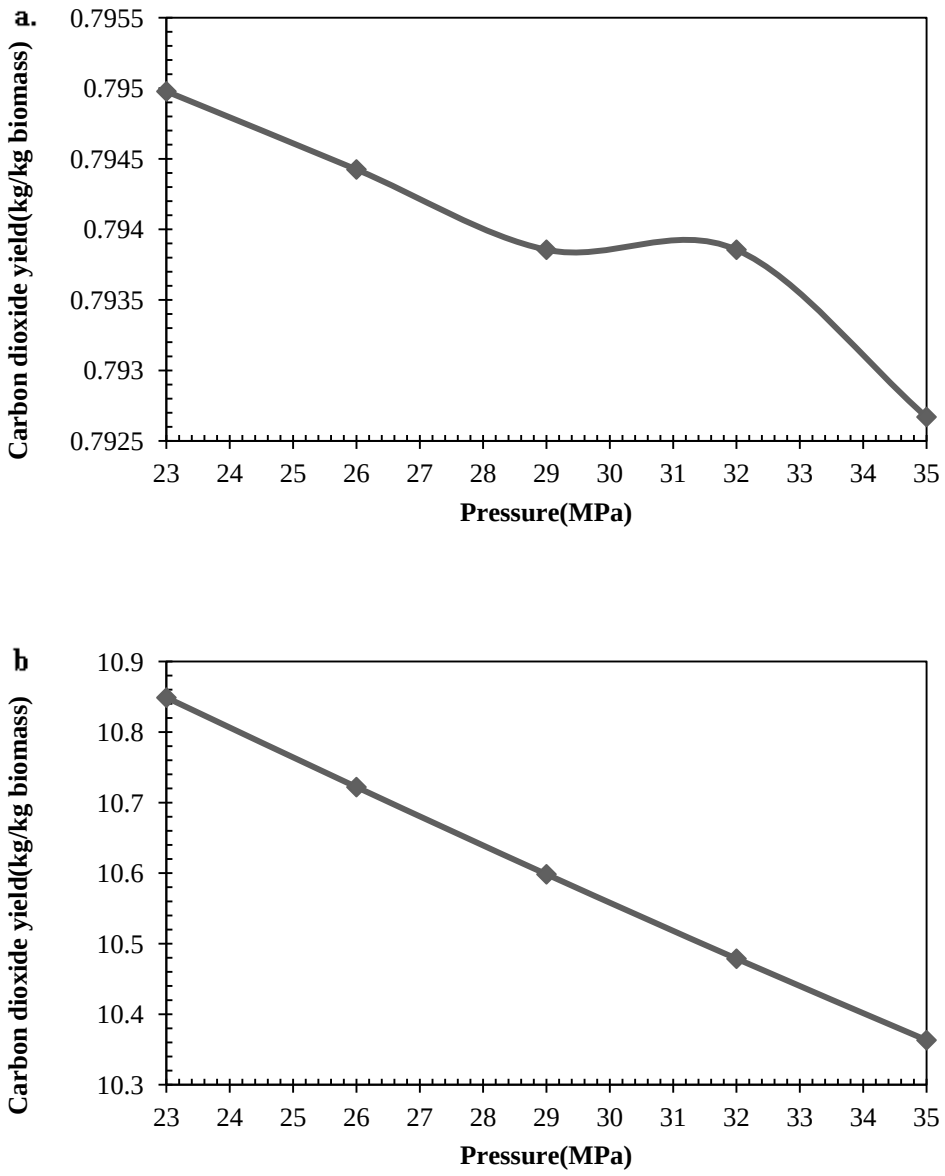

Figure 5.11 Effect of pressure on carbon monoxide yield (kg/kg biomass) at feedstock concentration 20 wt% and temperatures 800 ^{o}C (a) for water hyacinth and (b) for rice straw

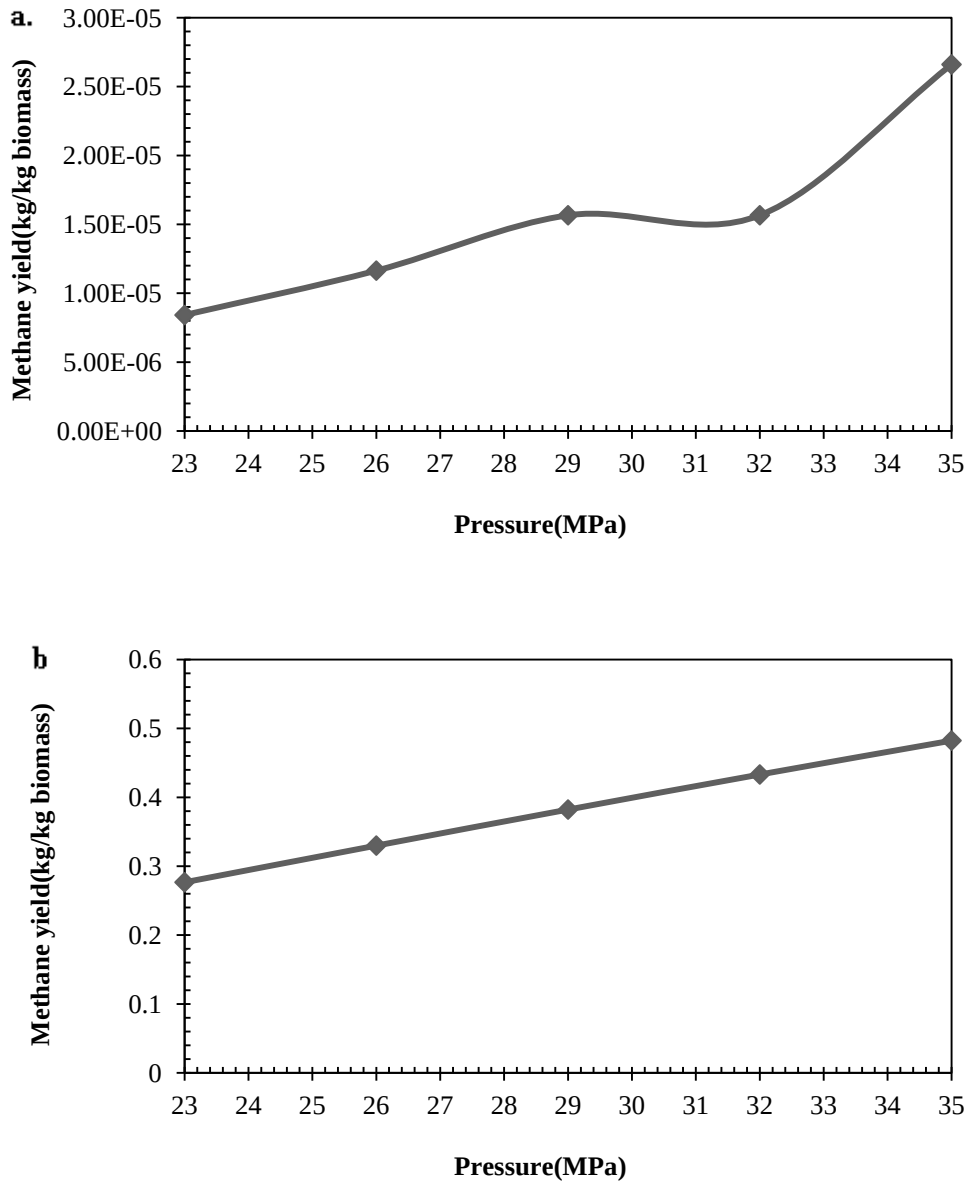

Figure 5.12 Effect of pressure on methane yield (kg/kg biomass) feedstock concentration 20 wt% and temperatures 800 ^{o}C (a) for water hyacinth and (b) for rice straw

5.4.3 Efficiency analysis

From the above sensitivity analysis, the highest hydrogen production can be achieved from model prediction presented above; nevertheless, the energy consumption for the system is also significant concern. Thus, the thermodynamic efficiencies of water hyacinth and rice straw were examined in order to define the

optimum operating conditions that can produce maximum yield of hydrogen with less energy consumption. The efficiency of the process was calculated as per the following definition:

$$\eta = \frac{\text{LHV of hydrogen in product gas}}{\text{LHV of biomass + all other energies}} \qquad (4.2)$$

$$\eta = \frac{n_{\mathrm{H}_2} \times LHV_{H_2}}{n_{\text{biomass}} \times LHV_{\text{biomass}} + (Q_{\text{gasifier}} + \text{HP} + \text{Compressor})} \qquad (4.3)$$

Where n_{H_2} is the flow rate of hydrogen production (kg/hr); n_{biomass} is the flow rate of biomass (kg/hr); LHV_{H_2} is the low heating value of hydrogen (kj/kg); LHV_{biomass} is the low heating value of biomass; Q_{gasifier} is energy of gasifier (kj/hr); HP is the energy of high pressure pump (kj/hr);.

Figure 5.14 (a) show the effect of gasifier temperature and feedstock concentration on efficiency for the supercritical water gasification process of water hyacinth process. The simulation result shows that the increasing gasifier temperature between 400 - 700 ^{o}C quickly improves the efficiency of process. However, it decreases slightly when increasing gasifier temperature up to 600 ^{o}C. Moreover, the increasing feedstock concentration increases efficiency of process. Figure 5.14 (b) show the efficient of gasifier temperature and temperature and feedstock concentration on efficiency for the supercritical water gasification at self-sufficient condition of rice straw fuel the simulation result shows that initially the efficiency increased with increasing temperature until reaching the optimum point and then it deceased at higher temperature. Moreover, the efficient increases (in the order of temperature 400 – 1000 ^{o}C) with increasing feedstock concentration. Therefore, the optimum operating conditions for the supercritical water gasification at self-sufficient condition of rice straw fuel are at 900 ^{o}C with inlet feedstock concentration 20 or 25 wt%. Figure 5.15 (a), (b) shows the predictions of the variation of the efficiency for

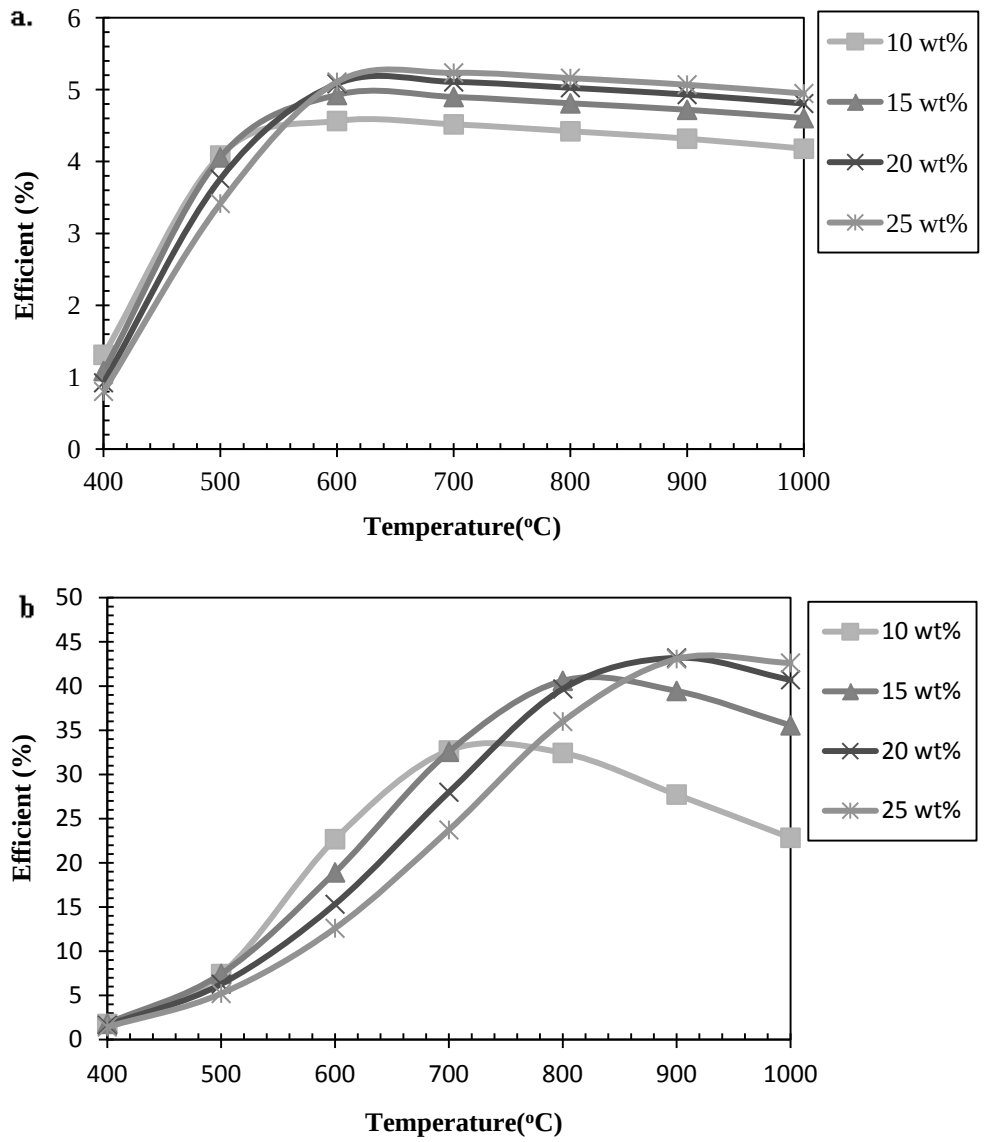

Figure 5.13 Efficiency (%) at different temperatures and at different feedstock concentration (a) for water hyacinth and (b) for rice straw

supercritical water gasification of water hyacinth and rice straw with variant pressures. The efficiency of process decrease as the pressure increases. This behavior can be explained by the pressure, from 20 MPa to 35 MPa, has no geat effect on the yield of hydrogen.

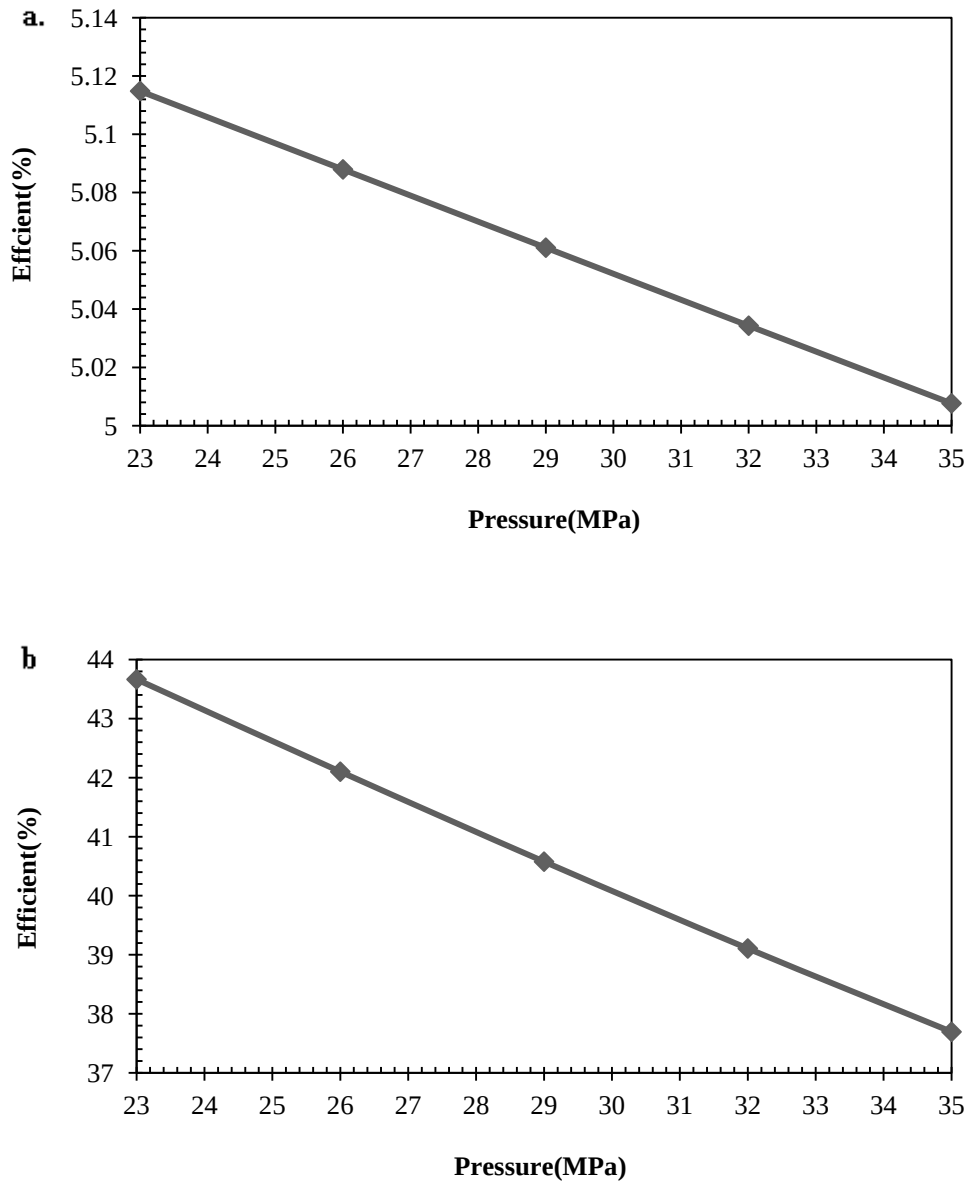

Figure 5.14 Effect of pressure on efficient (%) feedstock concentration 20 wt% and temperatures 800 ^{o}C (a) for water hyacinth and (b) for rice straw

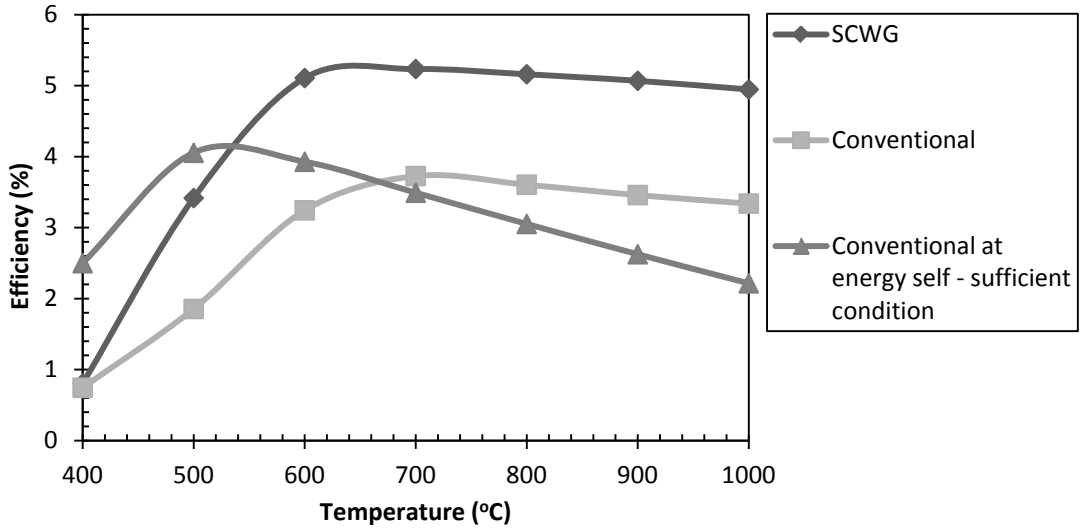

Figure 5.15 Efficiency (%) of water hyacinth at different temperatures and at different gasification technology.

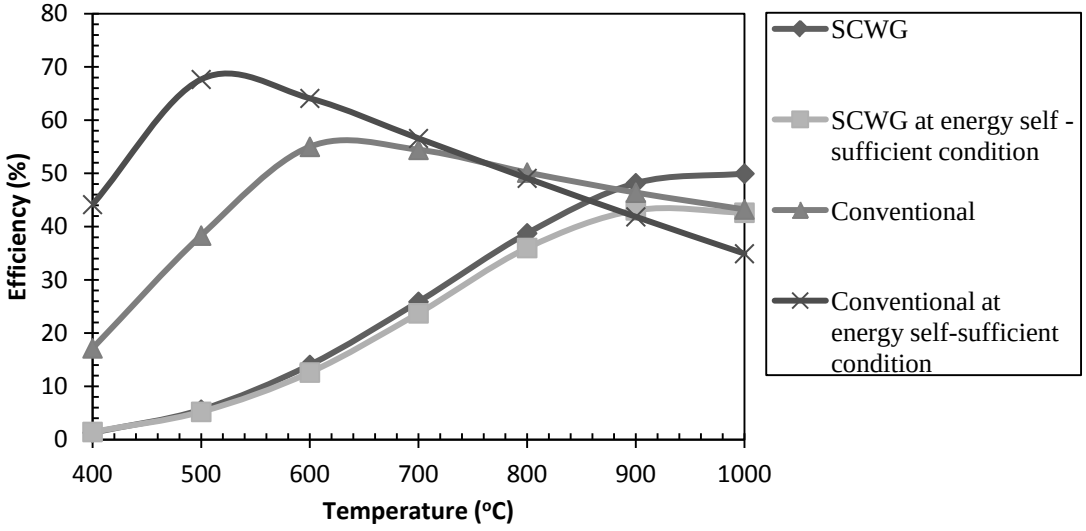

Figure 5.16 Efficiency (%) of rice straw at different temperatures and at different gasification technology.

5.5 Comparison of water hyacinth and rice straw gasification technology for syngas production

Total efficiency is compared between power generation methods. Following four processes are compared: conventional process, conventional process at energy self-sufficient condition, supercritical water gasification process and supercritical water gasification process at energy self-sufficient condition. In simulation the total efficiency, electricity consumption in the production process is converted to primary energy equivalents. Then, the total efficiency is defined as the energy content of the product divided by the energy content of all energy inputs to the process. Figure 5.6 shows efficiency percentage of water hyacinth at different temperatures. The comparison of simulation result shows that most appropriate technology for high moisture biomass (water hyacinth) is supercritical water gasification technology which is 5.2%. Using conventional technology with high moisture biomass (water hyacinth) will be less effective because the high moisture biomass must be substantially driven away before thermal gasification can begin; in addition, a large amount of the extra energy is consumed in its evaporation. Figure 5.7 shows efficiency percentage of rice straw at different temperatures. The comparison of simulation result shows that the conventional gasification at energy self-sufficient condition is the most efficient process for rice straw gasification and follow by conventional gasification technology, supercritical water gasification technology and supercritical water gasification technology at energy self-sufficient condition, respectively. For dry biomass, supercritical water gasification technology gave low efficiency because amount of the extra energy is consumed in high pressure pump. From Figure 5.15 and 5.16 we can conclude that although the conventional technology is good for dry biomass, the conventional technology used energy self – sufficient condition is suitable effective for dry biomass. The conventional technology used energy self-sufficient condition will allow the efficiency of the gasification process increasing. For high moisture biomass like water hyacinth, supercritical water gasification technology is the most appropriate. However, this technology is not suitable to the state energy self-sufficient condition because complete combustion takes place.

CHAPTER VI

OPTIMIZATION OF SUPERCRITICAL WATER GASIFICATION PROCESS

This section presents a optimization of the supercritical water gasification process. The aim is to determine key operating parameters maximizing the process efficiency. A statistical analysis using design of simulations is first described. The simulation data for process optimization is generated based on a central composite design (CCD) and then analyzed by using the response surface regression model, which is based on a second-order polynomial equation. Analysis of variance (ANOVA) is applied to estimate effects of the major operational variables and their potential interaction effects on the process efficiency. Finally, the mathematical model explaining a relation of process variables and process performance is developed and used to determine optimal process variables

6.1 Introduction

Conventionally, the optimization study for gasification process is performed with the variation of one component at a time and the response is a function of a single parameter (one-variable-at-a-time technique) which is time consuming and exorbitant in cost. This technique does not include interactive effects among the variables and it does not depict the complete effect of the parameters on the process (Lee et al., 2011). Response surface methodology (RSM) is a useful statistical technique, which has been applied in the research of complex variable processes (Myers and Montgomery, 2002). Multiple regression and correlation analysis are used as tools to assess the effects of two or more independent factors on the dependent variables. Furthermore, the central composite design (CCD) of RSM has been applied in the optimization of several biotechnological and chemical processes. It main

advantage is the reduction in the number of experimental runs required to generate sufficient information for a statistically acceptable result.

6.2 Statistical analysis using design of simulations

The effects of supercritical water gasification process parameter and the optimum conditions for the efficiency was studied by using design of simulations. Optimization process for syngas production is shown in figure 6.1. In this study, the design of simulation selected was Response Surface Method (RSM) coupled with Central Composite Design (CCD) using the Design-Expert Version 6.0.8 (State-Ease, Inc.) software. The process parameters selected for this study are feedstock concentration, gasifier temperature and pressure. The design matrix of the central composite design chosen together with the results for the three optimization parameters selected. The value of α was based on the number of optimization parameters (k = 3) as follows:

$$\alpha = (2^3)^{1/4} = 1.68$$

The total number of experiment trials (n_e) as follows:

$$n_e = 2^3 + 2(3) + 1 = 15$$

The independent variables are coded to two levels namely: low (-1) and high (+1), whereas the axial points are coded as -1.68 (-α) and +1.68 (+α). The α value was fixed at 1.68 which is the distance of the axial point from the center and make the design rotatable. A three-level-three-factor CCD requires 15 simulations, including 8 factorial points from full factorial design CCD for three variables, six axial points and one replicate at the center point were employed in this study.

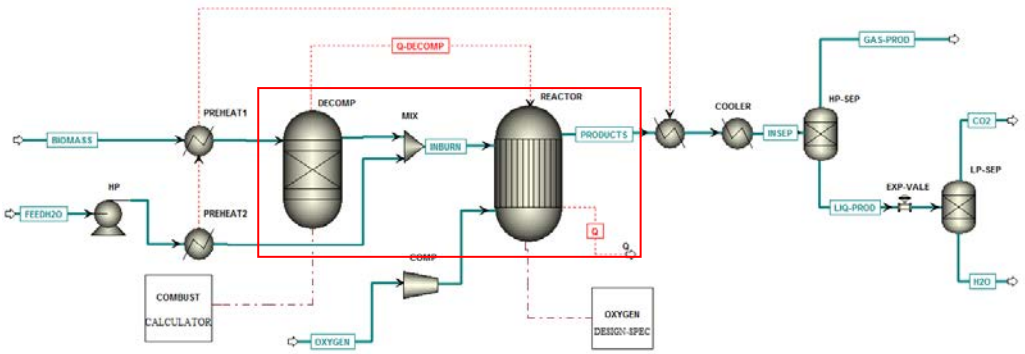

Figure 6.1 Optimization of supercritical water gasification process

Table 6.1 Process parameters in central composite design: coded and natural values

Factors	Symbols	Units	Levels				
			-1.68	-1	0	1	1.68
Concentration feedstock	X_1	wt%	10	22.16	40	57.84	70
Gasifier temperature	X_2	ºC	500	601.35	750	939.19	1000
Pressure	X_3	MPa	23	25.43	24	32.57	35

Table 6.1 shows the coded and actual value of the process parameters used in the design of simulations. The simulations were conducted based on the design matrix show in Table 6.2.

6.3 Development of regression model

Among the models that fitted to the response (linear, two factor interaction (2FI), quadratic and cubic polynomial), the quadratic model was selected as a best model due to its highest order polynomial with significant of additional terms and the model was not aliased (Table 6.3). The quality of the fit of polynomial model equation was evaluated by the coefficient of determination R^2, the coefficient of determination was shown as 0.8469. This indicated that, the accuracy and general availability of the polynomial model was considered to be reasonable. The empirical model is adequate to explain most of the variability in the assay reading which should be at least 0.75

Analysis of variance (ANOVA) is a collection of statistical models, and their associated procedures, in which the observed variance in a particular variable. The ANOVA was used for checking the significance of the quadratic model equation. Table 6.4 shows analysis of variance for the fitted quadratic polynomial.

6.3.1 Mean square of error

The mean squared of error (MSE) of an estimator is one of many ways to quantify the difference between values implied by an estimator and the true values of the quantity being estimated. From Table 6.4, the mean square of the error has a little value, it is indicated that the data obtained from simulation and optimization is very little difference. Mean of square regression (MS_{SSR}) and mean of square residual (MS_{SSE}) are obtained by divining sum of square (SSR) and sum of residual (SSE) over degree of freedom (DF), respectively.

6.3.2 F-value

The calculated *F*-value is defined as the ratio between MS_{SSR} and (MS_{SSE}). The significance testing *(F*-test) is used as a tool to check the significance of the variables to the model. The higher *F*-value indicated that the variable is significant. In single parameter effect, *F*-value indicated that gasifier temperature is the most significant variable and pressure, feedstock concentration are significant respectively. Two interaction term show significant effect on the efficiency; which are X_1X_2 (feedstock concentration and gasifier temperature) is the most significant effect on the efficiency, X_2X_3 (gasifier temperature and pressure) and X_1X_3 (concentration feedstock and pressure) are significantly reduced, respectively.

Table 6.2 Full factorial central composite design matrix of three independent variables in coded and the response of the dependent variable efficiency

RUN	Levels			Efficiency	
				Simulation	Predicted
1	-1.00	-1.00	-1.00	5.0906	4.62
2	1.00	-1.00	-1.00	4.25058	4.08
3	-1.00	1.00	-1.00	4.92314	4.79
4	1.00	1.00	-1.00	5.34955	5.67
5	-1.00	-1.00	1.00	4.87321	4.79
6	1.00	-1.00	1.00	3.75455	3.72
7	-1.00	1.00	1.00	4.86691	4.87
8	1.00	1.00	1.00	5.31939	5.62
9	-1.68	0.00	0.00	4.27479	4.84
10	1.68	0.00	0.00	5.34238	5.01
11	0.00	-1.68	0.00	2.4021	3.01
12	0.00	1.68	0.00	5.12314	4.75
13	0.00	0.00	-1.68	5.395	5.58
14	0.00	0.00	1.68	5.30343	5.35
15	0.00	0.00	0.00	5.35223	5.35

Table 6.3 Model summary statistics

Source	Standard Deviation	R-squared	Adjusted R-squared	Predicted R-squared	PRESS	
Linear	0.66	0.3530	0.2316	-0.1087	11.81	
2FI	0.67	0.4528	0.2002	-0.3453	14.33	
Quadratic	0.41	0.8438	0.7032	-0.1879	12.66	Suggested
Cubic	0.15	0.9872	0.9595	-1.8191	30.03	Aliased

6.3.3 P-value

The *P*-values are used as a tool to check the significance of each coefficient, which also indicate the interaction strength of each cross product. The value of "*P* > F" for models is less than 0.05, indicated that the terms in the model have a significant effect on the response. The value of P < 0.0001 indicates that there is only a 0.01% chance that a "model *F*-value" this large could occur due to noise. *P*-values lower than 0.05 indicate that the model is considered to be statistically significant at the 95% confidence level. In this study, λ_1, λ_2, $\lambda_1\lambda_2$, λ_1^2, λ_2^2 are significant model term. **(***P*-value for each variable is less than the significant size, which was used 0.05 in this test)

Table 6.4 Analysis of variance (ANOVA) for quadratic polynomial model

Source	Sum of Squares	df	Mean Square	*F*-value	*P*-value *(P) > F*
Model	8.99	9	1.00	6.00	0.0049
λ_1	0.038	1	0.038	6.23	0.0452
λ_2	3.66	1	3.66	21.97	0.0009
λ_3	0.067	1	0.067	0.40	0.5412
$\lambda_1\ \lambda_2$	1.01	1	1.01	6.05	0.0337
$\lambda_1\ \lambda_3$	7.97E-003	1	7.97E-003	0.048	0.8311
$\lambda_2\ \lambda_3$	0.049	1	0.049	0.30	0.5988
λ_1^2	0.32	1	0.32	1.91	0.0468
λ_2^2	3.87	1	3.87	23.27	0.0007
λ_3^2	0.026	1	0.026	0.16	0.7007
Residual	1.66	10	0.17		
Lack of Fit	1.66	5	0.33		
Cor Total	10.65	19			

6.3.4 Lack of fit

Lack of fit (LOF), this is the variation of the data around the fitted model. If the model does not fit the data well, the test will show significant. From table 6.4, lack of fit is not significance, it is indicated that the model fit the data.

6.3.5 Mathematical model

The quadratic model for the efficiency was regressed by considering the significant terms and was shown as below:

$$= 5.35 + 0.052X_1 + 0.52X_2 - 0.070x_3 + 0.35X_1X_2 - 0.032X_1X_3 + 0.078X_2X_3 - 0.15X_1^2 - 0.52X_2^2 + 0.043X_3^2$$

where *Y* is the total efficiency; X_1, X_2 and X_3 are the coded independent variables. From table 6.2, the model from CCD was considered to be accurate and reliable for predicting the efficiency of process.

Table 6.5 Regression analysis of a full second-order polynomial model for optimization of reaction conditions

Factor	Coefficient Estimate	Standard Error	95% CI Low	95% CI High
Intercept	5.35	0.17	4.97	5.72
λ_1	0.052	0.11	-0.19	0.30
λ_2	0.52	0.11	0.27	0.76
λ_3	-0.070	0.11	-0.32	0.18
$\lambda_1 \lambda_2$	0.35	0.14	0.033	0.68
$\lambda_1 \lambda_3$	-0.032	0.14	-0.35	0.29
$\lambda_2 \lambda_3$	0.078	0.14	-0.24	0.40
λ_1^2	-0.15	0.11	-0.39	0.091
λ_2^2	-0.52	0.11	-0.76	-0.28
λ_3^2	0.043	0.11	-0.20	0.28

*CI is confidence interval.

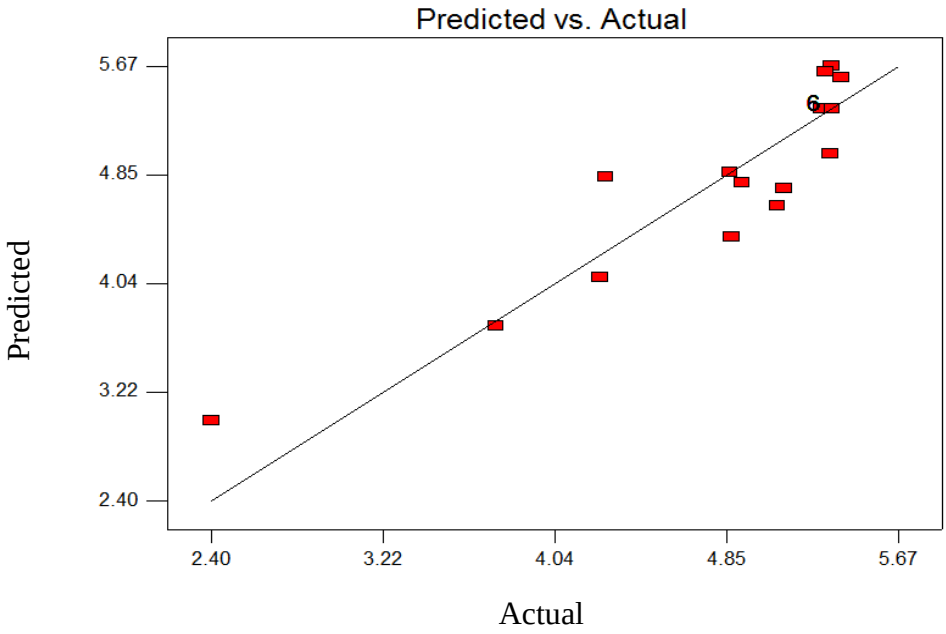

Figure 6.2 A comparative plot between simulation and predicted efficiency

6.4 Effect of process parameters

6.4.1 Effect of single parameter

Based on the developed model, all three single parameters were found to have significant positive effect on the yield of total efficiency as indicated by the positive values of all three regressions coefficient estimates.

6.4.1.1 Feedstock concentration

Figure 6.3 shows that the total efficiency of supercritical water gasification process increases with increasing feedstock concentration. The total efficiency of the process is defined the energy present in the produced gases divided by the energy present in the feed stream plus the energy content of all energy inputs to the process.

When decreasing the feedstock concentration will result in extra energy for high pressure pump as result in decreasing total efficiency. From table 6.4 F-value of the

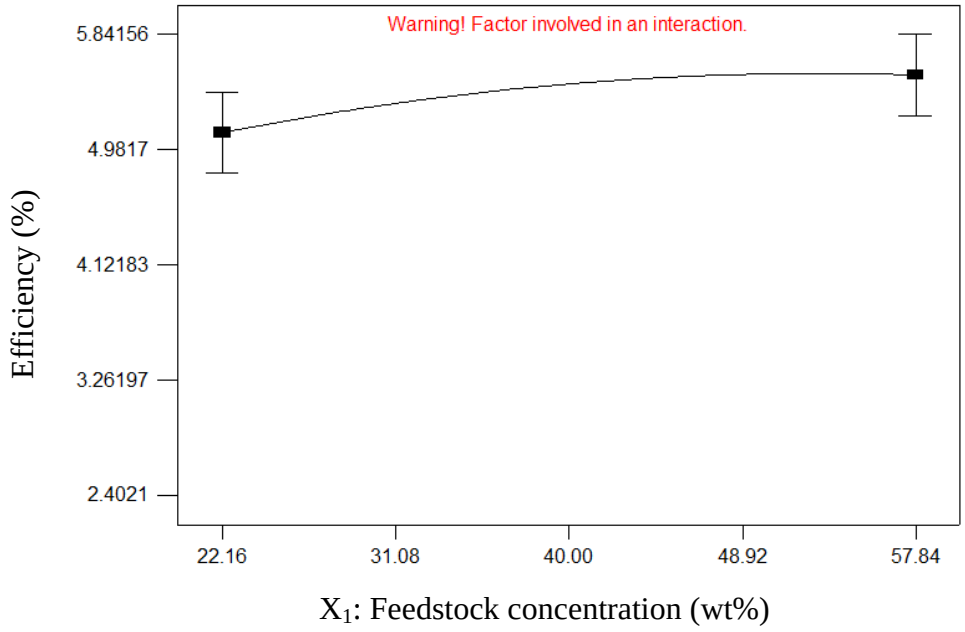

Figure 6.3 Effect of feedstock concentration on the efficiency

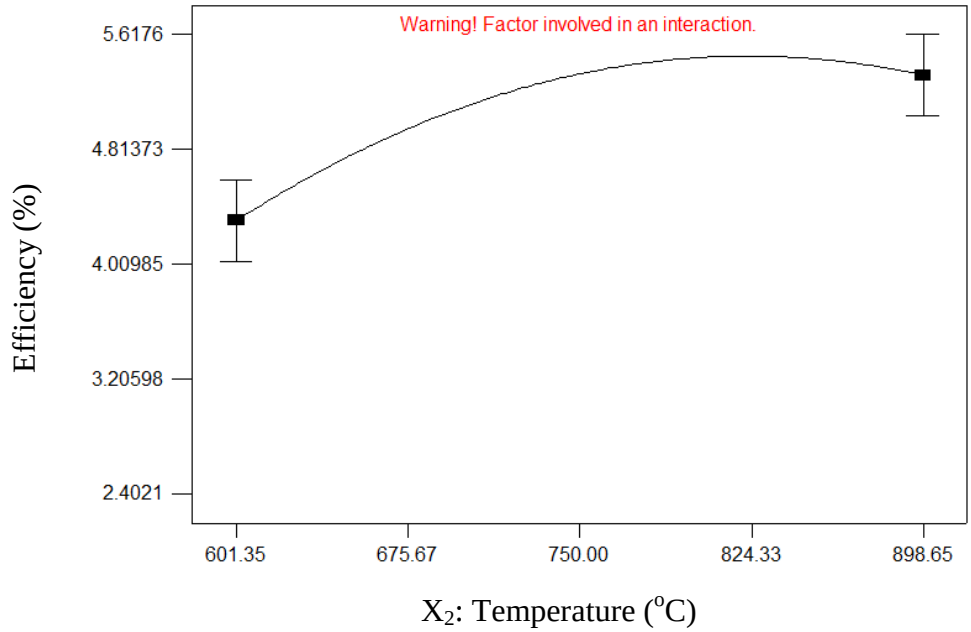

Figure 6.4 Effect of gasifier temperature on the efficiency

parameter is 6.23 and P-value is 0.0452, it is indicated that this parameter has the significant effect on the total efficiency of supercritical water gasification process.

6.4.1.2 Gasifier temperature

Figure 6.4 shows that the total efficiency of supercritical water gasification process increases and then decreasing with increasing gasifier temperature. When increasing the gasifier temperature will result in high hydrogen production. Moreover, at high gasifier temperature, more energy is needed for constant temperature. This increases the total efficiency and decreases. From table 6.4, F-value of the parameter is 21.97 and P-value is 0.0009, it is indicated that this parameter has the significant effect on the total efficiency of supercritical water gasification process.

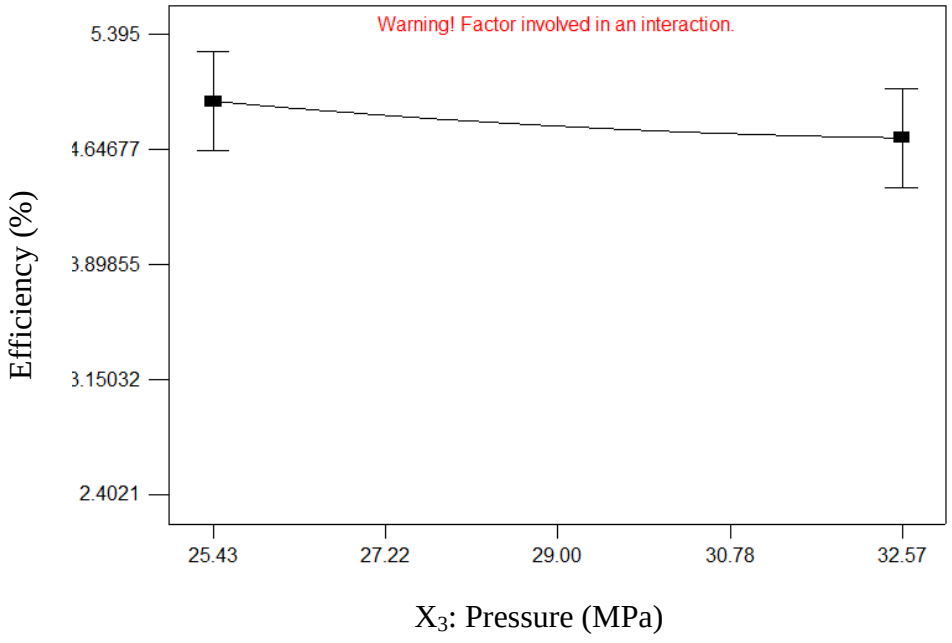

Figure 6.5 Effect of pressure on the efficiency

6.4.1.3 Pressure

Figure 6.5 shows that the efficiency of supercritical water gasification process decreases with increasing pressure. When increasing the pressure will result in low

hydrogen production, moreover extra energy for high pressure pump as result in decreasing the total efficient of supercritical water gasification process. From table 6.4, F-value of the parameter is 0.4 and P-value is 0.5412, it is indicated that this parameter has the non-significant effect on the total efficiency of supercritical water gasification process.

6.4.2 Effect of interaction between parameters

The contour plots described by the regression model were drawn to display the effect of the independent variable on the response variable. From the shape of contour plots one could estimate significance of the mutual interaction between the independent variables in that an elliptical profile of the contour plots indicates remarkable interaction strength as well as the optimal values ranges of the independent variables could be observed.

6.4.2.1 Gasifier temperature and feedstock concentration

According to the ANOVA presented in Table 6.4 term X_1X_2 F-value is 6.05 and P-value is 0.0337. Two interaction terms show significant effect on the total efficiency of supercritical water gasification process due to P-value > 0.005. From the graph in figure 6.8, the line from the A-axis bends toward the B-axis. The responses corresponding to the contour plot of second-order predicted model indicated that at low feedstock concentration, when the gasifier temperature increases the total efficiency of process increases and decreasing at high gasifier temperature. On the other hand, at high feedstock concentration, the line of graph from A-axis bends toword the B-axis. It is indicated when the gasifier temperature increase the total efficiency of supercritical water gasification process more than the operating at low feedstock concentration. The optimal conditions of two parameters for obtaining maximum total efficiency of supercritical water gasification process occurred at the elliptical nature of the contour plot at feedstock concentration 55 - 70 wt% and gasifier temperature about 800 – 900 ^{o}C. The maximum total efficiency of 0.57047 was obtained at feedstock concentration 62 wt% and gasifier temperature 875 ^{o}C.

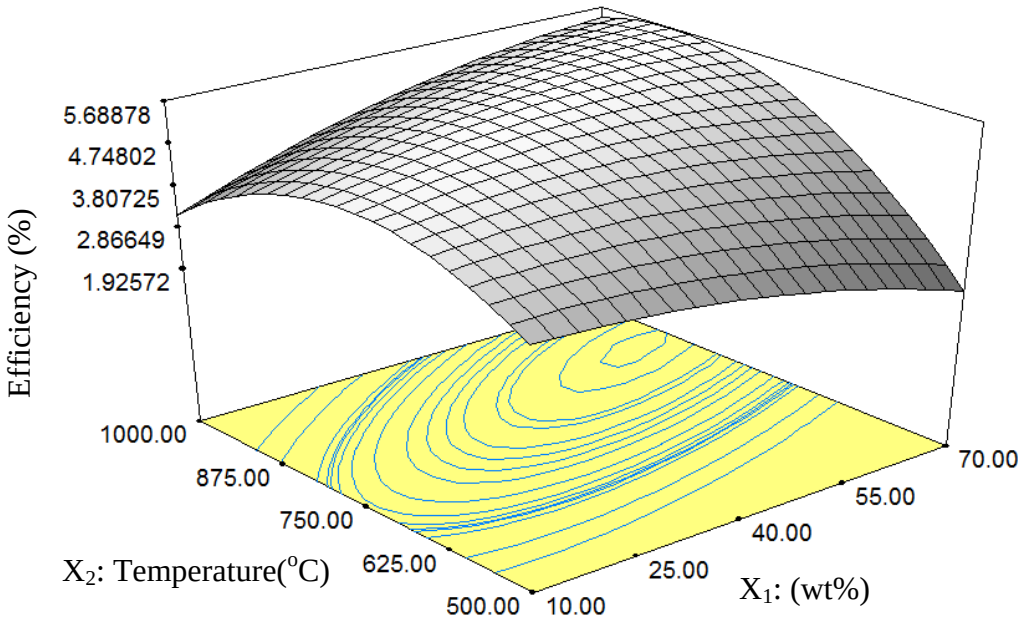

Figure 6.6 Contour plots of the combined effects gasifier temperature and feedstock concentration on the efficiency

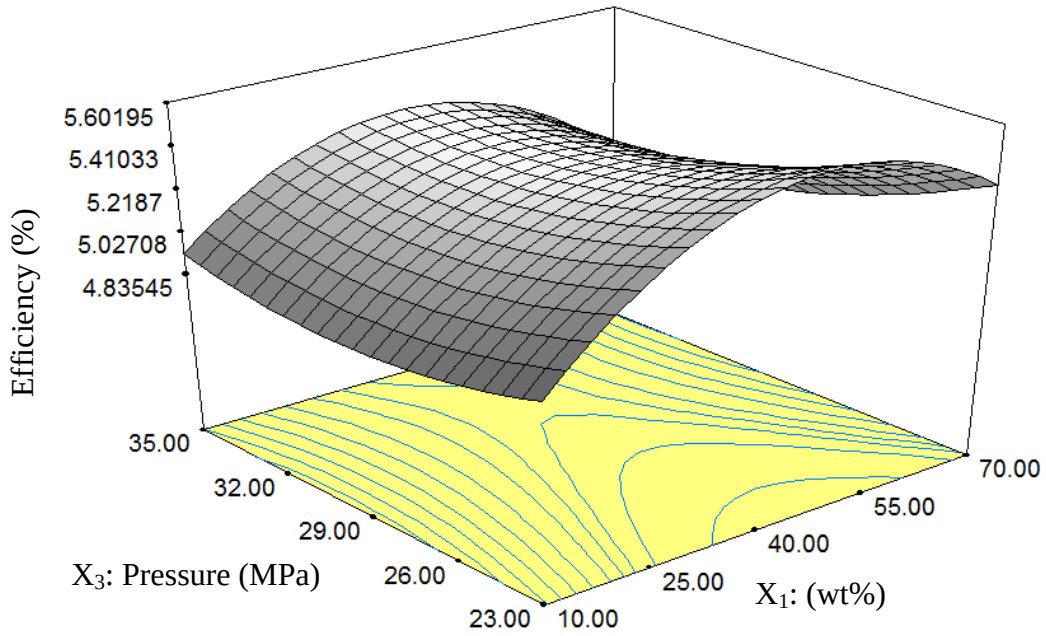

Figure 6.7 Contour plots of the combined effects pressure and concentration feedstock on the efficiency

6.4.2.2 Pressure and feedstock concentration

A response surface plot for total efficiency in figure 6.9 depicts the change of percentage of total efficiency with varying feedstock concentration and pressure, plotted for the case where gasifier temperature is 750. The sharp of three-D response surface plots is similar to the saddle. It can be seen that at low pressure, the total efficiency is found to initially increases with feedstock concentration, get to a maximum and then reduce at higher temperature, the behavior is similar at low pressure but gives relatively low efficiency because an increase in pressure result in a decrease in the yield of hydrogen and more energy is needed. According to the ANOVA presented in table 6.4, term F-value is 0.048 and P-value 0.8311. Two interaction terms show significant effect on the total efficiency of process. The maximum total efficiency of 0.57047 was obtained at feedstock concentration 48 wt% and pressure 23 MPa.

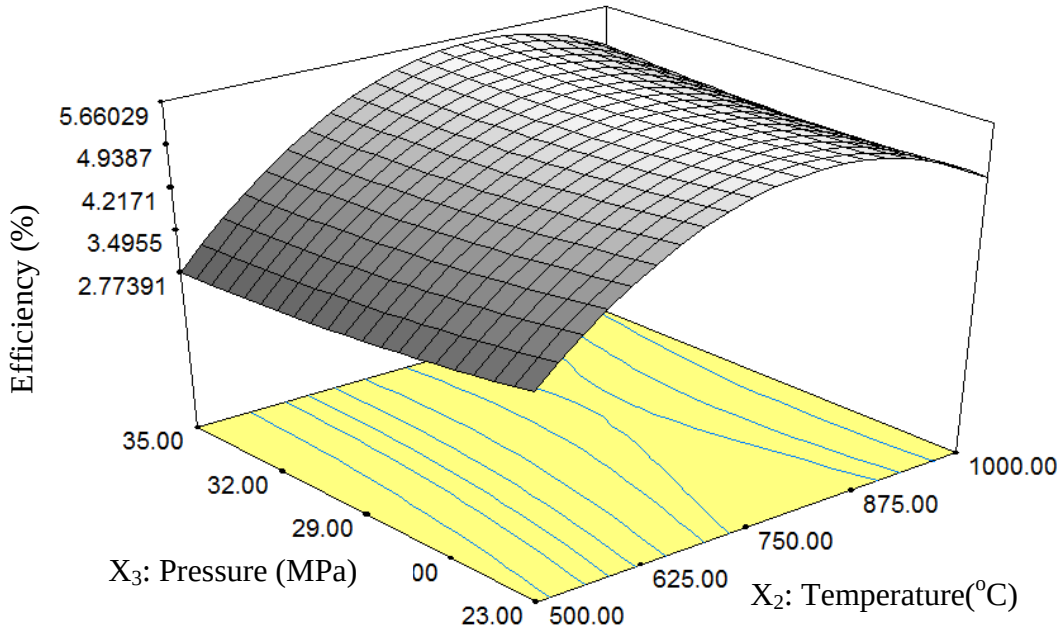

Figure 6.8 Contour plots of the combined effects pressure and gasifier temperature on the efficiency

6.4.2.3 Pressure and gasifier temperature

A response surface plot for total efficiency in Figure 6.10 depicts the change of percentage of efficiency with varying gasifier temperature and pressure, plotted for the case where feedstock concentration is 40 wt%. According to the ANOVA presented in table 6.4, term F-value is 0.30 and P-value 0.5988. Two interaction terms show significant effect on the total efficiency of process. In Figure 6.10, it can be seen that the total efficiency of process firstly increases with gasifier temperature, reach a maximum and then decreasing at high gasifier temperature. Pressure had little effect on the total efficiency of supercritical water gasification process for water hyacinth, when related with gasifier temperature. The maximum total efficiency of 5.63241 was obtained at gasifier temperature 813 ^{o}C and pressure 23 MPa.

6.5 Optimization of efficiency of a biomass gasification process

In this study, the optimization of the supercritical water gasification for water hyacinth process was performed to seek for an optimum combination of operating conditions at which the maximum total efficiency of process is achieved. The variables (feedstock concentration, gasifier temperature, pressure) were set in a range between low and high levels which coded -1.68 and 1.68 to achieve maximum response for the total efficiency of process (Table 6.6). The solutions with these three variables were generated by the software for the desired response of the system based on the model obtained and the simulation data input criteria. The overall average optimized conditions for the total efficiency were obtained as follows: feedstock concentration, gasifier temperature and pressure with total efficiency (Table 6.7). The predicted total efficiency was percentage. This means that the simulation value obtained was reasonably close to the predicted value calculated from the model (% of error). It can be conclude that the generated model showed reasonable predictability and sufficient accuracy for the total efficiency of process in the simulation conditions used.

The high correlation in the model indicates that the second order polynomial model could be used to optimize the total efficiency of supercritical water gasification

for water hyacinth. The conditions to get optimal total efficiency of supercritical water gasification for water hyacinth with % were found to be 53 wt% of feedstock concentration, 866 ^{o}C for gasifier temperature, 24.11 MPa for pressure. These results implicate that the optimization using a response surface methodology based on central composite design was useful software in improving the optimization of the total efficiency of supercritical water gasification for water hyacinth.

Table 6.6 Optimization criteria for maximum efficiency

Factor	Goal	Lower limit	Upper limit
Concentration feedstock	Is in range	10(-1.68)	70(+1.68)
Temperature gasifier	Is in range	500(-1.68)	1000(+1.68)
Pressure	Is in range	23(-1.68)	35(+1.68)
Efficiency	Maximize	-	-

Table 6.7 Results of model validation at the optimum conditions

Factors			Efficiency	
X_1	X_2	X_3	Simulation	Predicted
53.20	865.69	24.11	5.67234	5.71986

CHAPTER VII

CONCLUSIONS

7.1 Conclusions

In this study, the thermodynamic equilibrium analysis of syngas production from biomass was done by minimizing Gibbs free energy using Aspen Plus simulator software. The fuels used for model are water hyacinth (high moisture) and rice straw (low moisture). The biomass gasification technologies studied are fluidized bed technology (conventional gasification) at energy self-sufficiency condition and supercritical water gasification technology at energy self-sufficiency condition. The energy self – sufficient condition can be achieved when steam to biomass (SBR), equivalent ratio (ER), gasifier temperature and feedstock concentration are cautiously selected. These technologies are analyzed and compared in order to obtain the suitable process. The effect of operating parameters such as gasifier temperature, steam to biomass ratio on gas production composition and total efficiency were studied for conventional gasification process. The effect of operating parameters such as feedstock concentration, gasifier temperature and pressure on gas production composition and total efficiency were studied for supercritical water gasification process.

For convention gasification technology compared to water hyacinth, the use of rice straw to produce hydrogen gives a higher performance regarding with the yield of hydrogen produced in the gasifier due to higher number of carbon present in biomass, but general behavior is same. The equilibrium hydrogen yield is found to firstly increased with temperature, get to a maximum and reduce at higher temperature. In temperature range 400 - 500 ^{o}C, the hydrogen yield increases with steam to biomass ratio and decrease at gasifier temperature 600 - 1000 ^{o}C. For supercritical gasification with water hyacinth, the hydrogen yield firstly increases with increasing gasifier temperature and become constant since about 600 ^{o}C. The hydrogen yield initially

decreases with increase in feedstock concentration and then constant at gasifier temperature 600 - 1000 ^{o}C. For rice straw, the hydrogen yield increases first and then decreases with increase in gasifier temperature.

In case of the comparison of gasification technology, for water hyacinth, supercritical water gasification technology can produce the largest quantity of hydrogen, than conventional gasification technology and conventional gasification technology at energy self-sufficient condition, respectively. Supercritical water gasification technology is the most efficient one comparing to conventional gasification technology at energy self-sufficient condition and conventional gasification technology. For rice straw, conventional gasification technology can produce the largest quantity of hydrogen, than conventional gasification technology at energy self-sufficient condition, supercritical water gasification technology and supercritical water gasification technology at energy self-sufficient condition, respectively. Conventional gasification technology at energy self-sufficient condition is the most efficient than conventional gasification technology, supercritical water gasification technology and supercritical water gasification technology at energy self-sufficient condition, respectively.

In case of optimization of supercritical water gasification process with water hyacinth, response surface methodology (RSM) based on central composite design was used to optimize the three important variables. The mathematical model developed could predict the total efficiency of process at any point in the simulation domain as well as the determination of the optimal parameter conditions. The conditions to get optimal response with 5.71986% were found to be 53.20 wt% of feedstock concentration, 865.69^{o}C for gasifier temperature, 24.11 MPa for pressure. These results implicate that the optimization using a response surface methodology based on central composite design was useful software in improving the optimization of the total efficiency of process.

7.2 Recommendation

The present paper intended to present the simulation results of parametric study of the effects of gasifier temperature, feedstock concentration and pressure on gas composition and process efficiency**.** Due to expected high investment and maintenance cost of the supercritical water gasification process for syngas production, it is recommended to make economic analysis and a comparison with conventional gasification process.

REFERENCES

Antal Jr., M.J., Allen, S.G., Schulman, D.,Xu, X., Divilio, R.J. Biomass gasification in supercritical water. Industrial and Engineering Chemistry Research 39 (2000): 4040-4053.

Aslan, N. Application of response surface methodology and central composite rotatable design for modeling and optimization for a multi-gravity separator for chromite concentration. Powder Technology 185 (2008): 80-86.

Ashrafi, M., Prőll, T., Pfeifer, C., and Hofbauer, H. Experimental Study of Model Biogas Catalytic Steam Reforming: 1. Thermodynamic Optimization. Energy & Fuels 22 (2008): 4182-4189.

Bain, R.L., Dayton, D.C., Carpenter, D.L., Czernik, S.R., Feik, C.J., French, R.J., Magrini-Bair, K.A., Phillips, S.D. Evaluation of catalyst deactivation during catalytic steam reforming of biomass-derived syngas. Industrial and Engineering Chemistry Research 44 (2005): 7945-7956.

Balat, M., Balat, M., Kırtay, E., Balat, H., 2009, Main routes for the thermo-conversion of biomass into fuels and chemicals: Part 2: Gasification systems, Energy Conversion and Management 50 (2009): 3158-3168.

Barin I. Thermochemical data for pure substances, vol.1, 3rd ed. Weinheim : NY, 1995.

Basu, P. Biomass gasification and pyrolysi. Elsevier Inc: Academic Press, 2010.

Bos, J.D., Sillevis Smitt, J.H. Atopic dermatitis Journal of the European Academy of Dermatology and Venereology 7 (1996): 101-114.

Box, G.E.P., Wilson, K.B. On the experimental attainment of optimum conditions. Journal of the Royal Statistical Society. Series B, Statistical Methodology 13 (1951): 1-45.

Brown, R.C. Biorenewable Resources: Engineering New Products from Agriculture. Ames, Iowa: Iowa State Press, 2003.

Castello, D. and Fiori, L. Supercritical water gasification of biomass: Thermodynamic constraints. Bioresource Technology 102 (2011): 7574-7582.

Chen, G., Li, G., Glazer, M.P., Zhang, C.Andries, J. Operation of a circulating fluidised bed biomass gasifier. Proceedings of the ASME Turbo Expo 7 (2004): 87-92.

Devi, L., Ptasinski, K.J., Janssen, F.J.J.G., Van Paasen, S.V.B., Bergman, P.C.A., Kiel, J.H.A. Catalytic decomposition of biomass tars: Use of dolomite and untreated olivine. Renewable Energy 30 (2005): 565-587.

Doherty, W., Reynolds, A., Kennedy, D. The effect of air preheating in a biomass CFB gasifier using ASPEN Plus simulation. Biomass and Bioenergy 33 (2009): 1158-1167.

Elliott, Douglas C., Sealock Jr., L.John,Butner, Scott, R.Product analysis from direct liquefaction of several high-moisture biomass feedstocks. ACS Symposium Series (1988): 179-188.

Gómez-Barea, A., Leckner, B. Modeling of biomass gasification in fluidized bed. Progress in Energy and Combustion Science 36 (2010): 444-509.

Gutiérrez Ortiz, F.J., Ollero, P., Serrera, A. Thermodynamic analysis of the autothermal reforming of glycerol using supercritical water. International Journal of Hydrogen Energy 36 (2011): 12186-12199.

Hao X.H., Guo L.J., Mao X.M. and Chen H.J. Hydrogen production from glucose as a model compound of biomass gasified in supercritical water. International Journal of Hydrogen Energy 28 (2003): 53-64.

Herfjord, T., Osthagen, H., Saelthun, N.R. The Water Hyacinth. Oslo, Norwegian Agency for Development Cooperation.1994.

Ji, P., Feng, W., Chen, B., Yuan, Q. Finding appropriate operating conditions for hydrogen purification and recovery in supercritical water gasification of biomass. Chemical Engineering Journal 124 (2006): 7-13.

Kabyemela, B.M., Adschiri, T., Malaluan, R.M. and Arai, K. Glucose and fructose decomposition in subcritical and supercritical water: Detailed reaction pathway, mechanisms, and kinetics. Department of Chemical Engineering 38 (1999): 2888 -2895.

Kempegowda, R., Assabumrungrat, S.,Laosiripojana, N. Thermodynamic analysis for gasification of thailand rice husk with air, steam, and mixed air/steam for

hydrogen-rich gas production. International Journal of Chemical Reactor Engineering 8 (2010): A158

Knoef, H.A.M. Inventory of Biomass Gasifier Manufacturers and Installations, Final Report to European Commission, Contract DIS/1734/98-NL, in, Biomass Technology Group B.V. (2000).

Kumar, A.Demirel, Y., Jones, D.D., Hanna, M.A. Optimization and economic evaluation of industrial gas production and combined heat and power generation from gasification of corn stover and distillers grains. Bioresource Technology 101 (2010): 3696-3701.

Liao, C., Wu, C., and Yan, Y. The characteristics of inorganic elements in ashes from a 1 MW CFB biomass gasification power generation plant. Fuel Processing Technology 88 (2007): 149-156.

Lv, P., Chang, J., Xiong, Z., Huang, H.,Wu, C., Chen, Y., Zhu, J. Biomass air-steam gasification in a fluidized bed to produce hydrogen-rich gas. Energy and Fuels 17 (2003): 677-682.

Lu, Y., Guo, L., Zhang, X. and Yan, Q. Thermodynamic modeling and analysis of biomass gasification for hydrogen production in supercritical water. Chemical Engineering Journal 131 (2007): 233-244.

Mathieu, P. and Dubuisson, R. Performance analysis of a biomass gasifier. Energy Conversion and Management 43 (2002): 1291-1299.

Matsumura, Y., Minowa, T., Potic, B., Kersten, S., Prins, W., Vanswaaij, W., Vandebeld, B. and Elliott, D., Neuenschwander, G., Kruse, A. Biomass gasification in near- and super-critical water: status and prospects. Biomass and Bioenergy 29 (2005): 269-292.

Milne, T.A., Evans, R.J., Abatzoglou, N. Biomass Gasifier Tars: Their Nature, Formation, and Conversion, NREL/TP (1998): 570-25357.

Ortiz, F.J. G., Ollero, P. and Serrera, A. Thermodynamic analysis of the autothermal reforming of glycerol using supercritical water. International Journal of Hydrogen Energy 36 (2011): 12186-12199.

Osowski, S. and Fahlenkamp, H. Regenerative energy production using energy crops. Industrial Crops and Products 24 (2006): 196-203.

Pairojpiriyakul, T., Kiatkittipong, W.,Soottitantawat, A., Arpornwichanop, A.,Laosiripojana, N., Wiyaratn, W., Croiset, E., Assabumrungrat, S. Thermodynamic analysis of hydrogen production from glycerol at energy self-sufficient conditions. Canadian Journal of Chemical Engineering 90 (2012): 1112-1119.

Paviet, F., Chazarenc, F., Tazerout, M. Thermo chemical equilibrium modelling of a biomass gasifying process using ASPEN PLUS. International Journal of Chemical Reactor Engineering 7 (2009): A40.

Puig-Arnavat, M., Hernández, J.A.,Bruno, J.C., Coronas, A. Artificial neural network models for biomass gasification in fluidized bed gasifiers. Biomass and Bioenergy 49 (2013): 279-289.

Saelthun, N.R., Andersen, J.H. NEW PROCEDURES FOR FLOOD ESTIMATION IN NORWAY. Nordic Hydrology 17 (1986): 217-228.

Saisu, M., Sato, T., Watanabe, M., Adschiri, T. and Arai, K. Conversion of lignin with supercritical water–phenol mixtures. Energy Fuels 17 (2003): 922-8.

Shen, L., Gao, Y., Xiao, J. Simulation of hydrogen production from biomass gasification in interconnected fluidized beds. Biomass and Bioenergy. 32 (2008): 120-127.

Sheth, P.N., Babu, B.V. Experimental studies on producer gas generation from wood waste in a downdraft biomass gasifier. Bioresource Technology 100 (2009): 3127-3133.

Skoulou, V. , Zabaniotou, A., Stavropoulos, G. , Sakelaropoulos, G. Syngas production from olive tree cuttings and olive kernels in a downdraft fixed-bed gasifier. International Journal of Hydrogen Energy 33 (2008): 1185-1194.

Valderrama, J.O. The state of the cubic equations of state. Industrial & Engineering Chemistry Research 42 (2003): 1603-1618.

Van Paasen, S.V.B., Kiel, J.H.A. Tar formation in a fluidized bed gasifier: impact of fuel properties and operating conditions, Report ECN-C-04-013 (2004): 1-58.

Voll, F.A.P., Rossi, C.C.R.S., Silva, C.,Guirardello, R., Souza, R.O.M.A., Cabral, V.F., Cardozo-Filho, L.

gasification of methanol, ethanol, glycerol, glucose and cellulose. International Journal of Hydrogen Energy 34 (2009): 9737-9744.

Warnecke, R. Gasification of biomass: comparison of fixed bed and fluidized bed gasifier, Biomass and Bioenergy 18 (2000): 489-497.

Withag, J.A.M., Smeets, J.R., Bramer, E.A., Brem, G. System model for gasification of biomass model compounds in supercritical water - A thermodynamic analysis. Journal of Supercritical Fluids 61 (2012): 157-166.

Yan, Q., Guo, L. and Lu, Y. Thermodynamic analysis of hydrogen production from biomass gasification in supercritical water. Energy Conversion and Management 47 (2006): 1515-1528.

Yoshida, Y., Dowaki, K., Matsumura, Y.,Matsuhashi, R., Li, D., Ishitani, H.,Komiyama, H. Comprehensive comparison of efficiency and CO 2 emissions between biomass energy conversion technologies - Position of supercritical water gasification in biomass technologies. Biomass and Bioenergy 25 (2003): 257-272.

Zainal, Z.A. , R. Ali, C.H. Lean, K.N. Seetharamu, Prediction of performance of a downdraft gasifier using equilibrium modeling for different biomass materials. Energy Conversion and Management 42 (2001): 1499-1515.

APPENDIX A

FORTRAN subroutine

1. Calculator block to control drying

The material balance equations for this process define relations between the following quantities:

- Water content of the feed coal.
- Fractional conversion of coal to water.
- Water content of the dried coal.

$$Biomass_{in} \times \frac{H_2O_{in}}{100} = Biomass_{out} \times \frac{H_2O_{out}}{100} + Biomass_{in} \times Conv \quad (1)$$

$$Biomass_{in} = Biomass_{out} + Biomass_{in} \times Conv \quad (2)$$

Where: $Biomass_{in}$ = mass flow rate of biomass in stream BIOMASS

$Biomass_{out}$ = mass flow rate of biomass in stream DRY-BIOM

H_2O_{in} = percent moisture in the biomass in stream BIOMASS

H_2O_{dry} = percent moisture in the biomass in stream DRY-BIOM

Conv = fractional conversion of coal to H_2O in the block DRIER

Equation 1 is the material balance for water, and equation 2 is the overall material balance. These equations can be combined to yield equation 3:

$$Conv = \frac{(H_2O_{in} - H_2O_{out})}{(100 - H_2O_{out})} \quad (3)$$

Use equation 3 in calculator block to ensure these three specifications are consistent. The calculator block specifies the moisture content of the dried biomass and calculates the corresponding conversion of coal to water.

Fortran statements:

```
H2ODRY = 5.0
CONV   = (H2OIN – H2ODRY)/(100 – H20DRY)
```

2. Calculator block to calculate the yields

In this simulation, access the ultimate analysis of biomass in stream DRY-BIOM as a component attribute vector. Also define variables to access the moisture content of coal and the yield of each component in the DECOMP block.

Fortran statements:

```
FACT = (100 - WATER) / 100
H2O  = WATER  / 100
ASH  = ULT(1) / 100 * FACT
CARB = ULT(2) / 100 * FACT
H2   = ULT(3) / 100 * FACT
N2   = ULT(4) / 100 * FACT
CL2  = ULT(5) / 100 * FACT
SULF = ULT(6) / 100 * FACT
O2   = ULT(7) / 100 * FACT
```

Vitae

Nathapol Boonpithak, the first son of Nitat and Boonma Boonpithak, was born in Bangkok on October 12, 1987. After graduating high school from Taweethapisek School, he entered King Mongkut's University of Technology Thonburi in May 2006 and received his Bachelor of Engineering degree in Chemical Engineering in April 2010. He began his graduate study in May 2010 when he entered the Graduate School of Chulalongkorn University and joined the Control and Systems Engineering research group at Department of Chemical Engineering.